Training rivers with longitudinal walls
long-term morphological responses

Le, Binh

DOI
10.4233/uuid:cf588b41-0bcc-490f-9cf0-ea0d95a92678

Publication date
2018

Document Version
Final published version

Citation (APA)
Le, B. (2018). *Training rivers with longitudinal walls: long-term morphological responses*. [Dissertation (TU Delft), Delft University of Technology]. https://doi.org/10.4233/uuid:cf588b41-0bcc-490f-9cf0-ea0d95a92678

TRAINING RIVERS WITH LONGITUDINAL WALLS:

long-term morphological responses

TRAINING RIVERS WITH LONGITUDINAL WALLS:

long-term morphological responses

Proefschrift

ter verkrijging van de graad van doctor
aan de Technische Universiteit Delft,
op gezag van de Rector Magnificus Prof.dr.ir. T.H.J.J. van der Hagen;
voorzitter van het College voor Promoties,
in het openbaar te verdedigen op
woensdag 19 December 2018 om 12.30 uur

door

Thai Binh LE

Master of Science in Water Science and Engineering,
UNESCO-IHE, The Netherlands.
Geboren te Quang Nam, Vietnam.

Dit proefschrift is goedgekeurd door de promotor.

Samenstelling promotiecommissie bestaat uit:

Rector Magnificus,	voorzitter
Prof.dr.ir. W.S.J. Uijttewaal	TU Delft, *promotor*
Dr.ir. A. Crosato	IHE-Delft, *copromotor*

Onafhankelijke leden:

Dr. R.M.J. Schielen	Rijkswaterstaat
Prof.dr. M.J. Franca	IHE-Delft/Technische Universiteit Delft
Prof.dr. F. Klijn	Technische Universiteit Delft
Prof.dr.ir. A.J.F. Hoitink	Wageningen Universiteit & Research

Overige leden:

Assoc.prof.dr. T.T. Nguyen	Thuyloi Universiteit, Hanoi Vietnam

TU Delft Delft University of Technology

TRƯỜNG ĐẠI HỌC THỦY LỢI
THUYLOI UNIVERSITY - WWW.TLU.EDU.VN

Keywords: longitudinal training walls, river morphology, river bifurcation, river bars, Delft3D

Printed by: Ipskamp Printing

Front & Back: Photo taken by Rijkswaterstaat

ISBN 978-94-6384-002-6

An electronic version of this dissertation is available at
http://repository.tudelft.nl/.

No matter what happens, the Sky can not fall into one's head.
Why? Because if it can, human being were all gone, long time ago.

Lê Thúc Quang, my father, 2013.
One day before my PhD started.

Contents

List of Abbreviations and symbols **xi**

Summary **xv**

Samenvatting **xvii**

1 Introduction **1**
1.1 River training with groynes and longitudinal walls 2
1.2 Relevance and research scope 3
1.3 Scale of the problem 5
1.4 Approach 5
References 7

2 Experimental investigation **9**
2.1 Introduction 10
2.2 River bars and bifurcations 12
2.3 Methodology 13
2.4 Laboratory investigation 15
2.4.1 Experimental set up 15
2.4.2 Data collection and data processing 17
2.4.3 Results of the base-case scenario 18
2.4.4 Results of relative width variation 21
2.4.5 Sensitivity analysis 21
2.5 Numerical investigation 24
2.5.1 Model description 24
2.5.2 Upscaled-experiment model setup 25
2.5.3 Upscaled-experiment model results 26
2.5.4 Alpine Rhine model setup 28
2.5.5 Alpine Rhine model results 29
2.6 Discussion 32
2.7 Conclusions 33
References 34

3 Numerical investigation. **39**
3.1 Background and objective 40
3.2 Theoretical background 41
3.2.1 Stability of bifurcations and bars 41
3.2.2 Bifurcation stability analyses 43

3.3 Numerical investigations . . . 46
3.3.1 Model description . . . 46
3.3.2 Model setup . . . 46
3.3.3 Model runs . . . 49
3.4 Results . . . 51
3.4.1 Effects of starting location . . . 51
3.4.2 Effects of altering the width ratio between side and main channel . . . 54
3.4.3 Effects of variable discharge . . . 55
3.4.4 Sensitivity analysis on the effects of transverse bed slope 57
3.4.5 Sinuous planform . . . 60
3.5 Discussion . . . 61
3.6 Conclusions and recommendations . . . 62
References . . . 64

4 Case study **69**
4.1 Introduction . . . 70
4.1.1 Background information . . . 70
4.1.2 Study area . . . 72
4.2 Materials and Methods . . . 73
4.2.1 General description . . . 73
4.2.2 Numerical model setup . . . 77
4.2.3 Implementation of training wall and groynes . . . 79
4.3 Results . . . 80
4.3.1 Pre-runs . . . 80
4.3.2 Model calibration and validation . . . 80
4.3.3 Long-term morphological developments with and without interventions . . . 82
4.3.4 Results of the hydraulic models . . . 85
4.4 Discussion . . . 89
4.5 Conclusions and recommendations . . . 91
References . . . 92

5 Discussion **97**
5.1 Qualitative comparison with previous work and field observations . . . 98
5.2 Experimental tests . . . 99
5.3 Numerical simulations . . . 100
5.4 Future works . . . 102
5.4.1 Setting of longitudinal training walls . . . 102
5.4.2 On the river ecological potential . . . 102
References . . . 103

6 Conclusion **105**
6.1 Main conclusions . . . 105
6.2 Summary of conclusions and recommendations . . . 107

A Appendix **109**

Appendix **109**
References 111

Acknowledgements **113**

Curriculum Vitæ **115**

List of Publications **117**

List of Abbreviations and symbols

Abbreviations

1D	One dimension
2D	Two dimensions
2DH	Two-dimensional depth-averaged
3D	Three dimensions
A-A	Cross-section A-A
A'-A'	Cross-section A'-A'
AD	from Latin "Anno Domini" means "Year of the Lord", which indicating how many years have passed since the birth of Jesus
Delft3D	An open source code provided by Deltares, available online at: https://oss.deltares.nl/web/delft3d
DES	Detached Eddy Simulation
MF	Morphological Acceleration factor
MPM	Meyer-Peter and Muller
PTV	Particle Tracking Velocimetry
Rijkswaterstaat	Ministry of Public Works, the Netherlands
VIED	Vietnam International Education Development
Wallsamen	Data collected project along the ecological channel in the Netherlands, where three longitudinal dams were built along the Waal River

Experimental tests:

B	Base case
W1	Width ratio 1
W2	Width ratio 2
S1	Sensitivity analysis with sediment size 1
S2	Sensitivity analysis with sediment size 2

Numerical simulations:

W0	Base case constant discharge
W1	Width ratio 1
W2	Width ratio 2
V0	Base case variable discharge
V1	Width ratio 1
V2	Width ratio 2
A	Sensitivity analysis
S	Sinuous river

In the case study of River Waal:

W1	Longitudinal wall starts upstream of point bar top, navigation channel width 200 m
W2	Longitudinal wall starts downstream of point bar top, navigation channel width 200 m
W3	Longitudinal wall starts upstream of point bar top, navigation channel width 260 m
G1	Groynes scenario, river width 260 m
G2	Groynes scenario, river width 200 m

Symbols

A	A coefficient that weights the influence of the spiral flow [-]
A_{sh}, B_{sh} and C_{sh}	Calibration coefficients to calculate $f(\theta_0)$ [-]
b	The degree of non-linearity of the sediment transport formula as a function of flow velocity [-]
B	Normal width of original channel [m]
B_e	Width of the ecological channel [m]
B_n	Width of the navigation channel [m]
B/h	Width-to-depth ratio [-]
β_s	The direction of sediment transport [-]
β_τ	The bed shear stress [-]
C	The Chézy coefficient [$m^{1/2}/s$]
C_f	The friction factor defined by $C_f = \frac{g}{C^2}$[-]

C_D	The drag coefficient associated with the vegetation type [-]
D_{50}	Median sediment size [m]
D_{15}, D_{65}, and D_{90}	Sediment size that the percentages of 15%, 65%, and 90% of particles smaller than [m]
$\delta z/\delta y$	The transverse slope [-]
$\delta z/\delta x$	The streamwise slope [-]
Δ	Relative submerged sediment density [-]
ΔZ	Different in bed level of the two parallel channels [m]
E	A calibration coefficient to calculate $f(\theta_0)$ [-]
ε (≈ 1)	A calibration coefficient (in this study ε = 1) to calculate A [-]
$f(\theta_0)$	The function accounts for the effect of gravity on the direction of sediment transport over transverse bed slopes [-]
Fr	The Froude number [-]
g	The gravity acceleration [m/s^2]
h_0	Normal depth [m]
h_v	Vegetation height [m]
i	Longitudinal bed slope [-]
κ	The Von Kármán constant (= 0.4) [-]
L	River length [m]
L_p	Hybrid bar wavelength [m]
λ_w	2D flow adaptation length [m]
λ_S	2D water depth adaptation length [m]
λ_S/λ_w	2D interaction parameter [-]
m	Bars mode, number of bars in the river cross-section [-]
$M \times N$	Rectangular grid size [m × m]
n	The vegetation density [m^{-1}]
π	Pi number [-]
Q	Discharge of the original channel [m^3/s]
$Q_{50\%}$	Average discharge [m^3/s]
Q_{FW}	Fully wet discharge in Alpine Rhine model [m^3/s]
Q_{FT}	Fully transporting discharge in Alpine Rhine model [m^3/s]
Q_{cr}	Critical discharge for bar formation in Alpine Rhine model [m^3/s]
Q_{full}	Bank-full discharge in the Waal River [m^3/s]
Q_{low}	low discharge in the Waal River [m^3/s]
$Q_{history}$	Highest discharge in the last century in the Waal River [m^3/s]
Q_{design}	Design discharge for the Waal River [m^3/s]

R	The streamline radius of curvature [m]
t	Time step [minutes]
T	Simulation time [days]
θ_0	The Shields parameter [-]
u, v	The streamwise and transverse velocity [m/s]
Z_e	Bed level in ecological channel, averaged over the entire length of the training wall [m]
Z_n	Bed level in navigation channel, averaged over the entire length of the training wall [m]

Summary

Rivers have been trained for centuries by series of transverse groynes. This generally results in damages to their ecosystems as well as in undesirable long-term morphological developments. We analyze here the possibility to train rivers in a new way by subdividing their channel in parallel channels with specific functions with longitudinal training walls. In most cases, the goal is that of obtaining one deep, regular navigation channel and one shallower channel that is able to preserve some ecological functions of the river and to contribute to convey high flow discharges. The effectiveness of longitudinal training walls in achieving this goal and their long-term effects on the river morphology have not been thoroughly investigated yet. In particular, studies that assess the stability of the parallel channels separated by the training wall are still lacking.

This work studies the long-term morphological developments of river channels subdivided by one or two longitudinal walls, focusing on low-land rivers. These rivers are normally characterized by the presence of steady alternate bars, or point bars inside their bends. For this reason, the presence of these large deposits is taken into account. This is the first study dealing with the combined effects of bars and longitudinal walls. The methodology comprises both laboratory experiments and numerical simulations.

A series of laboratory investigations was performed to show the effects of placing a longitudinal training wall in a straight channel with steady alternate bars. The experimental tests include different types of bed material. The results show that the starting location of the wall with respect to a bar plays an important role in the evolution of the created parallel channel system.

The experiments were then reproduced numerically to assess the capability of a 2D morphological model of simulating the observed morphological behavior. The results show that Delft3D can be successfully used for this type of investigations. Considering this, 102 numerical simulations were subsequently carried out to study the effects of longitudinal training walls on the stability of the system. The numerical tests included straight and sinuous rivers, different widths of the parallel channels, and constant and variable discharges. The results show that the parallel channel system created by a longitudinal training wall is morphodynamically unstable, i.e. one channel tends to silt up whereas the other one becomes progressively deeper. The starting point of the wall with respect to a steady bar or point bar plays a major role in the morphological developments of the system. The numerical tests thus confirm the findings in the laboratory. The results show also that if the longitudinal training wall starts just upstream of a bar top the system is less unstable. Moreover, the morphological developments of the parallel channels slow down with variable discharge. The relative width of the channels does not affect the final evolution of the system, but equally wide channels take a longer time to evolve. These findings

suggest that an equal parallel channel system created by a wall starting near a bar top is manageable and could be a river training solution, considering that real rivers have variable discharge.

Finally, the numerical application on a real river case, the Waal River between the cities of Nijmegen and Tiel, supports the theoretical findings on idealized cases: a longitudinal training wall always creates one deep "navigation" channel and one shallow "ecological" channel. Compared to groynes producing the same channel width, training the river with a longitudinal wall results in the same level of navigability, whereas it improves high-flow conveyance and reduces river incision. In addition, the presence of a shallow channel offers the conditions for maintaining some ecological functions of the river.

This work comprises the first attempt towards the assessment of the long-term effects of training a river by means of a longitudinal training wall. More work needs to be done, in particular to assess the need to protect the river banks. The results of this study suggest that the only bank that needs to be protected against erosion is the one along the deeper navigation channel, but this is not enough to conclude that the bank of the ecological channel does not need protection.

Samenvatting

Rivierbeddingen zijn eeuwenlang gereguleerd met rijen kribben die dwars de rivier in steken. Dit resulteert in het algemeen in schade aan de ecosystemen van rivieren, en ook in ongewenste morfologische ontwikkelingen op lange termijn. We analyseren hier de mogelijkheden om rivierbeddingen te reguleren op een nieuwe manier door ze met langsdammen te verdelen in parallelle geulen die specifieke functies hebben. Het doel is in de meeste gevallen het verkrijgen van een diepe regelmatige vaargeul en een ondiepere geul die in staat is om bepaalde ecologische functies van de rivier in stand te houden en bij te dragen aan het afvoeren van hoge stroomdebieten. De effectiviteit van langsdammen bij het bereiken van dit doel en de langetermijneffecten van langsdammen op de riviermorfologie zijn nog niet grondig onderzocht. In het bijzonder ontbreken nog studies die de stabiliteit bepalen van de door de langsdam gescheiden parallelle geulen.

Dit werk bestudeert de morfologische ontwikkelingen op lange termijn van rivierbeddingen gescheiden door een of twee langsdammen, met een focus op laaglandrivieren. Deze rivieren worden normaal gesproken gekarakteriseerd door de aanwezigheid van stationaire alternerende banken, of kronkelwaardbanken in hun binnenbochten. Om deze reden wordt met deze grote afzettingen rekening gehouden. Dit is de eerste studie die zich richt op de gecombineerde effecten van banken en langsdammen. De methodologie omvat zowel laboratoriumexperimenten als numerieke simulaties.

Een reeks laboratoriumonderzoeken werd uitgevoerd om de effecten te tonen van het plaatsen van een langsdam in een rechte waterloop met stationaire alternerende banken. De experimentele proeven omvatten verschillende typen bodemmateriaal. De resultaten laten zien dat de startlocatie van de dam ten opzichte van een bank een belangrijke rol speelt in de ontwikkeling van het gecreëerde systeem van parallelle geulen.

De experimenten werden daarna numeriek gereproduceerd om de capaciteiten van een 2D morfologisch model te bepalen voor het simuleren van het waargenomen morfologische gedrag. De resultaten laten zien dat Delft3D met succes gebruikt kan worden voor dit type onderzoekingen. Dit overwegende werden vervolgens 102 numerieke simulaties uitgevoerd om de effecten van langsdammen op de stabiliteit van het systeem te bestuderen. De numerieke tests omvatten rechte en bochtige rivieren, verschillende breedtes van de parallelle geulen, en constante en variërende afvoeren. De resultaten laten zien dat het door een langsdam gecreëerde systeem van parallelle geulen morfodynamisch instabiel is, dat wil zeggen: één geul neigt aan te zanden terwijl de andere steeds dieper wordt. Het beginpunt van de dam ten opzichte van een stationaire bank of kronkelwaardbank speelt een voorname rol in de morfologische ontwikkelingen van het systeem. De numerieke tests bevestigen zo de bevindingen in het laboratorium. De resultaten laten ook

zien dat het systeem minder instabiel is als de dam juist stroomopwaarts van de top van de bank begint. Bovendien remmen de morfologische ontwikkelingen van de parallelle geulen af bij variërende afvoer. De relatieve breedte van de geulen heeft geen invloed op de uiteindelijke ontwikkeling van het systeem, maar voor geulen van gelijke breedte kost het meer tijd om zich te ontwikkelen. Deze bevindingen suggereren dat een systeem van gelijke parallelle geulen dat gecreëerd wordt door een langsdam die begint bij de top van een bank, beheersbaar is en een oplossing zou kunnen zijn voor rivierbedregulering, in overweging nemend dat echte rivieren een variërende afvoer hebben.

De numerieke toepassing op een echte riviercasus, de rivier de Waal tussen de steden Nijmegen en Tiel, ondersteunt ten slotte de theoretische bevindingen over geïdealiseerde casussen: een langsdam creëert altijd een diepe "scheepvaartgeul" en een ondiepe "ecologische geul". In vergelijking met kribben die dezelfde geulbreedte produceren, resulteert regulering van de rivierbedding met een langsdam in hetzelfde niveau van bevaarbaarheid terwijl dit het vermogen om hoge debieten af te voeren verbetert en insnijding van de rivier reduceert. Daar komt bij dat de aanwezigheid van een ondiepe geul de voorwaarden biedt voor het handhaven van bepaalde ecologische functies van de rivier.

Dit werk omvat de eerste poging in de richting van het bepalen van de langetermijneffecten van rivierbedregulering door middel van een langsdam. Meer werk is nodig, in het bijzonder om de noodzaak van het verdedigen van rivieroevers vast te stellen. De resultaten van deze studie suggereren dat de enige oever die tegen erosie verdedigd hoeft te worden de oever is langs de diepere scheepvaartgeul, maar dit is niet genoeg om te concluderen dat de oever van de ecologische geul geen verdediging behoeft.

1

Introduction

The journey of a thousand miles begins with one step.

Lao Tzu

This chapter presents the background of river training and introduces longitudinal training walls.

1

1.1. River training with groynes and longitudinal walls

Rivers have been trained for centuries by series of transverse groynes (Figure 1.1) with the aim to obtain a narrower and often also straighter river channel. This increases the river navigability and prevents the formation of ice jams [1, 2]. However, groynes decrease the channel conveyance during floods and trigger a morphological response characterized by channel incision in the narrowed reach and upstream. In the Waal River, apart from draining riparian habitats in floodplains and undermining hydraulic structures, channel incision also deteriorated the conditions for navigation. First, it turned local non-erodible areas of the river bed into obstacles. Second, the connection between the river and other elements of the inland waterway network, such as canals, ship locks and fluvial port facilities, became problematic. In addition, the fairway is spoiled by the shallow ridges that develop in response to the formation of local scour holes at groyne heads [3]. Finally, the transverse groynes hinder the flow at high discharge and therefore force the water level to increase. All this puts stress on the levees system, especially when we are facing the uncertainty of climate change that might cause the raising of high discharge events more than ever before.

In order to solve these problems, engineers and authorities are considering substituting the old groynes with longitudinal training walls (Figure 1.2). The goal is to obtain an equally-good navigation channel, while improving the river conveyance capacity during floods. In addition, the removal of groynes is expected to increase the river bank natural value (personal communication Rijkswaterstaat).

Figure 1.1: Examples of traditional river training with transverse groynes. Waal River near Druten, The Netherlands. Source: Google Earth © 2017. Red arrow indicates flow direction.

There are unsolved problems related to this new type of intervention. In particular, a longitudinal wall creates a parallel channels system, usually having different widths, with an upstream bifurcation. This is expected to change the river flow distribution and morphology. As river bifurcations are often unstable, the questions arise whether the parallel-channel system would be stable and, in case of instability,

which channel would silt up. The presence of steady bars and point bars inside river bends can be expected to influence this stability. This is because bars located near the upstream start of the wall would influence the sediment distribution between the two channels, particularly if the bar is steady [4–7].

Other issues regard the setup of the system with a longitudinal training wall. Which is the best setting of the wall? Which is the best location for the wall start if steady alternate bars or point bars are present in the original main river channel? What is the most suitable width to be assigned to the parallel channels? Which should be the elevation for the wall crest? Should the wall present openings at some locations?

1.2. Relevance and research scope

Three longitudinal training walls have been built in 2013-2015 in the Waal River, a branch of the Rhine, in the framework of a pilot project for testing this alternative approach to river training in The Netherlands (Figure 1.2.a). The main idea is to provide a narrow and deep navigation channel during low flows, while allowing more water to flow in the secondary channel behind the training wall at higher discharges. This would ideally reduce main channel erosion and lower the water levels during floods. Furthermore, the presence of the secondary channel would improve the ecological conditions of the river. Finally, the fairway would no longer be spoiled by the shallow ridges that develop in response to the formation of local scour holes at groyne heads [3].

Longitudinal training walls have been recently built also in other countries, for instance in Germany, where a longitudinal training wall was built in 1997 in the Rhine River in the reach between Walsum and Stapp (Figure 1.2.b). Longitudinal training walls have been proposed in Tra Khuc River, Vietnam, to stabilize the intakes for irrigation system [7].

Figure 1.2: Examples of river training with longitudinal training wall a) near Wamel in The Netherlands, b) near Walsum-Stapp in Germany. Source: Google Earth © 2017.

1

Although longitudinal walls have been already built or proposed as a promising solution, there is lack of studies related to their long-term effectiveness. Previous studies focus on maintaining a minimum water depth for navigation [8, 9] or on environmental issues (e.g. [10]). Additional investigations are required to assess whether longitudinal training walls are indeed effective in achieving the goals and whether they may also produce some undesirable effects, with particular attention to the morphological developments of the system. If undesirable effects are produced, then the geometrical characteristics of river channels and training walls should be optimized to mitigate the impact and reduce maintenance costs.

Longitudinal training walls appear particularly suitable for the training of low-land rivers used as water ways, like the Rhine in The Netherlands, because a two parallel-channel system system has potentially higher flood conveyance than a single channel crossed by series of groynes. Low-land rivers are characterized by the presence of migrating and steady alternate bars, and point bars inside their bends (Figure 1.3). Bars and point bars are large sediment deposits producing important transverse channel bed slopes and forcing the flow to follow a sinuous path. Steady alternate bars can thus be expected to influence the water and sediment distribution at channel bifurcations. Considering that a training wall creates a system of parallel channels, the bifurcation point being the upper end of the wall, the work focuses on the stability of the parallel-channel system. Sinuous channels present point bars inside their bends and relatively strong secondary currents (spiral flow) due to flow curvature which can influence the sediment distribution between the two bifurcating channels, too.

Figure 1.3: Examples of alternate bars and point bars in a low-land river. Ve River in Quang Ngai, Vietnam. Source: Google Earth © 2017.

The general goal of the study is ***to optimize the setting up of longitudinal training walls taking into account the long term morphological developments of the river system***. Factors that are important to assess the effectiveness of training a river with longitudinal walls are:

1. the morphodynamic stability of the parallel-channel system, which defines the need for regular maintenance;
2. the degree of river navigability;
3. the flood conveyance;
4. the long-term channel incision that can be expected;

The river ecological potential is not addressed here but discussed considering that morphological changes might affect the river ecology.

1.3. Scale of the problem

The river morphology can be described at different spatial scales. Morphological developments range from the development of small ripples, undulating the channel bed, to the evolution of the entire river planform and occur at different temporal scale. Morphological features such as ripples, bars, bends, etc. that characterize the river shape can be classified based on their spatial scale and on the temporal scale of their evolution as showed in Figure 1.4.

This thesis focuses on bars and cross sectional-profiles (cross-sectional scale), considering also issues at the river reach scale, such as longitudinal slope developments. The considered spatial scale is the river cross-section and the entire river reach. The considered temporal scale is ten to hundred years. The effects of features appearing at smaller scales are taken into account by parameterization (for instance the effects of ripples and dunes are parameterized as increased bed roughness). The effects of larger-scale features are considered as boundary conditions (inputs of water and sediment, water levels at the end of the study reach).

1.4. Approach

The method adopted in this study includes both experimental and numerical investigations using the open-source Delft3D code, integrated with a deep literature review. The latter allows assessing the state-of-the-art of the knowledge in the field of river training and morphodynamics and related fields, and is key to critical analysis of the numerical and experimental results. It includes: river training techniques, sediment transport, river morphodynamics, river bifurcations, bars, laboratory experiments techniques, analytical approaches, and two-dimensional (2D) numerical modeling of river hydrodynamics and morphodynamics. The description of the state-of-the-art arising from the literature review is found in the introductions of Chapters 2, 3 and 4.

The experiments are carried out at the Laboratory of Fluid Mechanics of the Delft University of Technology in a 14.4 m long and 0.4 m wide straight flume with a sandy bed presenting steady or slowly migrating alternate bars (Figure 1.5). In the experiments, longitudinal training walls are placed in the flume starting at different locations with respect to a steady bar. Different relative-widths of the parallel channels are considered. Moreover, different bed material with and without recirculation is used. The experimental investigation is reported in Chapter 2.

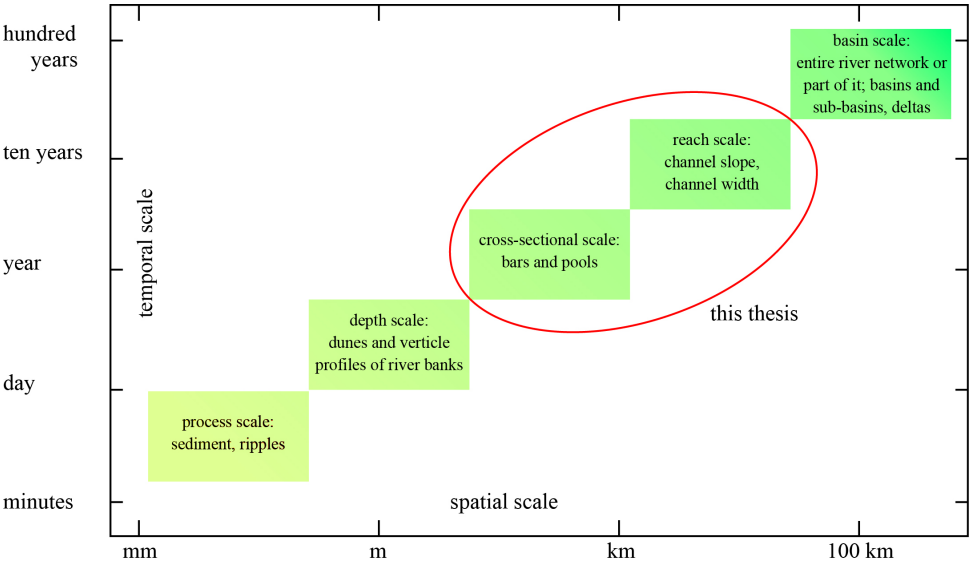

Figure 1.4: Typical spatial and temporal scales of morphological features in rivers. This thesis focuses on bars and cross sectional-profiles, but considers also the adaptation of the longitudinal slope (reach scale).

Figure 1.5: Flume used in this study and its components. a) General view with the formation of alternate bars; b) lasers devices to monitor bed and water level; c) high speed camera to monitor surface velocity.

The numerical simulations are carried out using the Delft3D code after having checked the ability of the code to simulate the processes that are relevant, namely the sediment and flow distribution at bifurcations, the effects of transverse slope and spiral flow on bed load transport direction, the effects of vegetation on the flood plains. The numerical tests allow extending the number of scenarios to be analyzed. In particular, the numerical simulations allow considering a large number of combinations of bifurcation points and steady bars; straight and sinuous channels; constant and variable discharge. The numerical tests include also the assessment of the long-term morphological developments in a channel with two longitudinal training walls. The numerical investigation is presented in Chapter 3.

The study ends with the application of the model on a real river. The selected case is the Waal River in The Netherlands. Considering that the present channel of this river is too narrow to be subdivided in two parallel channels without impeding navigability, the numerical simulations are based on the characteristics of the river before the training works, i.e. in 1800 AD. This exercise aims at studying navigability, high-flow conveyance and river incision. The ecological potential of a river trained with a longitudinal training wall is roughly considered by comparing the morphology of the same river trained with series of transverse groynes. The case study is described in Chapter 4.

All results of the work are discussed in Chapter 5 and then conclusions are drawn and recommendation given in Chapter 6.

References

[1] J. Wijbenga, J. Lambeek, E. Mosselman, R. Nieuwkamer, and R. Passchier, *Toetsing uitgangspunten rivierdijkversterkingen,* in *Deelrapport 2: Maatgevende belastingen, Waterloopkundig Laboratorium and European-American Center for Policy Analysis, Delft, the Netherlands.* (1993) (in Dutch).

[2] J. Wijbenga, J. Lambeek, E. Mosselman, R. Nieuwkamer, and R. Passchier, *River flood protection in the netherlands,* in *Proceedings of International Conference on River Flood Hydraulics. York, England, Eds. W.R. White & J. Watts, Wiley*, Paper 24 (1994) pp. 275–285.

[3] M. F. M. Yossef, *Morphodynamics of rivers with groynes*, Ph.D. thesis, Delft University of Technology (2005).

[4] A. de Heer and E. Mosselman, *Flow structure and bedload distribution at alluvial diversions,* in *River Flow*, Vol. 2004 (2004) pp. 801–806.

[5] M. Redolfi, G. Zolezzi, and M. Tubino, *Free instability of channel bifurcations and morphodynamic influence,* Journal of Fluid Mechanics **799**, 476 (2016), https://doi.org/10.1017/jfm.2016.389.

[6] T. B. Le, A. Crosato, and W. Uijttewaal, *Long-term morphological developments of river channels separated by a longitudinal training wall,* Advances in Water Resources **113**, 73 (2018), https://doi.org/10.1016/j.advwatres.2018.01.007.

[7] T. B. Le, A. Crosato, E. Mosselman, and W. Uijttewaal, *On the stability of river bifurcations created by longitudinal training walls. numerical investigation,* Advances in Water Resources **113**, 112 (2018), https://doi.org/10.1016/j.advwatres.2018.01.012.

[8] P. Paalvast, *Ecologische waarde van langsdammen.*, Tech. Rep. (Report PW-CG.95020, RIZA, Lelystad, p. 120., 1995) (In Dutch).

[9] M. Brabender, M. Weitere, C. Anlanger, and M. Brauns, *Secondary production and richness of native and non-native macroinvertebrates are driven by human-altered shoreline morphology in a large river,* Hydrobiologia **776**, 51 (2016).

[10] F. Collas, A. Buijse, L. van den Heuvel, N. van Kessel, M. Schoor, H. Eerden, and R. Leuven, *Longitudinal training dams mitigate effects of shipping on environmental conditions and fish density in the littoral zones of the river Rhine,* Science of The Total Environment **619-620**, 1183 (2017), https://doi.org/10.1016/j.scitotenv.2017.10.299.

2

Experimental investigation

Long-term morphological developments of river channels separated by a longitudinal training wall

Rivers have been trained for centuries by channel narrowing and straightening. This caused important damages to their ecosystems, particularly around the bank areas. We analyse here the possibility to train rivers in a new way by subdividing their channel in main and ecological channel with a longitudinal training wall. The effectiveness of longitudinal training walls in achieving this goal and their long-term effects on the river morphology have not been thoroughly investigated yet. In particular, studies that assess the stability of the two parallel channels separated by the training wall are still lacking. This work studies the long-term morphological developments of river channels subdivided by a longitudinal training wall in the presence of steady alternate bars. This type of bars, common in alluvial rivers, alters the flow field and the sediment transport direction and might affect the stability of the bifurcating system. The work comprises both laboratory experiments and numerical simulations (Delft3D). The results show that a system of parallel channels divided by a longitudinal training wall has the tendency to become unstable. An important factor is found to be the location of the upstream termination of the longitudinal wall with respect to a neighboring steady bar. The relative widths of the two parallel channels separated by the wall and variable discharge do not substantially change the final evolution of the system.

This chapter is published in **Advances in Water Resources (2018)** [1].

2

2.1. Introduction

Many low-land rivers are used for inland navigation, as for instance the Waal [2], the Elbe [3], the Thames [4], the Mississippi [5]. Important plans to improve inland navigation regard the White Nile and Nile Rivers in Sudan [6] as well as the Me Kong River in Vietnam [7], among others. These rivers still present long reaches with natural banks and new interventions should be planned in a way to preserve their most important ecological aspects. For this reason, it is important to study new training techniques that allow for the co-existence of navigation with natural banks, without affecting flood water levels.

The creation of a navigation route often includes channel narrowing. This results in a deeper river channel and reduces bar formation [8], which is good for navigation. Rivers are narrowed by constructing series of groynes along both sides of the river, as in the Rhine [9] and Rhone Rivers [10], or by bank protection works, especially in urban areas. As a result, bed degradation occurs in the narrowed reach and upstream. In the narrowed reach, the water depth increases; upstream, the water depth tends to remain the same as before the intervention, but both bed and water levels decrease, as shown by Jansen *et al.* [11]. Bed degradation is amplified by river shortening, another frequent intervention aiming at navigation improvement (e.g. [12]). Moreover, maintaining the navigation channel during low-flow conditions, when bars and other sediment deposits obstruct the navigation route often requires dredging, which is in some cases accompanied by dumping of dredged sediment in deep areas [13–15]. Without dumping, sediment extraction results in important incision processes along the entire river course, strengthening the effects of the other interventions aimed at navigation route improvement, such as channel narrowing and shortening (e.g. [2, 16]). Bed and water level degradation affect intakes and the foundations of structures along the river, including the groynes, and lower groundwater levels, with consequences for floodplain vegetation and agriculture in the area adjacent to the river. Excessive bed degradation can even cause problems to navigation if rock outcrops appear, as along the Rhine River between Cologne and Rees [17].

Another problem related to traditional river training is that banks protected by groynes or by revetments lose their natural value. This can be observed in many trained rivers, for which the restoration of the riverine environment has become a priority (e.g. [18]). However, at the same time, the restored river should have similar or even increased high-flow conveyance (e.g. [19]) to reduce the probability of floods along its course. All these issues show the need to define new, more sustainable, river management strategies [20].

In this chapter, we study the possibility of obtaining a stable navigation channel minimizing river ecosystem degradation, without affecting flood water levels. The idea is to create two parallel channels, one for navigation and one for ecology, which may have the same width or different widths, by means of a longitudinal wall. The system of parallel channels separated by a longitudinal wall starts with an upstream bifurcation. Previous work has shown that the stability of bifurcating channels depends on the distribution of flow and sediment at the bifurcation point [21]: if one branch receives more sediment than the flow can transport, it gradually

silts up; instead, if it receives less sediment than its transport capacity its bed is eroded. In the latter case, with the progression of bed erosion the branch receives increasing amounts of water, which intensifies the erosion process [22] and at the same time increases deposition in the other branch. Unbalanced sediment inputs therefore lead to the instability of the system.

This work focuses on the long-term stability of the two channels separated by a longitudinal wall in rivers with steady or slowly migrating alternate bars. These bars are common features in alluvial rivers (Figure 2.1). Steady bars in the river channel close to the bifurcation point permanently alter both the water flow pattern and the sediment transport direction. Therefore, bars are expected to affect the sediment distribution between the two channels, with possible consequences for their stability [23, 24].

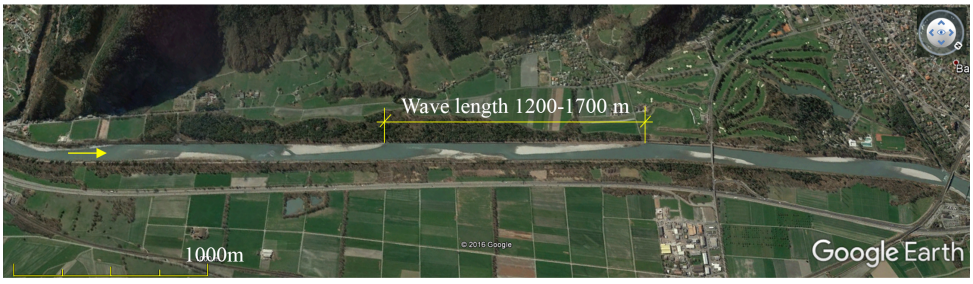

Figure 2.1: Bars migrate slowly and after 26 year they are more or less at the same location in the Alpine Rhine River between Landquart and Bad Ragaz, Switzerland [25](Google Earth © 2016).

The work includes laboratory and numerical investigations. The laboratory investigation analyses the morphological evolution of a straight channel with steady alternate bars divided by a longitudinal wall. Different width ratios and locations of the starting point of the structure with respect to one bar are considered, with the aim to define the conditions for obtaining a stable system. The numerical investigation, carried out using the open-source Delft3D code, analyses the applicability of the technology to real river cases. First, the most significant flume test is upscaled and simulated to establish whether the numerical model is able to reproduce the processes observed in the laboratory, but this time considering a similar system having a real river size. Then, the code is applied to the Alpine Rhine River [25], a natural system that is rather similar to the upscaled one and presents regular alternate bars with low migration rates. This part of the study focuses on the effects of variable discharge on the stability of the two-channel system, on bar formation inside the bifurcating channels and on flow conveyance. The work does not include any constructive issues (presence of openings, wall top level, etc.) that may influence the channel morphological changes and therefore the stability of the system.

2.2. River bars and bifurcations

River bars are large sediment deposits that become visible during low flows surrounded by deep areas (pools). Bars can be classified in three main categories: forced, free and hybrid [8]). Forced bars are local deposits that form due to persistent flow pattern imposed by the channel geometry or by external factors (forcing). A typical example of forced bars are the point bars inside river bends. Free bars are large bed undulations that form due an instability phenomenon of alluvial river beds [26–28] having a wavelength that compares with the channel width and amplitude that compares with the water depth. Their number in the river cross-section is represented by the "mode", m [29]. This is the integer of the ratio between the transverse half-wavelength of the bars that form in the channel and the channel width: $m = 1$ corresponds to a series of bars that alternately form near one side and then the other (alternate bars), typical of meandering rivers; $m = 2$ to central bars; and $m > 2$ to multiple bars. Modes larger than two correspond to a multiple-thread channel with more than one bar in the cross-section, typical of braided rivers [30–32]. Free bars normally migrate either in upstream or downstream direction [33]. The mode and the other bar characteristics, such as wave length, amplitude, migration celerity and growth rate depend on flow width-to-depth ratio, Shield number and other morphodynamic parameters (e.g. [34]). In particular, bars form only if the width-to-depth ratio exceeds a critical value and this critical value is larger for larger bar modes [29]. Hybrid bars are non-migrating bars similar to free bars. Their existence is due to the interaction of forcing and morphodynamic instability. Persistent geometric discontinuities of the channel (asymmetric narrowing, widening, and structures), which are rather common in rivers, act as forcing: they fix the location of the bars and impose to them zero celerity and a corresponding wavelength. The wavelength of hybrid alternate bars is generally 2-3 times longer than the wavelength of alternate free bars.

The effects of free migrating bars on bifurcations were studied by Bertoldi *et al.* [35]. Migrating bars arrive at the bifurcation alternatively on one side and then the other. They feed the downstream branches alternatively with a larger and then smaller amount of water and sediment. As a result, the bifurcation oscillates around an equilibrium or disappears due to closure of one of the branches.

Steady bars permanently affect the sediment transport distribution between the two branches of a bifurcation [24]. This is due to the combination of flow deformation and gravity. Due to the presence of bars, the flow follows a weakly meandering pattern and concentrates in the pools. For this, the branch closest to the pool receives most discharge and most sediment. Gravity alters the direction of bed material moving on bar slopes deviating sediment towards the pool [36]. Finally, bars impose a certain curvature to the stream lines, producing a (weak) spiral flow that deflects the sediment moving near the bed, this time towards the bar tops [37]. The effects of bars on bifurcation stability depends on the interaction between these phenomena.

Considering that water depth, channel width and other variables depend on flow characteristics, it can be expected that bars change shape and migration celerity due to discharge variations. This was investigated by Tubino [38] on free bars, but

works studying the effects of varying discharge on the characteristics of hybrid and forced bars are lacking. It is likely that also this type of bars changes geometry as a result of flow alterations, although to a lesser extent than free bars, because the effects of discharge are mitigated by the presence of the forcing. However, also the effect of geometrical discontinuities depends on discharge. This means that we can expect point bar and hybrid bar elongation or shortening due to the increase or decrease of flow discharge. This might mean that bars may affect the distribution of sediment and water between bifurcating channels in a different way depending on discharge and thus the hydrograph.

The morphological evolution of each branch of a bifurcation includes gradual changes of mode and other bar characteristics, as a direct consequence of bed elevation and water depth changes. We can generally expect bed degradation to contribute to gradual bar suppression (decreasing width-to-depth ratio) and bed aggradation to the opposite.

2.3. Methodology

The method adopted in this study includes both experimental and numerical investigations. The experiments were carried out at the Laboratory of Fluid Mechanics of Delft University of Technology in a 14.4 m long and 0.4 m wide straight flume with a sandy bed presenting steady or slowly migrating alternate bars. The longitudinal training wall was reproduced by a thin longitudinal plate which subdivided the original channel in two parallel channels, the bifurcation point being the location of the upstream termination of this plate. Considering that the water and sediment distribution between the parallel channels may depend on the location of the bifurcation with respect to a neighbouring steady bar, for every experiment two different locations were tested: one at the upstream part of a bar and the other one at the downstream part, in the pool area. Different subdivisions were studied to assess the role of relative channel width on the developments (timing and system stability): $B_e : B_n$ = 1:5, 1:3 and 1:1, being B_e and B_n the widths of the two branches of the bifurcation, here named the "ecological" and the "navigation" channel, respectively. The last one corresponds to a subdivision in two parallel channels having the same width. Additionally, extra tests were carried out using different sands to compare to the response of systems with different degrees of sediment suspension, also considering that the effects of transverse bed slope on sediment transport are relatively less important for small sediment sizes than for larger sediment sizes [39].

The formula by Crosato and Mosselman [32] was used for the preliminary selection of the morphodynamic characteristics of the laboratory stream. The formula allows deriving the mode m of hybrid bars that form in the channel. The formation of hybrid alternate bars is expected if the chosen combination of parameters results in m = 1:

$$m^2 = 0,17g\frac{(b-3)}{\sqrt{\Delta D_{50}}}\frac{B^3 i}{CQ} \tag{2.1}$$

where m is the bar mode, g is the gravity acceleration, b is the degree of non-linearity of the sediment transport formula as a function of flow velocity, B is the channel width, i is the longitudinal bed slope, Δ is the relative submerged sediment density, D_{50} is the median sediment size, C is the Chézy coefficient and Q is the discharge.

To allow observing the alternate bars in the 14 m long flume, the bar wavelength should not be too long. Ideally, 2-3 bars should be present in the channel. To check this, the theoretical hybrid bar wavelength was computed using the following equation [37]:

$$\frac{2\pi}{L_p} = \frac{1}{2\lambda_W}\left[(b+1)\frac{\lambda_W}{\lambda_S} - \left(\frac{\lambda_W}{\lambda_S}\right)^2 - \frac{(b-3)^2}{4}\right]^{1/2} \tag{2.2}$$

where L_p is the hybrid bar wavelength, λ_W is the 2D flow adaptation length, λ_S is the 2D water depth adaptation length.

$$\lambda_W = \frac{h_0}{2C_f} \tag{2.3}$$

$$\lambda_S = \frac{1}{(m\pi)^2} h_0 \left(\frac{B}{h_0}\right)^2 f(\theta_0) \tag{2.4}$$

in which h_0 is the normal depth, C_f is the friction factor defined by $C_f = \frac{g}{C^2}$, $f(\theta_0)$ accounts for the effect of gravity on the direction of sediment transport over transverse bed slopes. It is calculated as [36]

$$f(\theta_0) = \frac{0.85}{E}\sqrt{\theta_0} \tag{2.5}$$

where E is a calibration coefficient and θ_0 is the Shields parameter.

The ratio $\alpha = \lambda_S/\lambda_W$ is called "interaction parameter" and is a characteristic of the 2D response of an alluvial channel [37].

Equation. 2.2 was derived from a linear model and for this the value of L_p provides only a rough estimate of the wavelength of the bars in the final stages of their development. Nevertheless, the formula has been observed to function rather well on experimental settings [40]. Equation. 2.2 was applied in this study to check the experimental settings with the aim to obtain 2 to 3 bars in the flume.

Bars are expected to alter the subdivision of sediment between the parallel channels in a different way, depending on sediment transport mechanism and on transverse bed slope alteration of sediment transport direction. Considering that both mechanisms depend on sediment size, the laboratory investigation includes four extra tests with two different sands (sensitivity analysis).

The numerical simulations consisted of two investigations: the first one was meant to assess the capability of the numerical model to reproduce the morphological processes observed in the laboratory; the other one was an application of the model to a real river case. The first model application simulated the morphological evolution observed in the base-case laboratory scenario and consisted of two

runs. This was done on an upscaled numerical version of the experiments having the same longitudinal bed slope, Shields parameter, width-to-depth ratio, bar mode and 2D interaction parameter [41]. The two runs differ on the location of the bifurcation point with respect to a steady bar. The second model application was meant to simulate the hypothetical implementation of a longitudinal training wall on a real river presenting some similarity with the upscaled case. This river is the Alpine Rhine River [25]. The analysis focused on the effects of variable discharge, analysing the development of bars in the two bifurcating channels. Special attention was paid on high-flow conveyance of the bifurcating system with respect to the original channel. In both models, the longitudinal training wall was schematized as a thin longitudinal dam, assumed infinitely high, thus always separating the flow, even with the highest discharges.

Table 2.1 lists the morphodynamic characteristics of the systems reproduced in the laboratory and with the numerical model.

Table 2.1: Characteristics of laboratory experiments and numerical simulations in this study.

Parameters	Notation	Unit	Experiments*			Upscaled models	Alpine Rhine models**
			B, W1, W2	S1	S2		
Bar formative discharge	$Q_{50\%}$	m^3/s	$4.5*10^{-3}$	$4*10^{-3}$	$5*10^{-3}$	220	1845
River width	B	m	0.4	0.4	0.4	30	85
Normal depth	h_0	m	0.044	0.044	0.043	3.343	4.665
Average velocity	v	m/s	0.25	0.23	0.29	2.19	4.65
Longitudinal bed slope	i	-	0.0025	0.0027	0.0026	0.0025	0.0029
Chézy coefficient	C	$m^{1/2}/s$	24	21	27.5	24	40
Froude number	Fr	-	0.383	0.348	0.448	0.383	0.688
Shields parameter	θ_0	-	0.135	0.194	0.068	0.135	0.137
Median sediment size	D_{50}	m	$0.5*10^{-3}$	$0.37*10^{-3}$	$1.0*10^{-3}$	$37*10^{-3}$	$60*10^{-3}$
Relative density of sediment	Δ	-	1.65	1.65	1.65	1.65	1.65
Observed bar mode	mo	-					1
Observed bar length	L	m					1200-1700
Transport law			Meyer-Peter and Müller [42]				
Width-to-depth ratio	B/h	-	9	9	9	9	18
Bar mode according to Eq. 2.1	m	-	|0.78|	|0.99|	|0.59|	|0.78|	|0.95|
Theoretical hybrid bar wavelength	L_p	m	3.2	2.6	8	239	980
2D flow adaptation length	λ_W	m	1.31	0.98	1.66	98	380
2D water depth adaptation length	λ_S	m	0.23	0.28	0.17	17	98
2D interaction parameter	λ_S/λ_W	-	0.17	0.28	0.1	0.17	0.26

* Experiment scenarios B, W1, W2, S1 and S2 are explained in Table 2.3.

** Adami *et al.* [25], upstream reach from km 0.00 to km 12.27.

2.4. Laboratory investigation

2.4.1. Experimental set up

Following the method of Struiksma and Crosato [40], who imposed an upstream asymmetric flow restriction, the formation of hybrid bars was obtained by placing

a curved plate 2.5 m downstream of the inlet, obstructing 2/3 of the channel width (Figure 2.2). The training wall consisted of a longitudinal steel plate, placed at a certain distance from the glass side wall, separating two parallel channels. The length of the steel plate was equal to the theoretical longitudinal wave-length of the bars (Table 2.1). Two starting locations of the training wall with respect to the first steady bar were considered: one at the upstream part of the bar and the other one at the next pool. The two locations were selected after having obtained an equilibrium bed configuration presenting clear fully-formed hybrid alternate bars. Figure 2.2 shows the configuration corresponding to $B_e : B_n$ = 1:3 when the ecological channel is 10 cm wide and the navigation channel 30 cm.

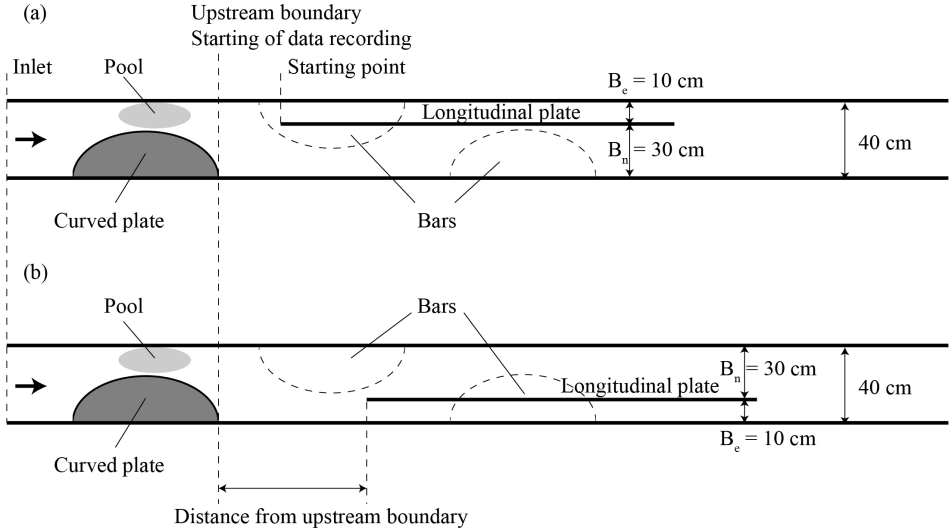

Figure 2.2: Flume schematization (not to scale) with curved plate and longitudinal training wall represented by a longitudinal steel plate for $B_e : B_n$ = 1:3 (base-case scenario). (a) Longitudinal plate starts at the upstream part of the first steady bar. (b) Longitudinal plate starts at the next pool.

Both water and sediment were recirculated. The sediment characteristics are summarized in Table 2.2. The use of sands with different grain sizes allowed studying cases differing in sediment transport mechanism (degree of suspension) and transverse bed slope alteration of sediment transport direction. The latter was expected to be smaller for sediment having smaller size (S1) and larger for larger sediment sizes (S2). The experimental tests S1 and S2 (sensitivity analysis) were carried out using the same width ratio as the base-case scenario (Table 2.3), $B_e : B_n$ = 1:3. For these tests, the upstream asymmetric flow restriction leading to the formation of hybrid alternate bars was obtained by placing a small transverse steel plate instead of a curved plate. The total number of performed laboratory tests is 13, see Table 2.3.

Table 2.2: Sediment characteristics used in the sensitivity analysis.

Characteristic diameter	Base-case (mm)	S1 (mm)	S2 (mm)
D_{15}	0.43	0.25	0.30
D_{50}	0.50	0.37	1.00
D_{65}	0.56	0.44	1.26
D_{90}	0.70	0.65	1.48

Table 2.3: Experimental tests carried out in this study.

N^{o}	Scenarios	Notation in graph	Location with respect to a bar	Width ratio	Upstream constriction
1	Base case	B	Reference case	No training wall	Curve plate
2			Upstream	$B_e : B_n$=1:3	
3			Pool		
4	Width 1	W1	Upstream	$B_e : B_n$=1:5	
5			Pool		
6	Width 2	W1	Upstream	$B_e : B_n$=1:1	
7			Pool		
8	Sensitivity 1	S1	Reference case	No training wall	Transverse plate
9			Upstream	$B_e : B_n$=1:3	
10			Pool		
11	Sensitivity 2	S2	Reference case	No training wall	Transverse plate
12			Upstream	$B_e : B_n$=1:3	
13			Pool		

2.4.2. Data collection and data processing

Bed level and water level were recorded by 5 laser devices three times a day. Since lasers can penetrate water, the measurements were carried out during the experiment without drying up the channel. One laser device measured the water level and the other ones measured the bed level at four locations in transverse direction.

Due to the presence of relatively large dunes and ripples, the rough bed level data were filtered to clean out the bar signal. The filter used is based on the Matlab software ProcessV3 and optimized for bed forms having wavelengths larger than 1 m. The filtering procedure reduced the bar amplitude but allowed recognizing the bar geometry (pool, bar top, upstream and downstream parts of a bar). Bed level data were used to derive the temporal evolution of the averaged difference in bed level between the two parallel channels:

$$\Delta Z = Z_e - Z_n \tag{2.6}$$

in which Z_e and Z_n are the bed level in the ecological and the navigation channels, respectively, averaged over the entire length of the training wall.

The velocity field was measured using a Particle Tracking Velocimetry (PTV).

2.4.3. Results of the base-case scenario

All the tests of the base-case scenario started with the same bed topography (reference bed topography), presenting clear alternate bars, which was obtained after 10 days of morphological developments (Figures 2.3 and 2.4.a). The flow characteristics after 10 days are summarized in Table 2.1 and the characteristics of the sediment used are given in Table 2.2 (base-case scenario). The first two bars were steady with a wave length of about 3.2 m, while the remaining bars were shorter and migrating. The two bifurcation points were located 0.8 m and 1.8 m from the upstream boundary, respectively. In the first case the longitudinal steel plate started in the upstream part of the first steady bar. In the second case the longitudinal plate started in the pool. In both cases the "ecological channel" had a width of 10 cm and the "navigation channel" of 30 cm (Figure 2.2).

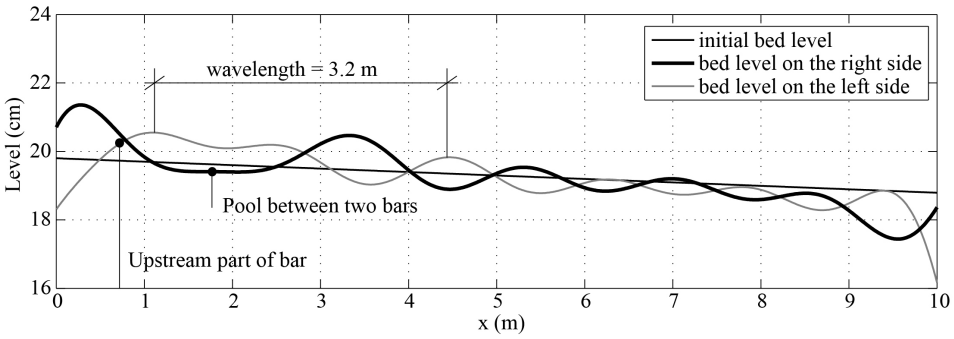

Figure 2.3: Longitudinal bed level profiles showing hybrid alternate bars in the first 4 m after 10 days in the reference layout of the base-case scenario: filtered data.

The final configuration of the channel system at the end of the investigations is shown in Figure 2.4. The temporal evolution of (averaged) bed topography (Figure 2.5) shows progressive aggradation of the ecological channel and progressive degradation of the navigation channel if the longitudinal plate started in the upstream part of the bar (red line). After 10 days, the difference in averaged bed elevation between the two channels was ΔZ = 1.44 cm, and this difference arose mainly due to sediment deposition in the ecological channel. The flow velocity in the ecological channel became gradually smaller than in the navigation channel. Figure 2.6.a shows the transverse velocity field after 10 days, at the end of this experimental test.

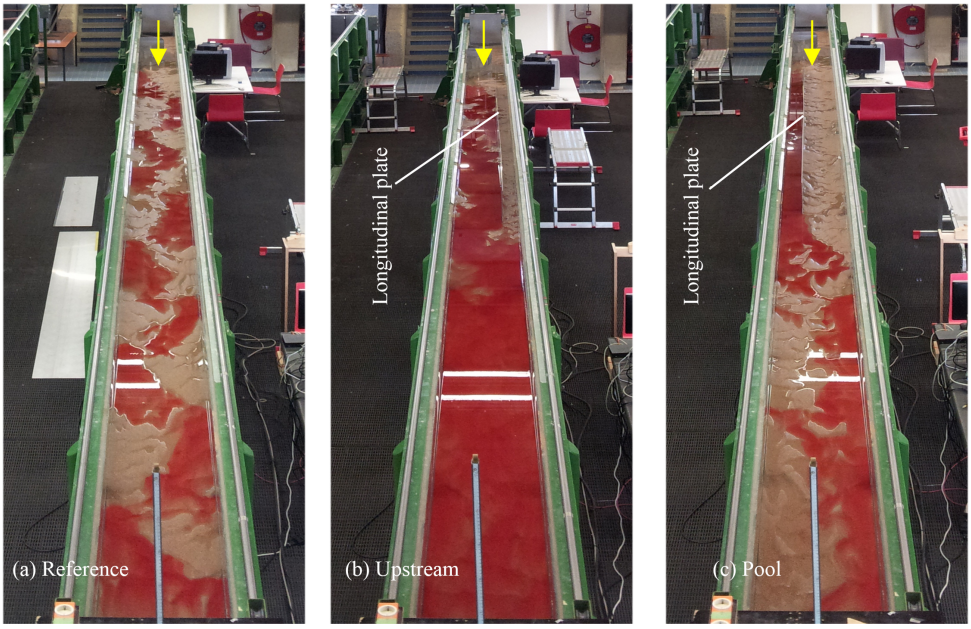

Figure 2.4: Bed configuration of the base-case scenario at the end of the experiment after draining most of the water. (a) Hybrid and free alternate bars in the reference run without longitudinal plate. (b) Longitudinal plate starting in the upstream part of a steady bar: bed aggradation in the ecological channel and navigation channel deepening. (c) Longitudinal plate starting in a pool between two bars: bed aggradation in the navigation channel and ecological channel deepening. The yellow arrow indicates the flow direction. The blue line at the end of the flume is a ruler. The white crossing lines are the reflection of the neon light at the celling.

The ecological channel became increasingly deeper and the navigation channel shallower if the longitudinal plate started in the pool (Figure 2.5, blue line). After 10 days, the difference in averaged bed elevation between the two channels was ΔZ = -2.6 cm, which was mainly due to ecological channel bed erosion. The flow velocity in the ecological channel became progressively higher than in the navigation channel. Figure 2.6.b shows the transverse velocity field after 10 days, at the end of this experimental test.

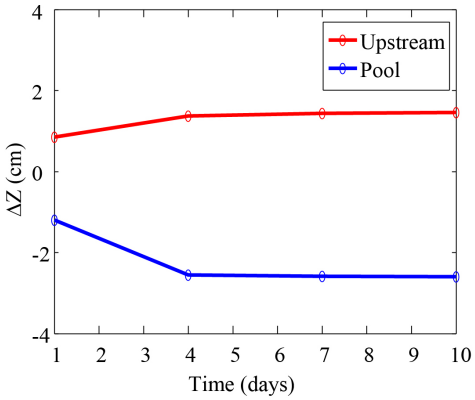

Figure 2.5: Temporal evolution of the difference in bed elevation between the two parallel channels in the base-case scenario. "Upstream" refers to the case in which the longitudinal plate started in the upstream part of the first steady bar (red line). "Pool" refers to the case in which the plate started in the pool (blue line).

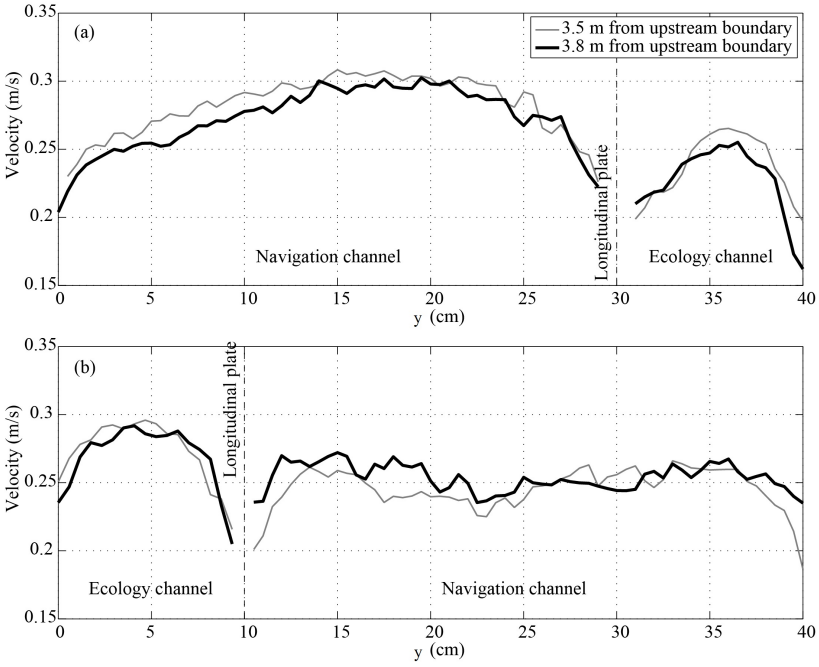

Figure 2.6: Transverse velocity field in the base-case scenario after 10 days. (a) Longitudinal plate starting in the upstream part of the bar. (b) Longitudinal plate starting in the pool.

2.4.4. Results of relative width variation

Changing the width of the parallel channels did not change the trends observed in the base-case scenario. If the longitudinal plate started in the upstream part of the bar the ecological channel silted up and the navigation channel became deeper. The opposite occurred if the longitudinal plate started in the pool. This means that the starting point of the longitudinal plate with respect to a steady bar influences the morphological process of the system more than the width distribution between the two channels. The latter was found to mainly influence the intensity and the speed of the process: the smaller the width ratio was, the faster the morphological evolution was. Figure 2.7 shows the temporal evolution of the difference in bed elevation between the two channels for all cases. After 10 days, if the longitudinal plate started in the upstream part of the bar, the difference in bed elevation, ΔZ, was 2 cm for $B_e : B_n$ = 1:5 (case W1); 1.46 cm for $B_e : B_n$ = 1:3 (base case B) and 0.93 cm for $B_e : B_n$ = 1:1 (case W2). On the contrary, when the longitudinal plate started in the pool, the results were -3.13 cm, -2.6 cm and -2.02 cm, respectively. These results suggest that the largest width ratio (channels having the same width), leading to the smallest difference in bed elevation between the two channels, may offer the best configuration in term of long-term morphology.

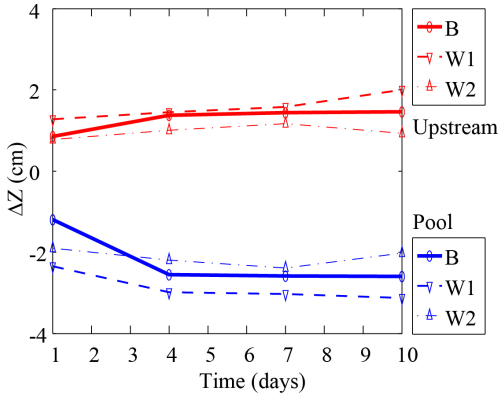

Figure 2.7: Temporal evolution of the difference in bed elevation between the two parallel channels. "Upstream" refers to the case in which the longitudinal plate started in the upstream part of the first steady bar (red lines). "Pool" refers to the case in which the plate started in the pool (blue lines). The speed of the process is represented by the steepness of the curve.

2.4.5. Sensitivity analysis

The sensitivity analysis was meant to qualitatively study the effects of varying sediment on the morphological trends of the system. This was done based on the initial trends, without reaching morphodynamic equilibrium. For this, the duration of the sensitivity-analysis tests was shorter: 3 days for each run. The longitudinal plate was placed 10 cm from the right side of the flume ($B_e : B_n$ = 1:3). Each run started with a flat bed. The forcing offered by a small transverse plate assured

that the hybrid bars always formed at the same location [8]. The starting points of the longitudinal plate were selected at the end of the reference scenario. The characteristics of the physical parameters are listed in Table 2.1. The characteristics of the sediment are listed in Table 2.2: S1 corresponds to the finer sand and S2 to the coarser one.

Results with finer sediment: test S1

In the reference scenario without longitudinal plate, hybrid alternate bars with a wavelength of 2.5 m and amplitude of 1 cm became well recognizable after 3 days (Figure 2.8). In the subsequent tests, the longitudinal plate started either in the upstream part of the second bar or in the pool between the second and the third bar, 3.8 m and 5.0 m from the upstream boundary, respectively.

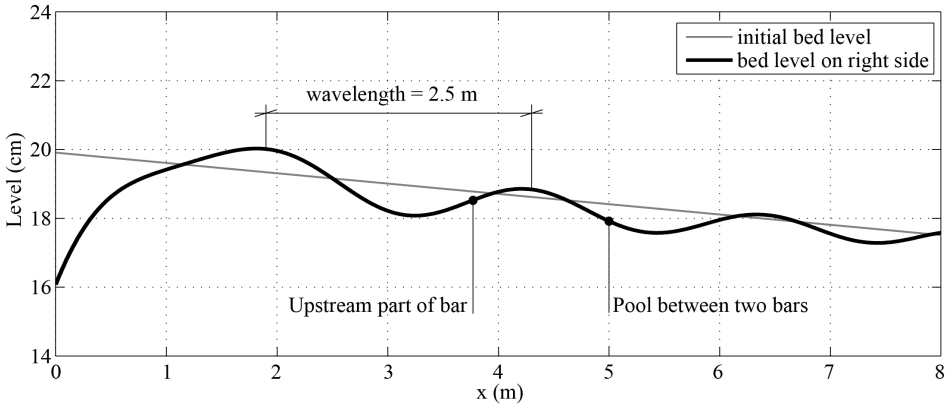

Figure 2.8: Longitudinal bed level profile showing hybrid alternate bars after 72 hours with finer sediment (test S1): filtered data.

Figure 2.9 shows the evolution of the difference in averaged bed elevation between the two channels (case S1 is represented by continuous lines).

When the longitudinal plate started in the pool, the ecological channel became progressively deeper than the main channel and the flow velocity in the ecological channel gradually became larger than in the navigation channel, confirming the results of the base case.

The ecological channel became slightly deeper and slightly conveyed more discharge also in the other test with the longitudinal plate starting in the upstream part of the bar. However, the results in this case might not be correct due to some discharge oscillations which were recognized only afterwards, when the experiment was finished already. In any case this result requires further checks.

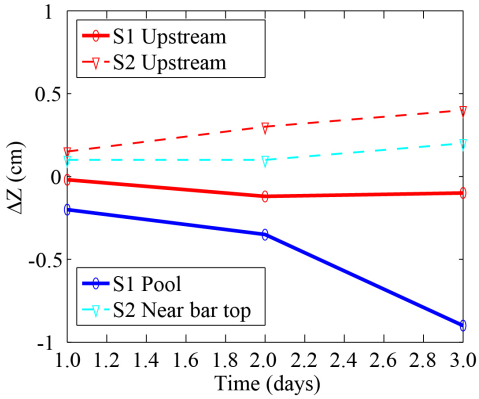

Figure 2.9: Temporal evolutions of the difference in bed elevation between the two parallel channels (sensitivity analysis). Continuous lines refer to sediment S1 and dash lines to sediment S2. Red lines refer to the cases in which the longitudinal plate started in the upstream part of the bar. The blue line represents the case in which the longitudinal plate started in the pool and the light blue line near the bar top.

Results with coarser sediment: test S2

In the reference scenario without a longitudinal wall, hybrid alternate bars with a wave length of 8 m were fully formed after 3 days. The long wavelength made the experiment particularly difficult, because the bars had also a rather small amplitude and this made it impossible to select a clear pool location. For the case of the plate starting in the upstream part of a bar, the starting point was placed at a distance of 4.4 m from the upstream boundary. Another starting location was investigated, this time close to the first bar top, at a distance of 6.7 m from the upstream boundary (Figure 2.10).

The results are shown in Figure 2.9 (dotted lines). When the training wall started in the upstream part of a bar, the ecological channel bed became gradually higher than the navigation channel bed. At the end of Day 3, the difference was 0.4 cm, mainly due to sediment deposition in the ecological channel. At the same time the flow velocity in the ecological channel became smaller than in the navigation channel. Although the duration of this test was only 72 hours (3 days), this result shows a clear trend of deposition in the ecological channel, confirming the results of the base case.

For the training wall starting near the bar top, the ecological channel slightly aggraded, whereas the flow velocity in the two channels remained almost the same. This could be a sign of ongoing aggradation or of a balance and should be further investigated.

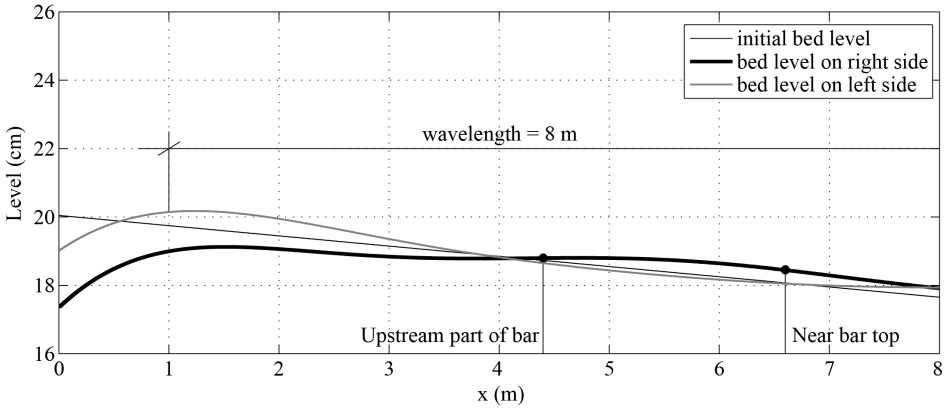

Figure 2.10: Longitudinal bed level profiles showing hybrid alternate bars after 72 hours with coarser sediment (test S2): filtered data.

2.5. Numerical investigation

2.5.1. Model description

This study constructed two two-dimensional (2D) depth-averaged morphodynamic models using the Delft3D software. One model represented an upscaled version of the experimental flume and the other one a real river case. Delft3D has a finite difference scheme to solve the three-dimensional Reynolds equations for incompressible fluid under shallow water approximation and includes a morphodynamic module to account for sediment transport and bed level changes [43]. The two models were based on the depth-averaged version of the basic equations, which was demonstrated to be sufficient to reproduce bars with sufficient accuracy (e.g. [8, 44–46]). The influence of the spiral flow in curved reaches was accounted for according to the formulation of Struiksma *et al.* [37]. The roughness was represented by a constant Chézy coefficient (values in Table 2.1) and the bed-load transport rate was computed by means of the Meyer-Peter and Müller [42] (MPM) formula, valid for sand and gravel-bed rivers. The effects of transverse bed slope on sediment transport direction were taken into account according to Bagnold [47] formulation (default in Delft3D). Not considering these effects would result in an un-realistic unstable model [48].

The hydrodynamic boundary conditions of the models consisted of downstream water level and upstream discharge. In the upscaled model, these boundary conditions were constant values, whereas in the Alpine Rhine model they were variable, according to the discharge variations. The boundary conditions for the sediment component were defined by upstream balanced sediment transport, which prevented the bed level from changing at the boundary, and downstream free sediment transport condition, which may result in bed level changes. The lateral banks were fixed and treated as free-slip fixed boundaries.

The time step of the flow was 0.1 minutes to ensure numerical stability as evaluated by the Courant criterion for fluid advection. To fully reproduce the interaction between flow and sediment, the computations were carried out without any morphological acceleration. The longitudinal training wall was schematized as a thin, infinitely high and deep, dam. This ensured that the structure always divides the two channels. The length of the wall was equal to the bar wave length and obtained after completion of a reference run. A transverse groyne obstructing 2/3 of the width was placed at the right side wall at a certain distance from the upstream boundary to trigger hybrid bars. Table 2.4 shows the exact distance and the numerical parameters in both models.

Table 2.4: Values of variables and parameters used in the numerical simulations studying an upscaled version of the laboratory experiments.

Parameters	Notation	Unit	Upscale	Alpine Rhine
Length of computational domain	L	m	2250	4250
Rectangular grid size	M×N	m	2.5×7.5	7.08×21.25
Time step	t	minutes	0.1	0.1
Simulation time	T	days	10	3×365
Location of forcing (transverse groyne)	-	m	375	510
Morphological factor	MF	-	1	1
Transport law			Meyer-Peter and Müller [42]	

2.5.2. Upscaled-experiment model setup

This numerical simulation aimed at establishing whether a 2D morphodynamic model constructed using the Delft3D software provides reliable results when studying the effects of subdividing a straight river channel with alternate bars with a longitudinal training wall.

The hydraulic and morphology parameters in the upscaled version of the laboratory tests are presented in Table 2.1. The numerical parameters are summarized in Table 2.4.

The reference case, without longitudinal wall, started with a flat bed. A transverse groyne, located 375 m from the upstream inlet on the right side was used to assure the formation of the hybrid bars as in Duró *et al.* [8], reproducing the effects of the curved plate placed in the flume. The results obtained after 10 days of morphological development are shown in Figure 2.11. In this figure, the results are plotted from the transverse groyne to the end of the reach. The shape of the alternate bars qualitatively resembles the one obtained in the laboratory for the reference case (Figure 2.3), with a long steady bar opposite to the groyne and smaller migrating bars more downstream. This means that the similarity based on longitudinal slope, Shield parameter, width-to-depth ratio, bar mode, interaction parameter (Table 2.1), does not result in quantitative geometric similarity, but only in qualitative geometric similarity.

In the same way as in the experiment, two locations for the starting point of the longitudinal wall were considered: one in the upstream part of the first steady

bar and one in the pool opposite to it (Figure 11). For each location, three different width ratios were considered: $B_e : B_n$ = 1:5, 1:3 and 1:1. All upscaled-experiment scenarios (Table 2.5) started from the bed topography shown in Figure 2.11. The computations simulated a period of 10 days.

Table 2.5: Overview of the upscaled-experiment simulations.

Nº	Scenarios	Notation in graph	Location with respect to a bar	Width ratio	Initial bed level	Description
1	Base case	B	Reference case	No training wall	Flat bed	B runs study the effects of starting location of the training wall
2			Upstream	$B_e : B_n$=1:3	Hybrid bars	
3			Pool			
4	Width 1	W1	Upstream	$B_e : B_n$=1:5		W runs study the effects of width ratio
5			Pool			
6	Width 2	W1	Upstream	$B_e : B_n$=1:1		
7			Pool			

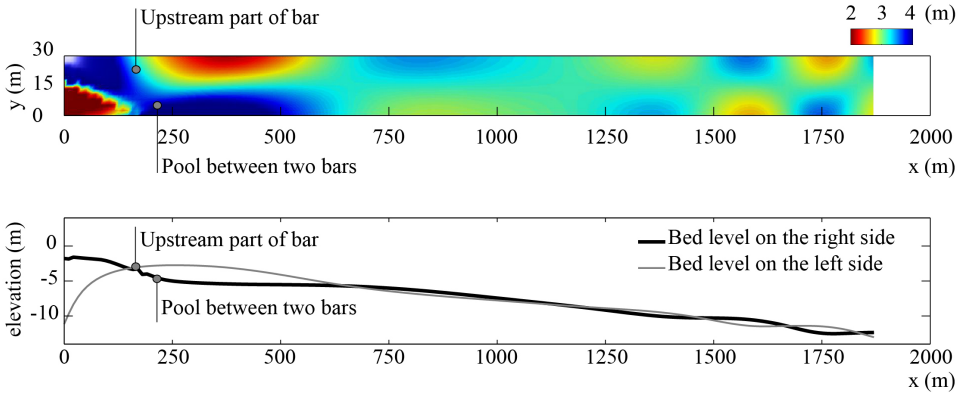

Figure 2.11: Water depth distribution showing alternate bars in the reference case of the upscaled model and locations of the starting points of the longitudinal wall (grey dots).

2.5.3. Upscaled-experiment model results

In the base-case scenario (B runs), when the longitudinal training wall starts from the upstream part of a bar, the result shows that the smaller ecological channel silts up (Figure 2.12.a). The opposite occurs, when the training wall starts at a pool location (Figure 2.12.b).

The trends are the same also for different width ratios. If the training wall

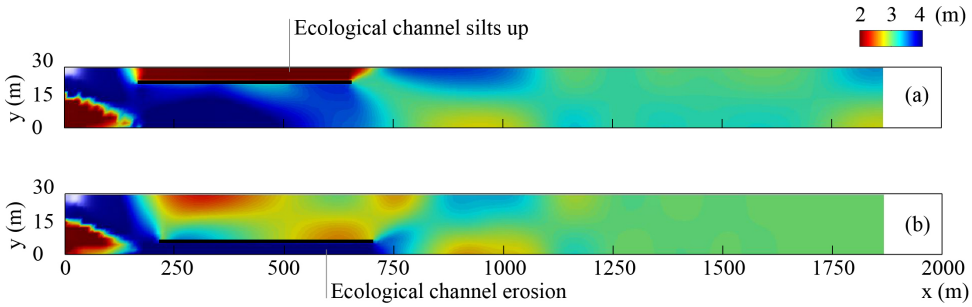

Figure 2.12: Water depth distribution showing the morphological development in base-case scenario. (a) Longitudinal wall starting in the upstream part of a steady bar. (b) Longitudinal wall starting in the pool between two bars.

starts in the upstream part of the bar the ecological channel silts up. Instead, if the training wall starts in the pool between two bars the ecological channel deepens whereas the navigation channels aggrades. As in the experiments, also in the numerical simulations the width ratio influences the speed of the process (Figure 2.13) in the same way as in the experimental test (Figure 2.7).

All the obtained numerical results are similar to the ones obtained in the laboratory, supporting the use of the numerical model to study a real river case with variable discharge.

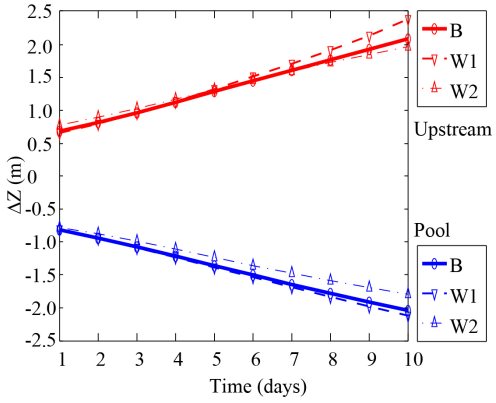

Figure 2.13: Temporal evolution of the difference in bed elevation between the two parallel channels. Red lines represent the cases in which the training wall started in the upstream part of the bar and the blue lines the cases in which the training wall started in the pool. The speed of the process is represented by the steepness of the curve.

2.5.4. Alpine Rhine model setup

This numerical investigation aimed at studying the effects of variable discharge in a real river case that is rather similar to the upscaled version of the system studied in the laboratory. The analysis focused on conveyance capacity and bar formation. The selected case study is the Upper Reach of the Alpine Rhine River described by Adami *et al.* [25]. The characteristics of the system are listed in Table 2.1. The numerical parameters are summarized in Table 2.4.

The hydrograph used in this model considered the three discharge levels indicated by Adami *et al.* [25] fully wet discharge Q_{FW} = 381 m^3/s, fully transporting discharge Q_{FT} = 829 m^3/s, and critical discharge for bar formation Q_{cr} = 1845 m^3/s. The duration of these discharges was derived from Figure 2 in Adami *et al.* [25] to roughly describe a typical year (Figure 2.14).

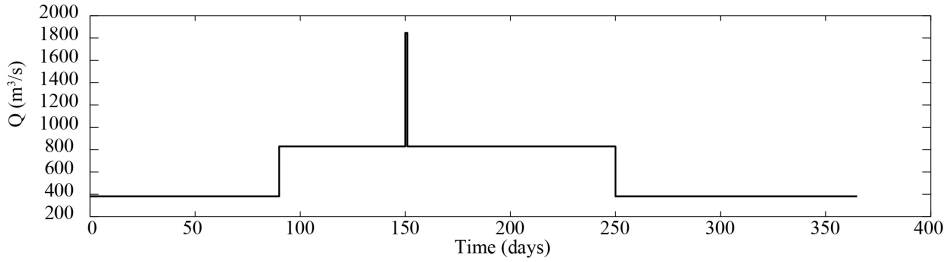

Figure 2.14: Hydrograph for a typical year used in Alpine Rhine model.

The model schematized the river reach as straight, although the channel presents a slight curvature (Figure 2.1). Since the model was not meant to reproduce each bar observed in the study reach, but to simulate the effects of subdividing the river channel with a longitudinal wall, a transverse groyne, located 500 m from the upstream boundary was placed at the right side to obtain hybrid bars, in the same way as in the upscaled-experiment model. For this the model was not calibrated, but validated in terms of bar mode and bar wave-length.

The reference case, without longitudinal wall, started with a flat bed. The bed topography obtained after 3 years is shown in Figure 2.15. In this figure, the bed elevation is plotted from the transverse groyne to the end of the reach. The computed steady alternate bar configuration corresponds rather well to the observed one, considering that also the celerity of the observed bars in the real river reach is zero or close to zero. Moreover, the computed wave length of the alternate bars is 1500 m, which nicely falls within the observed range [25] (Figure 2.1).

Two locations for the starting point of the longitudinal wall were considered: one in the upstream part of the first steady bar and one in the pool opposite to it. Only one width ratio was considered: B_e : B_n = 1:3. All the Alpine Rhine scenarios (Table 2.6) started from the bed topography shown in Figure 2.15. Each computation simulated a period of 3 years.

Table 2.6: Overview of the Alpine Rhine simulations.

Nº	Scenarios	Notation in graph	Location with respect to a bar	Width ratio	Initial bed level	Description
1	Variable discharge	V	Reference case	No training wall	Flat bed	V runs study the effects of variable discharge
2			Upstream	$B_e : B_n$=1:3		
3			Pool			

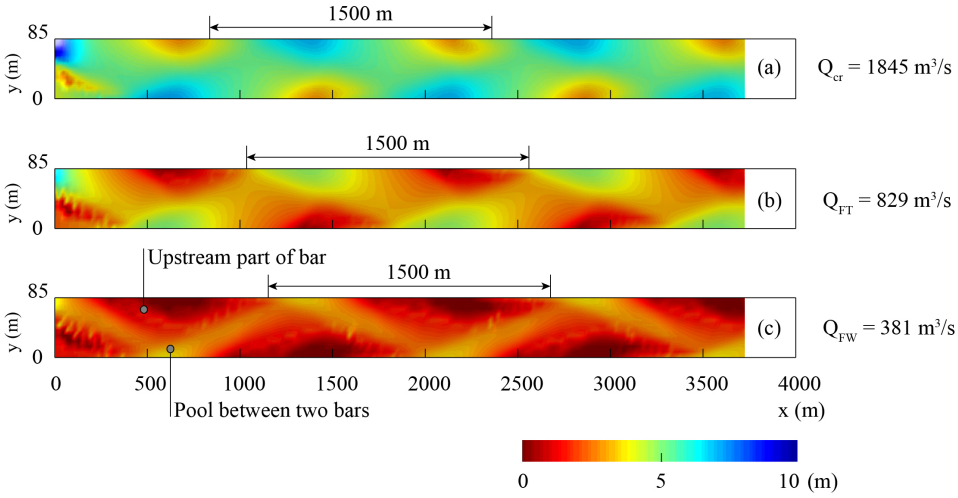

Figure 2.15: Alpine Rhine model results: water depth distributions showing alternate bars in the reference scenario, without longitudinal wall, at the end of the each discharge in the third year. The gray dots in (c) indicate the location of the starting points of the longitudinal wall.

2.5.5. Alpine Rhine model results

In general, based on the results obtained after 3 years, the morphological trends computed for the Alpine Rhine with variable discharge agree with the results of the laboratory tests and upscaled model. When the longitudinal training wall starts in the upstream part of a steady bar the smaller ecological channel silts up (Figure 2.16). The opposite occurs when the training wall starts in a pool location (Figure 2.17).

Figure 2.16 shows that when the training wall started in the upstream part of a bar, under high discharge, the ecological channel silts up but both channels remain open (Figure 2.16.a) whereas under low discharge, the ecological channel is completely closed and the navigation channel conveys the entire discharge (Figure 2.16.b and c). When all water flows in the navigation channel smaller and shorter bars are found compared to the reference case. Downstream of the training wall, the bars remain of the same type as in the reference case. In this scenario,

the training wall helps to reduce the hinder of the bars in the navigation channel.

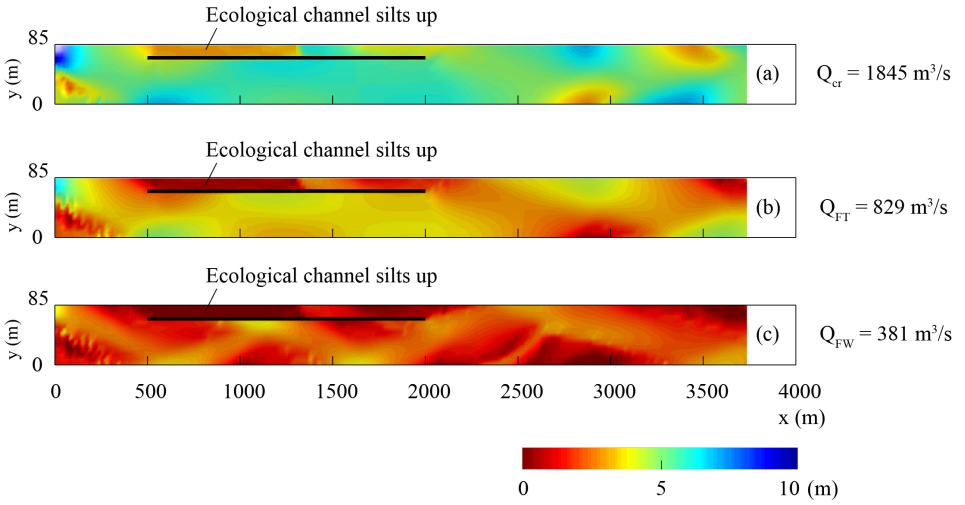

Figure 2.16: Water depth distribution showing the morphological developments if the longitudinal wall started in the upstream part of a steady bar.

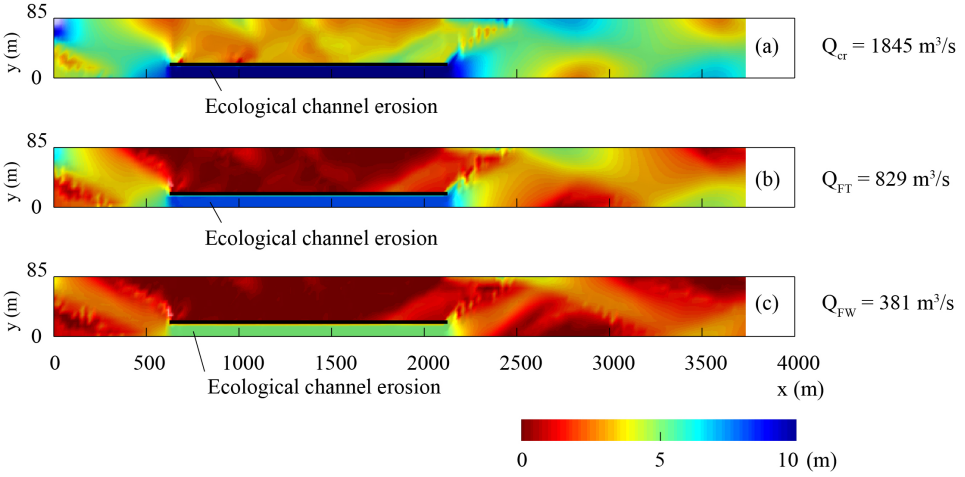

Figure 2.17: Water depth distribution showing the morphological developments if the longitudinal wall started in the pool between two bars. Ecological channel always erosion.

When the longitudinal training wall starts in the pool between two bars, with high discharge the ecological channel conveys almost all water but both channels remain open (Figure 2.17.a). With the smallest discharge the navigation channel closes and all water flows in the ecological channel (Figure 2.17.b and c). In this

scenario the navigation channel is not functional at all at low water.

Figure 2.18 shows the longitudinal profiles of water and bed levels in both the ecological and the navigation channel during the highest discharge. These results show that the longitudinal training wall does not hamper the flood conveyance during high flows.

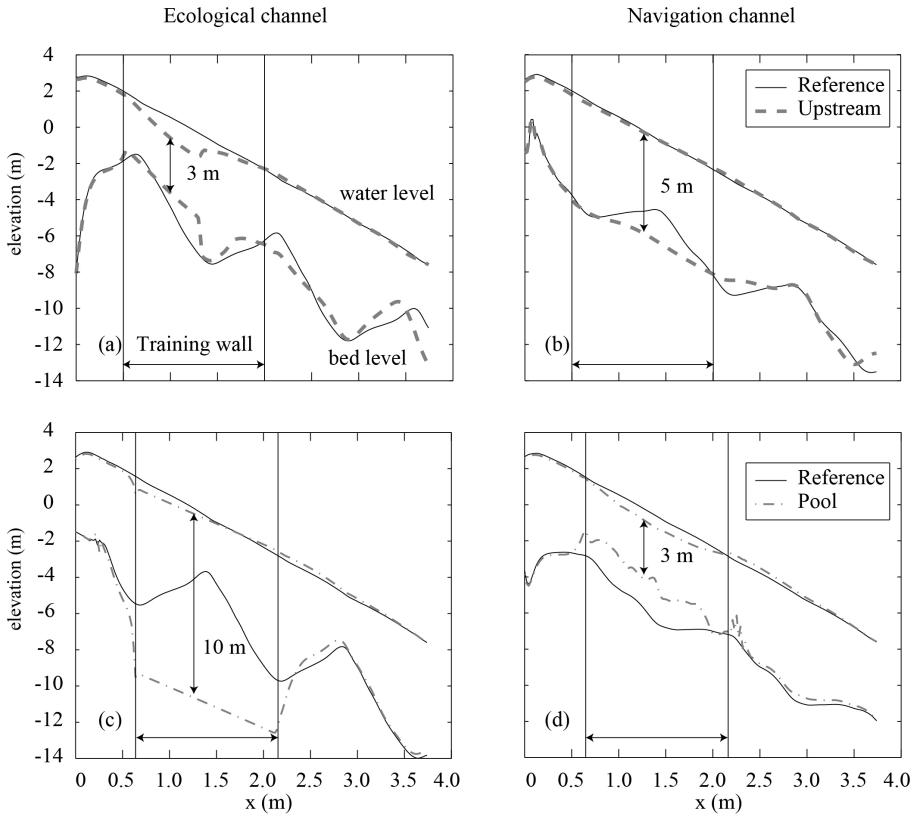

Figure 2.18: Longitudinal profiles along the center line of the ecological and navigation channels during high flow (Q_{cr} = 1845 m^3/s). In (a) and (b) the longitudinal wall started in the upstream part of a steady bar (upstream), whereas in (c) and (d) the longitudinal wall started in the pool between two bars (pool). "Reference" refers to the case without longitudinal wall.

If the training wall starts in the upstream part of a bar, there is a 1.2 m drop of water level in the ecological channel (Figure 2.18.a) whereas in the navigation channel the water level is almost the same as in the reference case (Figure 2.18.b). At the downstream end of the training wall there is a slight increasing in water level compared to the reference case (10 cm). This could be the influence of the confluence where the parallel channels merge again.

If the training wall starts in the pool between two bars the water level in the

ecological channel drops by maximum 50 cm (Figure 2.18.c) and in the navigation channel by a maximum of 65 cm (Figure 2.18.d). However, near the downstream end of the training wall the water level rises up to 28 cm. In this scenario, the rise of water level due to the confluence appears more important.

The effects of using a constant Chézy coefficient might have resulted in overestimating the conveyance of the aggrading channel for which the roughness is most likely underestimated. At the same time, the conveyance of the deepening channel might be slightly underestimated.

2.6. Discussion

The experiments were carried out on straight channels, whereas real rivers present numerous curves. The point bars at the inner side of bends may act as steady alternate bars in affecting the distribution of water and sediment between the two parallel channels, but river bends also result in spiral flow formation and this might alter the direction of sediment transport. For this, the presence of river bends might affect the results of this study. We therefore recommend studying the effects of a longitudinal training wall in a meandering channel.

The numerical results were obtained assuming constant hydraulic resistance, represented by Chézy coefficient. However, channel deepening might result in smaller hydraulic resistance (larger Chézy coefficient) whereas the channel becoming shallower might result in higher hydraulic resistance (smaller Chézy coefficient). Small-scale (sub-grid) bedform formation would influence the Chézy coefficient as well. These effects are not taken into account in the computations. Moreover, due to the alternation of high and low discharges, vegetation might colonize the shallow channel during low flow and drastically increase its bed roughness during high flow. This can reduce the flood conveyance of the parallel channel system. A sensitivity analysis should take into account vegetation on side channel to check whether this really reduce the flood conveyance at high flow.

The work considered gravel-bed rivers, since the laboratory experiments, even though sand was used, represented a river with gravel bed (the characteristics of the laboratory experiments and of the upscaled river are shown in Table 2.1). The subsequent real-river case was again a gravel-bed river with alternate bars. This means that the results are strictly valid only for gravel-bed rivers and their applicability on sand-bed systems requires further investigation.

The strategy we propose to train rivers by creating a navigation and ecological channel with a longitudinal wall presents advantages and disadvantages. We have shown that the bifurcation created with a longitudinal wall results in an unstable system in which one of the two channels inevitably becomes shallower, ideally the ecological channel. This channel closes completely only if the discharge is constant; with variable discharge, it becomes dry at low flows only. This would be an advantage for navigation, because the flow then concentrates in the other channel, increasing the low-flow water depth. The temporary, seasonal, closure of the ecological channel, however, might be a disadvantage for the riverine ecology and this should be further investigated by experts in this field.

In rivers with hybrid alternate bars (rather common in real cases), the results

show also that if the training wall starts in the upstream part of a steady bar the smaller ecological channel experiences sediment deposition and the navigation channel becomes deeper. In this case, the flood conveyance of the river is not reduced, which means that the construction of the longitudinal wall does not increase flood risk in the area adjacent to the river. The opposite happens if the training wall starts in the pool between two bars: the navigation channel silts up and the flood conveyance of the river reduces. These results show the importance of well designing the starting point of the longitudinal wall.

The time scales involved in the processes plays an important role too. If the morphological development is slow, it could be possible to maintain both channels open by, for instance, dredging and dumping the deposited sediment from one channel to the other. This means that the applicability of the proposed technique requires more research.

2.7. Conclusions

We studied the possibility of subdividing a river channel in one relatively narrow "ecological channel" and one "navigation channel" by means of a longitudinal training wall in the laboratory and by means of numerical simulations. We considered channels characterized by the presence of steady alternate bars, which are common morphological features hindering river navigation.

The laboratory experiments show that subdividing a channel presenting steady or slowly migrating alternate bars with a longitudinal training wall might lead to an unstable system, in which one of the two parallel channels tends to silt up. The results show that the starting point of the longitudinal wall with respect to a bar plays an important role for the morphological evolution of the two channels. When the training wall starts at a location in the upstream part of a bar, the narrower ecological channel silts up. Instead, when the training wall starts in the pool area between two subsequent bars, the same channel deepens and the navigation channel silts up. Changing the widths of the channels did not change the trends observed in the base-case scenario. The most stable system is obtained if the longitudinal wall subdivides the river in two equally-wide parallel channels. Changing sediment did not alter the observed trends too, with the exception of test S1 (finer sediment) for which some problems encountered during the experiment did not allow to draw any conclusions for the case starting in the upstream part of a bar. One experimental test (S2: coarser sediment) indicates that a stable system might be obtained if the training wall starts near a bar top, but this might not be true with a variable discharge regime and should be further investigated.

These observations were reproduced numerically in an upscaled version of the laboratory experiments, supporting the use of a 2D model based on the numerical code Delft3D to investigate this type of systems on a real river case.

The subsequent use of the code to study the effects of placing a longitudinal training wall in the Upper Reach of the Alpine Rhine River described by Adami *et al.* [25] confirms the observed trends and shows that a variable discharge regime does not change the observed trends.

The conveyance of the channel was studied by comparing the water levels in

presence of longitudinal wall with those in a reference scenario without wall. The results show that the longitudinal training wall affects high-flow water levels only slightly if it starts in the upstream part of a bar. In this case, a small increase of water level is observed near the downstream end of the longitudinal wall. However, if the training wall starts in the pool between two bars the raise of high-flow level near the end of the longitudinal wall is not negligible, even if limited.

Acknowledgments

This work is sponsored by Vietnam International Education Development (VIED), project 911. The authors wish to thank Floortje Roelvink, Anouk Lako and the technical staff of the Environmental Fluid Mechanics Laboratory of Delft University of Technology.

References

[1] T. B. Le, A. Crosato, and W. Uijttewaal, *Long-term morphological developments of river channels separated by a longitudinal training wall,* Advances in Water Resources **113**, 73 (2018), https://doi.org/10.1016/j.advwatres.2018.01.007.

[2] H. de Vriend, *The long-term response of rivers to engineering works and climate change,* in *Proceedings of the Institution of Civil Engineers-Civil Engineering*, Vol. 168 (Thomas Telford Ltd, 2015) pp. 139–144, https://doi.org/10.1680/cien.14.00068.

[3] Elbe Promotion Centre, website, (2017), www.elbpro.com/en/elbe/waterway-in-a-cultural-landscape.html.

[4] British Marine Federation and Environment Agency, *Cruising guide to the river thames and connecting waterways 2013-2014,* Environment Agency, LIT 6689 (2013), www.gov.uk/government/publications/river-thames-and-connecting-waterways-cruising-guide.

[5] Army Corps of Engineers, *Upper Mississippi River Navigation Charts: Minneapolis, MN to Cairo, IL Upper Mississippi River Miles 866 to 0, Minnesota and St. Croix Rivers*, Vol. 286 pp (Defense Dept., Army Corps of Engineers, Mississippi Valley Division, 2011).

[6] NEPAD Agency, *Construction of navigational line between lake victoria and the mediterranean sea,* (2013), www.nepad.org/content/construction-navigational-line-between-lake-victoria-and-mediterranean-sea.

[7] Mekong River Commission, *Strategic plan 2016 - 2020,* (2016), http://www.mrcmekong.org/assets/Publications/strategies-workprog/MRC-Stratigic-Plan-2016-2020.pdf.

[8] G. Duró, A. Crosato, and P. Tassi, *Numerical study on river bar response to spatial variations of channel width,* Advances in Water Resources **93**, 21 (2015), https://doi.org/10.1016/j.advwatres.2015.10.003.

[9] H. Havinga, M. Taal, R. Smedes, G. Klaassen, N. Douben, and C. Sloff, *Recent training of the lower rhine river to increase inland water transport potentials: a mix of permanent and recurrent measures,* in *Proceedings of International Conference on Fluvial Hydraulics–River Flow* (2006) pp. 31–50, ISBN 0-415-40815-6.

[10] F. Scerri, C. Lescoulier, C. Boudong, and C. Hémain, *2d modelling of the rhone river between arles and the sea in the frame of the flood prevention plan,* in *Advances in Hydroinformatics* (Springer, 2016) pp. 253–273, https://doi.org/10.1007/978-981-287-615-7_18.

[11] P. Jansen, L. van Bendegom, J. van den Berg, M. de Vries, and A. Zanen, *Principles of river engineering. The non-tidal alluvial river.* (Pitman, London, Facsimile edition. Published in 1994 by Delftse Uitgevers Maatschappij., 1979) ISBN 90 6562 146 6.

[12] B. Spinewine and Y. Zech, *An ex-post analysis of the german upper rhine: data gathering and numerical modelling of morphological changes in the 19th century,* Journal of Flood Risk Management **1**, 57 (2008), https://doi.org/10.1111/j.1753-318X.2008.00007.x.

[13] E. Mosselman, P. Kerssens, F. van der Knaap, D. Schwanenberg, and K. Sloff, *Sustainable river fairway maintenance and improvement-literature survey*, Tech. Rep. (WL | Delft Hydraulics, Delft, the Netherlands, 2004).

[14] J. Sieben, *Sediment management in the dutch rhine branches,* International Journal of River Basin Management **7**, 43 (2009), https://doi.org/10.1080/15715124.2009.9635369.

[15] S. van Vuren, A. Paarlberg, and H. Havinga, *The aftermath of "room for the river" and restoration works: Coping with excessive maintenance dredging,* Journal of Hydro-environment Research **9**, 172 (2015), https://doi.org/10.1016/j.jher.2015.02.001.

[16] H. H. Visser P.J. and W. ten Brinke, *Hoe houden we de rivier bevaarbaar?* Land + Water **39(9)**, 24 (1999), (in Dutch).

[17] R. M. Frings, R. Döring, C. Beckhausen, H. Schüttrumpf, and S. Vollmer, *Fluvial sediment budget of a modern, restrained river: The lower reach of the rhine in germany,* Catena **122**, 91 (2014), https://doi.org/10.1016/j.catena.2014.06.007.

[18] M. M. Schoor, H. P. Wolfert, G. J. Maas, H. Middelkoop, and J. J. Lambeek, *Potential for floodplain rehabilitation based on historical maps and present-day processes along the river rhine, the netherlands,* Geological Society, London, Special Publications **163**, 123 (1999).

[19] J. A. Villada Arroyave and A. Crosato, *Effects of river floodplain lowering and vegetation cover,* Proceedings of the Institution of Civil Engineers - Water Management **163**, 457 (2010), https://doi.org/10.1680/wama.900023.

[20] J. Rijke, S. van Herk, C. Zevenbergen, and R. Ashley, *Room for the river: delivering integrated river basin management in the netherlands,* International journal of river basin management **10**, 369 (2012), https://doi.org/10.1080/15715124.2012.739173.

[21] C. Flokstra, *De invloed van knooppuntsrelaties op de bodemligging bij splitsingspunten.*, Report R2166 (Waterloopkundig Laboratorium (WL | Delft Hydraulics), 1985) (in Dutch).

[22] Z. B. Wang, R. J. Fokkink, M. de Vries, and A. Langerak, *Stability of river bifurcations in 1D morphodynamic models,* Journal of Hydraulic Research **33**, 739 (1995).

[23] K. Sloff and E. Mosselman, *Bifurcation modelling in a meandering gravel–sand bed river,* Earth Surface Processes and Landforms **37**, 1556 (2012), https://doi.org/10.1002/esp.3305.

[24] M. Redolfi, G. Zolezzi, and M. Tubino, *Free instability of channel bifurcations and morphodynamic influence,* Journal of Fluid Mechanics **799**, 476 (2016), https://doi.org/10.1017/jfm.2016.389.

[25] L. Adami, W. Bertoldi, and G. Zolezzi, *Multidecadal dynamics of alternate bars in the alpine rhine river,* Water Resources Research **52**, 8938 (2016), https://doi.org/10.1002/2015WR018228.

[26] E. Hansen, *On the formation of meanders as a stability problem. progress report 13,* Coastal Engineering, Laboratory, Techn. Univ. Denmark, Basis Research (1967).

[27] R. Callander, *Instability and river channels,* Journal of Fluid Mechanics **36**, 465 (1969), https://doi.org/10.1017/S0022112069001765.

[28] M. Tubino, R. Repetto, and G. Zolezzi, *Free bars in rivers,* Journal of Hydraulic Research **37**, 759 (1999).

[29] F. Engelund, *Instability of erodible beds,* Journal of Fluid Mechanics **42**, 225 (1970).

[30] J. Fredsøe, *Meandering and braiding of rivers,* Journal of Fluid Mechanics **84**, 609 (1978).

[31] G. Parker, *On the cause and characteristic scales of meandering and braiding in rivers,* Journal of fluid mechanics **76**, 457 (1976).

[32] A. Crosato and E. Mosselman, *Simple physics-based predictor for the number of river bars and the transition between meandering and braiding,* Water Resources Research **45** (2009), 10.1029/2008WR007242, https://doi.org/10.1029/2008WR007242.

[33] G. Zolezzi and G. Seminara, *Downstream and upstream influence in river meandering. Part 1. General theory and application to overdeepening,* Journal of Fluid Mechanics **438**, 183 (2001), https://doi.org/10.1017/S002211200100427X.

[34] M. Tubino and G. Seminara, *Free–forced interactions in developing meanders and suppression of free bars,* Journal of Fluid Mechanics **214**, 131 (1990).

[35] W. Bertoldi, L. Zanoni, S. Miori, R. Repetto, and M. Tubino, *Interaction between migrating bars and bifurcations in gravel bed rivers,* Water resources research **45** (2009), 10.1029/2008WR007086, https://doi.org/10.1029/2008WR007086.

[36] A. Talmon, N. Struiksma, and M. V. Mierlo, *Laboratory measurements of the direction of sediment transport on transverse alluvial-bed slopes,* Journal of Hydraulic Research **33**, 495 (1995), https://doi.org/10.1080/00221689509498657.

[37] N. Struiksma, K. Olesen, C. Flokstra, and H. De Vriend, *Bed deformation in curved alluvial channels,* Journal of Hydraulic Research **23**, 57 (1985), https://doi.org/10.1080/00221688509499377.

[38] M. Tubino, *Growth of alternate bars in unsteady flow,* Water Resources Research **27**, 37 (1991).

[39] V. Chavarrías, A. Blom, C. Orrú, and E. Viparelli, *Laboratory experiment of a mixed-sediment gilbert delta under varying base level,* in *RCEM 2013, 9-13 June*, IAHR (Santander, Spain, 2013) p. 114.

[40] N. Struiksma and A. Crosato, *Analysis of a 2-D Bed Topography Model for Rivers* (Wiley Online Library, 1989) ISBN 0-87590-316-9.

[41] M. G. Kleinhans, W. M. van Dijk, W. I. van de Lageweg, R. Hoendervoogt, H. Markies, and F. Schuurman, *From nature to lab: scaling self-formed meandering and braided rivers,* in *Proc. River Flow*, Vol. 2 (2010) pp. 1001–1010, ISBN 978-3-939230-00-7.

[42] E. Meyer-Peter and R. Müller, *Formulas for bed-load transport,* in *Proc., 2nd Meeting, IAHR* (Stockholm, Sweden, 1948) pp. 39–64.

[43] G. Lesser, J. Roelvink, J. Van Kester, and G. Stelling, *Development and validation of a three-dimensional morphological model,* Coastal engineering **51**, 883 (2004).

[44] A. Defina, *Numerical experiments on bar growth,* Water Resour. Res. **39**, 1092 (2003), https://doi.org/10.1029/2002WR001455.

[45] F. Schuurman, W. A. Marra, and M. G. Kleinhans, *Physics-based modeling of large braided sand-bed rivers: Bar pattern formation, dynamics, and sensitivity,* Journal of geophysical research: Earth Surface **118**, 2509 (2013), https://doi.org/10.1002/2013JF002896.

[46] U. Singh, A. Crosato, S. Giri, and M. Hicks, *Sediment heterogeneity and mobility in the morphodynamic modelling of gravel-bed braided rivers,* Advances in Water Resources **104**, 127 (2017), https://doi.org/10.1016/j.advwatres.2017.02.005.

[47] R. A. Bagnold, *An approach to the sediment transport problem from general physics* (Washington : U. S. Govt. Print. Off, 1966) https://doi.org/10.1017/S0016756800049074.

[48] E. Mosselman and T. B. Le, *Five common mistakes in fluvial morphodynamic modeling,* Advances in Water Resources **93**, 15 (2016), https://doi.org/10.1016/j.advwatres.2015.07.025.

3

Numerical investigation.

On the stability of river bifurcations created by longitudinal training walls.

To maintain a navigable channel and improve high-flow conveyance, engineers have recently proposed constructing longitudinal training walls as an alternative to the traditional transverse groynes. However, previous work has shown that the system of parallel channels created by a longitudinal training wall might be unstable in rivers with alternate bars. Many questions remain unanswered, particularly whether a stable system can be obtained by carefully designing the bifurcation point. This work analyses the stability of the bifurcating system created by a thin longitudinal wall in sand-bed rivers with alternate bars or point bars. The methodology includes performing 102 numerical tests using the Delft3D code to reproduce an idealized lowland river, either straight or meandering. The results show that the system of parallel channels separated by a training wall may indeed become unstable. An important factor is found to be the location of the bifurcation point with respect to a neighboring bar or point bar. The same trends are observed for both constant and variable discharge, in straight and meandering channels. The results suggest that cyclic growth and decline of the bifurcating channels may arise as inherent system behavior, without the need of any additional external forcing. We explain this from changes in the relationship between sediment transport ratio and discharge ratio as the bifurcation evolves. This cyclic behavior can be regarded as a form of system stability and can be obtained by carefully placing the starting point of the longitudinal training wall, and thus the bifurcation point, near the top of a bar.

This chapter is published in **Advances in Water Resources (2018)** [1].

3.1. Background and objective

Lowland rivers have been trained for centuries with transverse groynes to prevent bank erosion and to improve and maintain a navigable channel. Longitudinal training walls are less commonly applied, but they can serve the same purposes.

In the Netherlands, series of transverse groynes have been built to prevent ice jams during the winter and improve channel navigability by channel narrowing (Figure 3.1.a). The large-scale narrowing of the Rhine branches, along with bend cutoffs and sediment mining, triggered a morphological response of incision at rates up to over 2 cm/year. Apart from draining riparian habitats in floodplains and undermining hydraulic structures, this incision also deteriorated the conditions for navigation. To mitigate these effects, groynes in the river Waal near Tiel were replaced by longitudinal training walls in the years 2013-2015, as a pilot for testing this alternative approach to river training (Figure 3.1.b). The main idea was to provide a narrow and, hence, deep main channel during low flows, while allowing more water to flow in the secondary channel behind the training wall at higher discharges in order to reduce main channel erosion and to lower the water levels during floods. Furthermore, the presence of the secondary channel was expected to improve the ecological conditions of the river. Finally, the fairway would no longer be spoiled by the shallow ridges that develop in response to the formation of local scour holes at groyne heads.

Figure 3.1: (a) Classical transverse groynes versus (b) longitudinal training wall in the Waal River near Tiel. Source: Rijkswaterstaat.

Another pertinent example is the Quang Ngai irrigation system in central Vietnam which was built in the period 1985-1997 in the framework of the Thach Nham project. It comprises two main intakes upstream and many small free inlets further downstream along both sides of the Tra Khuc River. During the dry season the main low-flow stream sways inside the main channel changing location every year (Figure 3.2). This creates the need to guarantee water flow to the intakes without hindering the water conveyance during the rainy season. Two solutions are proposed to solve the problem. The first one is to move the intakes to other locations where the main stream is more stable. The second solution proposes constructing longitudinal training walls along the river banks in the reach with the

intakes. This solution is expected to be more easily accepted by the local community, since it would not change the old channel system and the land use along the river. Therefore, longitudinal training walls appear as a promising solution to clear the entrances of water inlets and intakes along the Tra Khuc River.

Figure 3.2: Tra Khuc River (Vietnam). The small branch on the right might become the main low-flow stream in the future (Photograph Le Thai Binh).

A longitudinal training wall divides a river in two parallel channels, usually having different widths, with an upstream bifurcation. As river bifurcations are often unstable, the question arises whether the two-channel system will be stable and, in case of instability, which channel would silt up. The pattern of steady bars in the river can be assumed to be a major factor for this stability, because bars influence the sediment distribution between the two channels [2–4]. We address this question in the present research by carrying out a long series of numerical tests using the Delft3D code, considering that this code has already proven to be successful in simulating the morphological development of this type of systems [4]. The objective is to assess the stability of the channels on either side of a longitudinal training wall in single-thread sand-bed rivers with steady or slowly migrating alternate bars or point bars. Several cases are considered: different locations of the bifurcation point with respect to a bar or point bar, different channel widths, constant and variable discharges, as well as straight and sinuous channels.

3.2. Theoretical background

3.2.1. Stability of bifurcations and bars

Bifurcation stability depends on the flow and sediment transport in the upper reaches of the branches below the bifurcation. If more sediment enters the branch than the flow can transport, the branch will experience sedimentation. If less sediment enters, the bed of the branch will erode. If the amount of sediment entering each branch is exactly equal to the transport capacity of the flow, the bifurcation is in equilibrium. This equilibrium is stable if it is restored after a small perturbation, e.g. if occasional erosion in a branch generates sediment overloading, producing counteracting sedimentation. It is unstable if the small perturbation grows further, for instance if occasional erosion in a branch generates a shortage of sediment

entering this branch, giving rise to further erosion.

The stability of a bifurcation is therefore governed by the interplay between the distributions of water and sediment between the two branches. These distributions depend on the structure of flow and sediment transport in the area immediately upstream of the bifurcation. Most alluvial rivers have wavy channel beds due to the presence of bars (Figure 3.3). This makes the structure of flow and sediment transport complex. Bars are associated with lateral flow redistribution, transverse bed slopes and helical flow that alter the sediment transport direction [5]. These features affect the distribution of sediment at bifurcations [6]. The presence of a bar, and in particular a steady bar [3, 4], might therefore lead to the silting up and closure of one of the two parallel channels divided by the longitudinal wall.

Figure 3.3: Examples of bars in low-land rivers. (a) Han River in Danang, Vietnam. © Google Earth, 2015. (b) Cauca River, Colombia (photograph Erik Mosselman).

Bars develop due to either morphodynamic instability occurring at sufficiently large width-to-depth ratios or morphodynamic forcing, or both. The bars that arise from morphodynamic instability are called "free bars". These bars are typically periodic and can migrate in downstream or in upstream direction [7–9]. The linear stability analyses carried out since the 1970s show that a flat alluvial bed may develop into a pattern of alternate or multiple bars (unstable bed), depending on the flow width-to-depth ratio and other morphodynamic parameters (e.g., [10–15]). Zolezzi and Seminara [7] showed that free bars migrate in downstream direction if the flow width-to-depth ratio is smaller than the resonant one (sub-resonant conditions), and in upstream direction if it is larger (super-resonant conditions). At resonant conditions free bars present zero celerity. Notwithstanding the presence of simplifying assumptions, such as a constant discharge, the results of these analyses are successfully used as physics-based predictors of the alluvial channel pattern (e.g. [14, 16, 17]).

"Morphodynamic forcing" is the result of permanent flow curvature that arises from a local change of channel geometry, which can be caused by a bend, a struc-

ture, and a local width change. Curved flow results in outer-bend scour and inner-bend sediment deposition. Typical "forced bars" are the point bars that become visible during low flows at the inner side of river bends.

Forcing can also fix the location of free bars [5, 18]. Such bars with zero celerity can give rise to a more extensive pattern of periodic non-migrating sediment deposits. These deposits are called "hybrid bars" because they depend on both forcing and morphodynamic instability [19]. Recent theoretical analyses show that steady bars may arise upstream of the bifurcation point as a result of the perturbation generated by the start of the longitudinal wall if the original channel exceeds the width-to-depth ratio that allows for upstream morphodynamic influence, i.e. is at super-resonant conditions [3].

Forced and hybrid bars are rather common in low-land rivers, since natural channels are generally irregular, resulting in numerous forcings, and this is why the presence of these bars is considered central in this study.

3.2.2. Bifurcation stability analyses

Non-linear phase-plane stability analyses of one-dimensional bifurcation models by Flokstra [20] and Wang *et al.* [21] show how sensitive bifurcations are to the distribution of sediment transport. These analyses use simple hypothetical relationships in which the ratio of sediment transports into the two branches is a function of the ratios of discharges and widths of the two branches:

$$\frac{Q_{s1}}{Q_{s2}} = \left(\frac{Q_1}{Q_2}\right)^k \left(\frac{B_1}{B_2}\right)^{1-k} \tag{3.1}$$

where Q_{s1} and Q_{s2} are the sediment transport rates entering branch 1 and 2, respectively; Q_1 and Q_2 are the water discharges; B_1 and B_2 are the channel widths; and k is a number that has to be determined empirically. For low values of k, this relation is destabilizing, because a higher discharge into one branch would generate a higher (stabilizing) sediment input but an even higher (destabilizing) sediment throughput due to the nonlinear relation between sediment transport capacity and discharge. The stabilizing effect of the higher sediment input prevails only if k is sufficiently large. Wang *et al.* [21] found that bifurcations are stable (both channels remain open) for $k > 5/3$ and unstable (one of the channels silts up) for $k < 5/3$ if the sediment transport capacity is computed with Engelund and Hansen [22] formula, which is valid for sand-bed rivers.

In principle, 2D and 3D models can be used to calculate the distribution of sediment transport into the branches of a bifurcation. In 1D models, however, the 2D and 3D details of flow and sediment transport at the bifurcation are lost. Several researchers attempted to improve the relationships for sediment transport distribution over bifurcated branches in 1D models by accounting in a parameterized way for various mechanisms that may play a role (Figure 3.4).

Bolla Pittaluga *et al.* [23] extended Wang *et al.* [21] formula by incorporating transverse flows due to the redistribution of discharges over the cross-section and by incorporating the effects of transverse bed slope in the final reach of the upstream channel with normal width, flow discharge and sediment transport rate

Mechanism		Inclusion in nodal point relation * WFVL	BRT	KJMS	BZMRT	MM
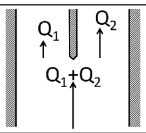	Discharge distribution	+	+	+	+	+
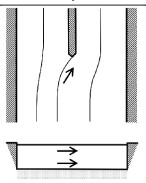	Transverse velocity due to redistribution of flow over cross-section	-	+	+	+	+
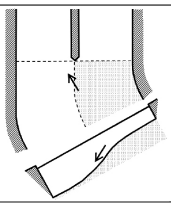	Transverse bed slope due to upstream bars (e.g. point-bars in bends or alternate bars in straight reaches)	-	-	-	+	-
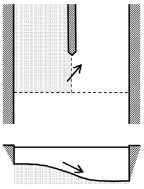	Transverse bed slope due to downstream bed elevation difference	-	+	+	+	-
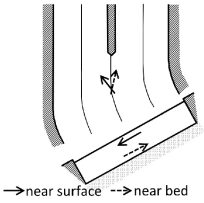	Helical flow due to upstream bend	-	-	+	-	-
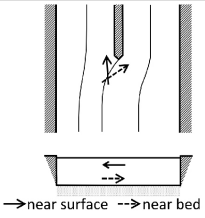	Helical flow due to redistribution of flow over cross-section	-	-	-	-	+
* WFVL = Wang et al (1995), BRT = Bolla Pittaluga et al (2003), KJMS = Kleinhans et al (2008), BZMRT = Bertoldi et al (2009), MM = Van der Mark & Mosselman (2013)						

Figure 3.4: Mechanisms affecting the distribution of sediment at bifurcations and their incorporation in sediment distribution relationships for 1D models.

equal to B_0, Q_0 and Q_{s0}, respectively. The additions by Bolla Pittaluga *et al.* [23] imply that more sediment is transported towards the largest and deepest channel downstream. They thus have a stabilizing effect. Indeed, Bolla Pittaluga *et al.* [23] found that for low values of the channel aspect ratio and large values of the Shields parameter of the flow, symmetrical bifurcation geometries are stable. As the channel aspect ratio increases (or the Shields number decreases) this configuration loses stability. de Heer and Mosselman [2] commented that the relationship of Bolla Pittaluga *et al.* [23] does not account for upstream asymmetries, such as the presence of bars. They expressed the expectation that an extension with more mechanisms of sediment distribution would reveal that bifurcations can be unstable under more conditions than suggested by the analysis of Bolla Pittaluga *et al.* [23]. Such extensions were proposed subsequently by Kleinhans *et al.* [24], Bertoldi *et al.* [25], van der Mark and Mosselman [26].

Bertoldi *et al.* [25] included the effect of migrating bars according to relations by Colombini *et al.* [27] for free alternate bars that occur in long straight channels with uniform width. Bars arriving at the bifurcation feed the downstream branches alternatively with a larger amount of water and sediment. The time period of this feeding is set by the ratio between bar length and migration speed. As a result, the bifurcation oscillates around an equilibrium or disappears due to closure of one of the branches. The findings of Bertoldi *et al.* [25] do not hold, however, for the point-bars and hybrid steady bars that are encountered more generally in rivers than free bars.

Kleinhans *et al.* [24] added the effects of helical flow in upstream river bends to the sediment distribution relation of Bolla Pittaluga *et al.* [23] by modifying the direction of the sediment transport by taking into account the effects of transverse slope. However, the transverse bed slope is still calculated from the elevation difference between the bed levels in the downstream branches, not from the topography of the upstream point-bar that is formed in alluvial river bends.

van der Mark and Mosselman [26] proposed a relationship for the effects of helical flow in which the streamline curvature generating this helical flow is related to redistribution of the flow over the cross-section rather than related to an upstream river bend. They tested their relationship as well as other relationships against field data, concluding that all relationships perform poorly and that reliable models of river bifurcations should be at least two-dimensional. Systematic 2D numerical simulations by Kleinhans *et al.* [24] shed more light on the effects of different sediment distribution mechanisms on bifurcation stability. Unstable bifurcations can be nearly balanced if mechanisms favoring the closure of one channel are compensated by mechanisms favoring the closure of the other channel. Such nearly balanced bifurcations develop more slowly than unbalanced bifurcations. Furthermore, the numerical simulations showed the sediment distribution relationships to change as a bifurcation evolves. In this way an initially unstable bifurcation may become stable in a strongly asymmetrical configuration, without reaching full closure of the declining branch.

3.3. Numerical investigations

3.3.1. Model description

We analysed the results of a large number of 2D numerical simulations reproducing the behavior of an idealized low-land river with alternate bars or point bars which is divided into two parallel channels by a thin longitudinal wall.

The Delft3D code solves the three-dimensional Reynolds equations for incompressible fluid and shallow water with a finite-difference scheme [28]. A variety of sediment transport formulas is available to compute the sediment transport rate. Bed level changes are derived by either applying the Exner principle (bed load or fast adapting suspended load) or from a sediment balance equation in which sediment deposition and entrainment rates are derived as a function of suspended-solid concentrations and hydrodynamic parameters. The models developed in the framework of this study were based on the depth-averaged version of the basic equations (2D approach). Duró *et al.* [19], Defina [29], Schuurman *et al.* [30] and Singh *et al.* [31] demonstrated that this type of approach is able to simulate bar processes with sufficient accuracy. The approach is also supported by the experience of Le *et al.* [4], who successfully reproduced the long-term morphological developments of this type of systems at the laboratory scale with a 2D model built using the Delft3D code.

3.3.2. Model setup

We selected values of the hydraulic and morphological variables and parameters that represent a "typical lowland river with alternate bars or point bars". Such variables and parameters were inspired by the Waal River in the Netherlands (Figure 3.1) and are listed in Table 3.1. The computational case, however, is not a scaled version of the Waal River, since the two systems differ, for instance in the value of the Shields parameter.

Figure 3.5 shows part of the numerical grids (45 km total length) for the straight and the sinuous channel, the rectangular grid size being 15×45 m^2 (straight channel). In all models $B_0 = B_1 + B_2$ where B_0 is the original river width, B_1 is the side (smaller) channel width and B_2 is the main (larger) channel width. Three width combinations are investigated, including the scenario in which $B_1 = B_2$. In the curved channel, the wavelength of the meanders along the straight line connecting their inflection points was chosen to be equal to the equilibrium hybrid-bar wavelength (1350 m). The meander amplitude was equal to 100 m.

The hydrodynamic boundary conditions of the models consisted of downstream water level and upstream discharge. These boundary conditions were either constant (most scenarios), with a discharge of 200 m^3/s, or variable (see Table 3.3). The discharge hydrograph adopted in the variable-discharge scenarios was inspired by the Waal River (Table 3.1). The typical hydrological year is depicted in Figure 3.6. The boundary conditions for the sediment component were upstream balanced sediment transport, which prevented the bed level from changing at the boundary, and a downstream free sediment transport condition, which allows undisturbed level changes up to the boundary. The banks were kept fixed and treated as free-slip boundaries.

Table 3.1: Characteristics of the Waal River and numerical simulations in this study

Parameters	Notation	Unit	Waal River	Computational case
Hydrological characteristics				
Average discharge	$Q_{50\%}$	m^3/s	1587	200
Minimum discharge	Q_{min}	m^3/s	939	118
Maximum discharge	Q_{max}	m^3/s	4680	590
Discharge ratio between Q_{max} and Q_{min}	Q_{max}/Q_{min}	-	4.98	5.00
Discharge ratio between Q_{max} and $Q_{50\%}$	$Q_{max}/Q_{50\%}$	-	2.95	2.95
1D hydraulic and morphological characteristics at average discharge				
River width	B	m	250	90
Normal depth	h	m	6.0	3.0
Longitudinal bed slope	i	-	10^{-4}	10^{-4}
Chézy coefficient	C	$m^{1/2}/s$	43	43
Froude number	Fr	-	0.137	0.137
Shields parameter	θ	-	0.365	0.906
Median sediment grain size	D_{50}	m	$1.0*10^{-3}$	$2*10^{-4}$
Relative density of sediment	Δ	-	1.65	1.65
Transport law	Engelund and Hansen [22]			
2D hydraulic and morphological characteristics at average discharge				
Width-to-depth ratio	B/h	-	42	30
Theoretical bar mode Crosato and Mosselman [17]	m	-	1	1

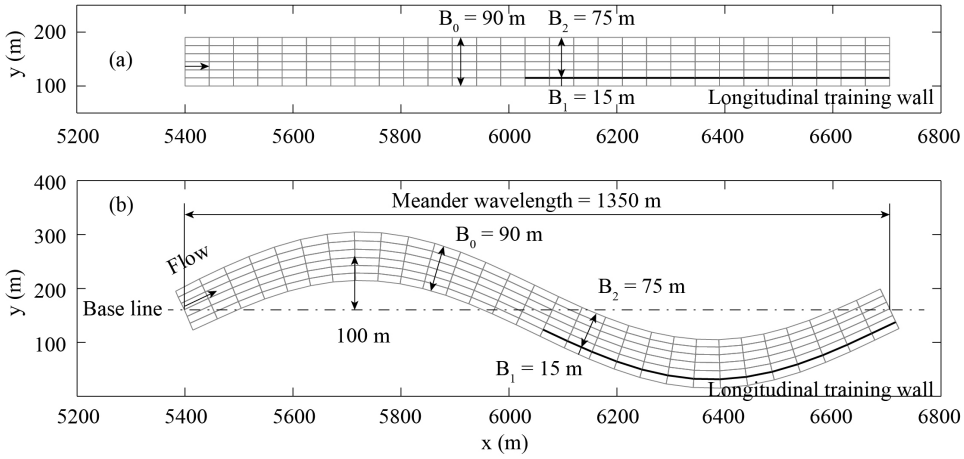

Figure 3.5: Numerical grid and longitudinal training wall for $B_1 : B_2$ = 1:5. (a) Straight channel models. (b) Sinuous channel models.

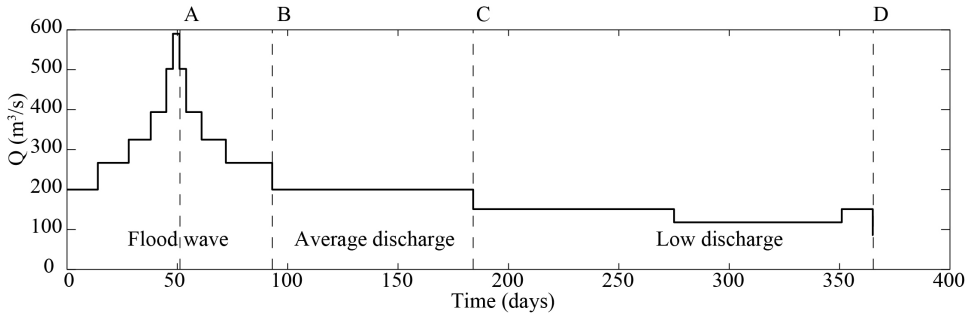

Figure 3.6: Discharge hydrograph used in the variable-discharge scenarios (average discharge = 200 m^3/s). A, B, C, D indicate the moments of the plots in Figure 3.13.

The morphodynamic conditions of the simulated system correspond to a river channel with alternate bars. The theoretical mode m is the integer representing the type of bars that form in the river channel; it was here computed according to Crosato and Mosselman [17]'s theory. The value $m = 1$ (Table 3.1) refers to alternate bars. Applying the linear theory, both the Waal River at average discharge and the computational case result in super-resonant conditions, but very close to resonance [32]. In such a case, a finite flow discontinuity near the upstream boundary leads to the formation of a series of hybrid alternate bars [9, 18]. Such a discontinuity was obtained in the straight channel simulations by placing a transverse thin dam obstructing 1/2 of the channel width at a distance of 900 m from the upstream boundary, ten times the width of the channel B_0. The sinuous-channel simulations did not need an external disturbance to obtain the formation of point bars which spontaneously form at the inner side of bends.

The longitudinal training wall was schematized as a thin, infinitely high and deep, dam to ensure that the structure always divides the two channels, even at the highest flow rates.

The bed roughness was represented by a constant Chézy coefficient (value in Table 3.1) and the bed-load transport rate was computed by means of the Engelund and Hansen [22] formula, valid for sand bed rivers. The situation in which transverse bed slopes do not affect sediment transport is not considered here, since it leads to unreliable computations [33]. The bed slope effect on sediment transport direction was taken into account in all simulations. Two formulations were considered: Bagnold [34] (default in Delft3D) and Koch and Flokstra [35]. Koch and Flokstra [35]'s formulation was adopted solely for the sensitivity analysis meant to study the effects of transverse bed slope on bifurcation stability, since it allows having a stronger vs. smaller effect of transverse bed slope on sediment transport direction by changing the value of one or more coefficients. The influence of the spiral flow in curved reaches was accounted for according to the formulation of Struiksma *et al.* [5].

In Delft3D, the drying of wet cells is imposed based on a threshold water depth. Cells that become dry are removed from the hydro-morphological computational

domain and remain dry. They may become wet again by bank erosion, but this is not considered in our computations. In our simulation this threshold water depth was 10 cm (default in Delft3D).

The time step of the flow computations was 0.5 minute to ensure numerical stability and accuracy, as evaluated by the criterion that the Courant number is smaller than 10.

The morphological developments in all simulations with constant discharge were accelerated by using a morphological acceleration factor (MF) equal to 10, after having checked that this does not affect the results in a way that is relevant for the scope of the study. This approach is also justified because previous studies in river channels with similarly small Froude numbers (e.g. [19, 36]) showed that it hardly affects the development of the 2D bed topography in a river with hybrid bars. For the simulations with variable discharge, we did not accelerate the computations (MF=1). As a result, the running times were 10 years for all constant discharge scenarios (with MF=10) and 100 years for the variable discharge scenarios (with MF=1). This means that we computationally cover 100 years in all cases. The computational time proved to be long enough to reach a new morphodynamic equilibrium, characterized by negligible temporal changes of the average bed elevation of the parallel channels (see Section 3.4). Table 3.2 summarizes the numerical parameters used in the simulations.

Table 3.2: Values of numerical parameters used in the simulations.

Parameters	Notation	Unit	Value
Size of computational domain	$L \times B$	m×m	45,000×90
Rectangular size of grid cell	-	m×m	45×15
Number of grid cells	$M \times N$	-	1000×6
Time step	t	s	30
Simulation time	T	year	100
Running time and morphological factor	T_{run} & MF	-	10, MF=10 (constant discharge) 100, MF=1 (variable discharge)

3.3.3. Model runs

The investigation comprises 102 different model runs. These are meant to study the effects on bifurcation stability of: longitudinal wall starting point (Runs W_0); width ratio (Runs W_0, W_1 and W_2); and variable discharge (Runs V_0, V_1 and V_2, with different width ratios). The investigation includes a sensitivity analysis to assess the effects on bifurcation stability of the deviation of bed load direction due to transverse bed slope (Runs A). In addition, four runs are carried out to study bifurcation stability in a sinuous channel (Runs S). These are especially meant to investigate whether accounting for the effects of spiral flow on bed load direction may result in different morphological trends, since spiral flow deviates bed load transport in opposite direction compared to transverse bed slope [5, 24, 37]. The performed simulations are listed in Table 3.3.

All scenarios included a reference case without longitudinal wall, but with a

transverse wall to generate the initial bed topography with alternate hybrid bars. This bed topography is then the starting condition of all the other runs. To study the influence of bars on the stability of the bifurcation created by the start of the longitudinal wall, several starting locations were identified with respect to a selected steady bar (Figure 3.7). These locations are numbered from 1 to 18 (Location 18 corresponds to Location 1 with respect to the next bar). The effects of the starting location were then analysed for different width ratios, namely: $B_1 : B_2$ = 1:5 (W_0) - base-case scenario; 1:2 (W_1) and 1:1 (W_2) (see Table 3.3).

Table 3.3: Overview of the simulations in this study

Run	Scenarios	Starting location	Width ratio* $B_1 : B_2$	Initial bed level	Descriptions
Constant discharge (55 simulations)					
Reference case with constant discharge			No wall	Flat bed	Reference run to obtain hybrid steady bars with constant discharge and Bagnold [34] formulation
W_0	Width ratio 0 (base-case constant discharge)	1 - 18	1:5	Hybrid bars	W runs study the effects of different width ratios and starting point of the longitudinal wall with respect to a hybrid bar
W_1	Width ratio 1	1 - 18	1:2	Hybrid bars	
W_2	Width ratio 2	1 - 18	1:1	Hybrid bars	
Variable discharge (10 simulations)					
Reference case with variable discharge			No wall	Flat bed	Reference run to obtain hybrid steady bars with variable discharge and Bagnold [34] formulation
V_0	Width ratio 0 (base-case variable discharge)	4, 10, 17	1:5	Hybrid bars	V runs study the effects of starting location considering that hybrid bars are expected to change due to discharge variation. Three width ratios are considered.
V_1	Width ratio 1	4, 10, 17	1:2	Hybrid bars	
V_2	Width ratio 2	4, 10, 17	1:1	Hybrid bars	
Sensitivity analyses (33 simulations)					
Reference case with constant discharge			No wall	Flat bed	Reference runs to obtain hybrid steady bars with constant discharge and Koch and Flokstra [35] formulation. One run per value of A_{sh} **
A	Sensitivity analysis	4, 17	1:5	Hybrid bars	A runs study slope effects of transverse slope on bed load direction. Two locations for each value of A_{sh}
Sinuous river (4 simulations)					
Reference case with constant discharge			No wall	Flat bed	Reference run to obtain point bars inside bends
S	Sinuous planform	4, 10, 17	1:5	Hybrid bars	S runs study the effects of spiral flow on a sinuous river with constant discharge

* B_1 = side channel width and B_2 = main channel width

** A_{sh} is a parameter in Koch and Flokstra [35] formulation (see section 4.4).

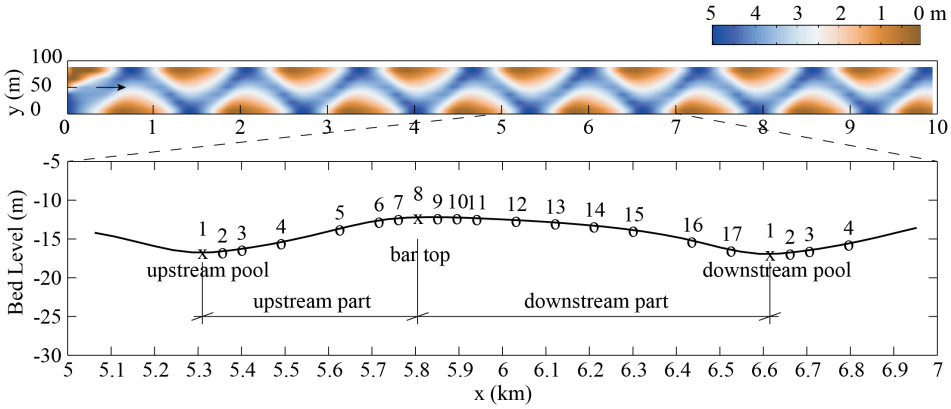

Figure 3.7: Equilibrium state of bars and starting locations of the training wall with respect to a bar. Bar wavelength: 1350 m, bar amplitude: 2.85 m, B/h = 30. Upper graph: water depth at the constant discharge of 200 m^3/s after 100 years. Lower graph: zoomed in longitudinal profile along the right bank from km 5 to km 7.

3.4. Results

3.4.1. Effects of starting location

The 18 simulations reproducing the long-term morphological developments of the base-case scenario (W_0 runs with $B_1 : B_2$ = 1:5 and constant discharge) differ solely in the starting location of the longitudinal wall. The results show that if the training wall starts in the upstream part of a steady bar, i.e. at Locations 3 to 7, the side channel silts up (Figure 3.8.b). Instead, if the training wall starts in the downstream part of the bar, i.e. at Locations 11 to 17, the side channel deepens and it is the main channel that silts up. In this case, the side channel eventually conveys almost all the water discharge (Figure 3.8.d).

A different morphodynamic behavior is observed if the training wall starts near the bar top, at Locations 8 to 10. In this case, the results show a dynamic balance in which the side channel experiences cycles of erosion and sedimentation and remains open (Figure 3.8.c). Every cycle comprises three steps (Figure 3.9): 1) rise of side-channel bed; 2) bar formation near the upstream end of the side channel and side-channel bed erosion; 3) upstream bar erosion and return to the initial state. These cycles repeat continuously during the 100 years covered by the computations. The first cycle is illustrated in Figure 3.9.

The simulated systems were slightly super-resonant at average flow. In this case, the perturbation caused by the starting of the longitudinal wall might affect the shape of the steady bars upstream [3]. However, the obtained results do not always show upstream influence of the bifurcation point. Indeed, when the training wall starts in the upstream part (Figure 3.8.b) or near the bar top (Figure 3.8.c), upstream bars do not show any changes compared to the reference case (Figure 3.8.a). When the training wall starts in the downstream part, a bar deformation

extends to a distance upstream of about 3 bar wavelengths (Figure 3.8.d). Independently from the bifurcation point, no bars formed upstream of the transverse forcing dam that was placed to generate the series of hybrid bars downstream (not in the figures).

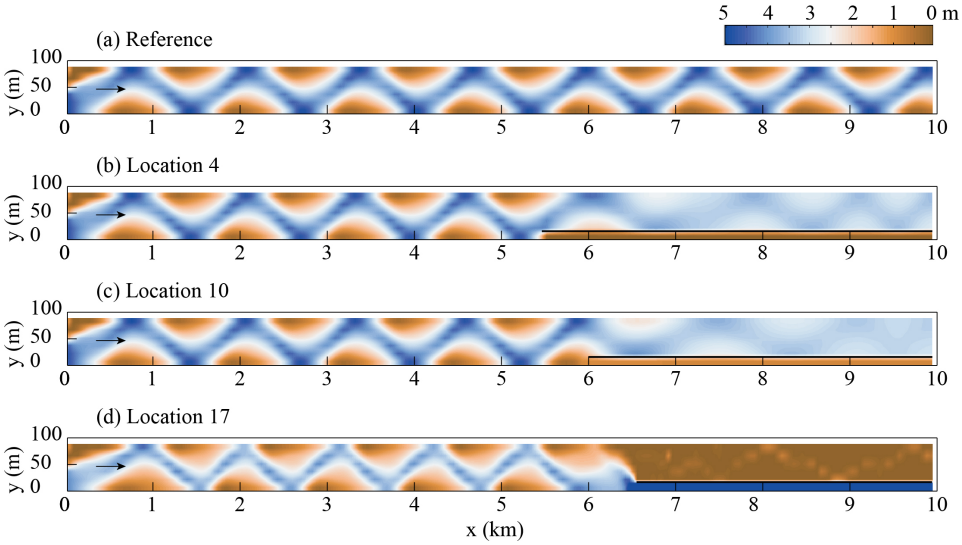

Figure 3.8: Water depth at the constant discharge of 200 m³/s after 100 years (first 10 km after the transverse dam). (a) Reference case without training wall. (b) Training wall starting at Location 4: the side channel closes and bars in the main channel tend to disappear for a distance. (c) Training wall starting at Location 10: both channels remain open. (d) Training wall starting at Location 17: the side channel deepens and the main channel is closed.

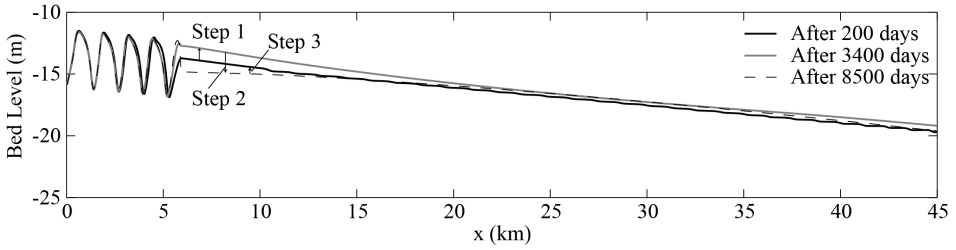

Figure 3.9: Longitudinal bed level profile of the side channel when the training wall starts at Location 10: first cycle of dynamic balance.

Figure 3.10.a shows the temporal variations of the proportion of total discharge that flows in the side channel, Q_1/Q_0, in some representative cases. If $Q_1/Q_0 = 0$ all the discharge is conveyed by the main channel. If $Q_1/Q_0 = 1$ all the discharge

is conveyed by the side channel. The fastest developments pertain to the cases in which the side channel becomes increasingly deep.

Figure 3.10.b shows the variations of sediment transport ratio versus discharge ratio during the computations, the initial discharge ratio Q_1/Q_2 being about 1/8. This figure shows also theoretical sediment transport ratios as a function of Q_1/Q_2 for $B_1 : B_2$ = 1:5 (base-case scenario), computed using Equation 3.1 [21]. In the logarithmic-scale graph, the values of the exponent k are represented by the slope of the straight lines. According to Wang *et al.* [21], the bifurcation is stable (both channels remain open) for $k > 5/3$ and unstable (one of the channels silts up) for $k < 5/3$ in case sediment transport capacity is governed by the formula of Engelund and Hansen [22]. This is the transport formula adopted in the simulations. The application of Wang *et al.* [21]'s theory implies deriving the constant value of k by calibration. For the performed numerical tests, this would lead to the selection of a value of k within the instability conditions for most cases. For location 10, however, the numerical results show that the system assumes a dynamic balance in which it alternates between a stable bifurcation, with a slope, k, in Figure 3.10.b that is steeper than 5/3, and an unstable bifurcation, with a slope that is less than 5/3. Temporal variations thus allow a limit cycle that is not a possible solution in the theoretical analysis of Wang *et al.* [21] that uses a constant value of k. This suggests that an oscillating distribution of discharges can arise as inherent system behavior, not necessarily imposed by the alternating arrival of migrating bars from upstream as in Hirose *et al.* [38] and Bertoldi and Tubino [6] because in our system we do not have migrating bars at the longitudinal wall starting location. This behaviour can be theoretically described only when allowing for temporal variations of k in Wang *et al.* [21] formula (Equation 3.1).

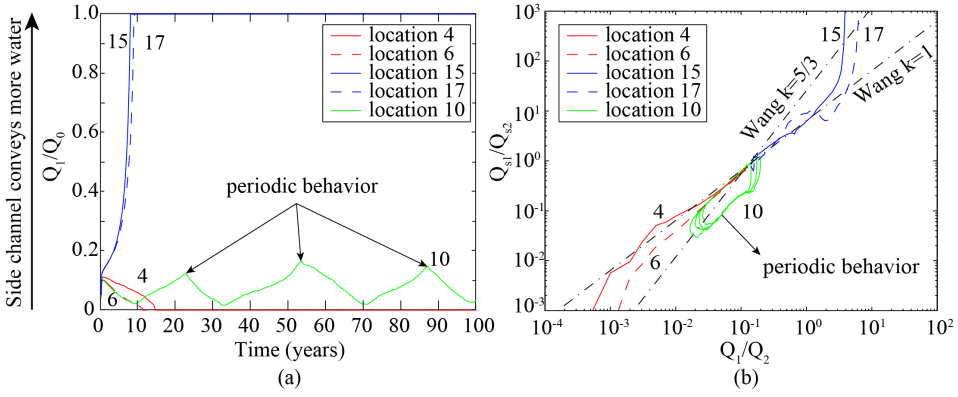

Figure 3.10: Temporal variations of discharge and sediment redistribution at the bifurcation. (a) Temporal variation of the ratio between the discharge entering the side channel and the total discharge Q_1/Q_0. (b) Sediment distribution Q_{s1}/Q_{s2} versus discharge distribution Q_1/Q_2 between side and main channel. Locations 4 and 6 lead to side channel silt up (in red); Locations 15 and 17 lead to side channel erosion (in blue); location 10 leads to a dynamic balance showing a periodic behavior (in green).

3.4.2. Effects of altering the width ratio between side and main channel

The results of the long-term morphological simulations show that altering the width ratio does not change the final result. The trends are the same as in the base-case scenario (Figure 3.11): if the training wall starts in the upstream part of a hybrid bar the side channel silts up (Figure 3.11.a), instead, if the training wall starts in the downstream part of the same bar the side channel deepens and the main channel aggrades (Figure 3.11.c). If the training wall starts near the bar top, both channels remain open (Figure 3.11.b).

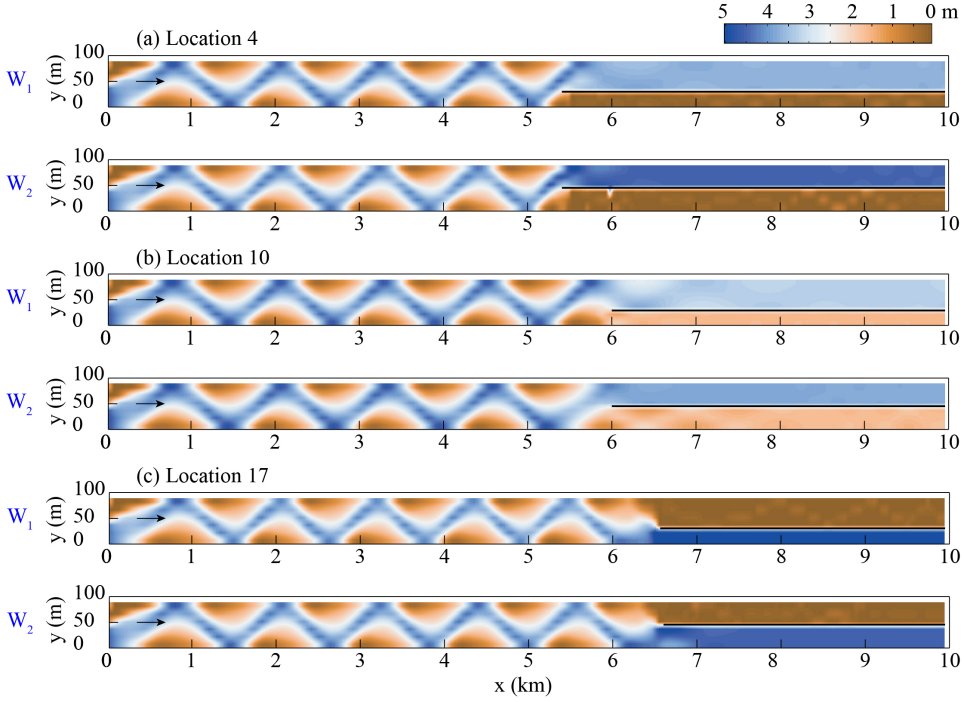

Figure 3.11: Results of different width ratios: water depth at the constant discharge of 200 m^3/s after 100 years (first 10 km after the transverse dam). (a) Training wall starting at Location 4. (b) Training wall starting at Location 10. (c) Training wall starting at Location 17.

Figure 3.12 shows the temporal variations of the proportion of total discharge that flows in the side channel (Q_1/Q_0) for various width ratios. If the training wall starts in the upstream part of a bar, the side channel silts up completely (Q_1/Q_0=0, dash-dot lines) as seen in the previous section. This happens for all considered width ratios, except for $B_1 : B_2$ = 1:1 (side and main channel having equal width) where the process is slower (red line) and does not result in complete closure of one of the channels. If the training wall starts in the downstream part of a bar, the side channel eventually conveys most water discharge (dash lines). It conveys 100% of

the water (main-channel closure) only for $B_1 : B_2$ = 1:5 (black line), whereas the main channel remains open for the larger width ratios ($B_1 : B_2$ = 1:2 and $B_1 : B_2$ = 1:1). However, also in these cases the side channel still conveys the major part of the discharge, with $Q_1/Q_0 > 0.95$. In the new equilibrium, bars are not observable in the deeper channel, whereas some low-amplitude bars are present in the silting-up channel. They are the remains of bars that formed during the transition period.

When the training wall starts near the bar top, both channels remain open (continuous lines). The larger the width ratio, the more water flows through the side channel. These results suggest that enlarging the width ratio increases the stability of the bifurcation.

In general, the evolution with constant discharge is relatively fast. When it does not reach a dynamic balance, it reaches the dominant configuration in which one of the parallel channels silts up within the first 14 years.

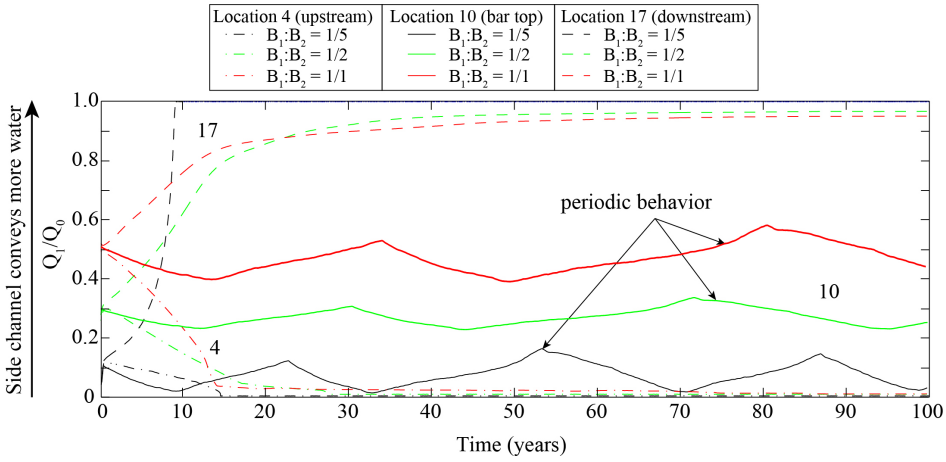

Figure 3.12: Temporal evolution of the ratio between the discharge entering the side channel and the total discharge Q_1/Q_0 for different width ratios. The dash-dot lines correspond to the cases in which the training wall starts at the upstream location, the continuous lines to the bar top location, and the dash lines to the downstream location.

3.4.3. Effects of variable discharge

A set of runs was carried out to study the effects of variable discharge on bifurcation stability, considering that flow variations can influence the bar location and geometry as well as the sediment distribution between the two channels. As in the previous set of runs, three different width ratios were considered: $B_1 : B_2$ = 1:5 (base-case scenario), $B_1 : B_2$ = 1:2, and $B_1 : B_2$ = 1:1. The following three starting locations were analysed: 4 (upstream of bar top), 10 (bar top), and 17 (downstream of bar top), see Figure 3.7.

The reference case with variable flow started with a flat bed. The bars that formed after 100 years can be recognized from Figure 3.13, showing their evolution

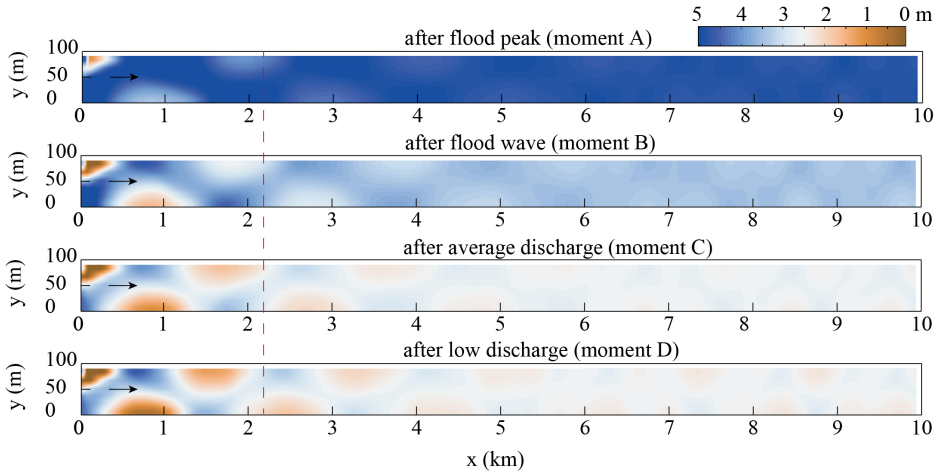

Figure 3.13: Reference case without longitudinal wall: evolution of water depth with variable discharge during the 100th year. The yearly hydrograph is shown in Figure 3.6. The figure shows the first 10 km after the transverse dam. The dash line identifies the initial location of the second bar top.

during the tenth year due to discharge variations. Bars tend to disappear at peak discharge (Q = 590 m^3/s), when the width-to-depth ratio is the minimum (B/h = 15). At peak discharge low-amplitude migrating bars are observable in the straight reach with the exception of a forced bar near the transverse wall and a strongly damped hybrid bar further downstream at the opposite side. Bars start to reform after the peak discharge since small-amplitude bars are already visible at the end of the flood wave, at a discharge of Q = 267 m^3/s, when the width-to-depth ratio has increased to B/h = 25. It can be observed that the small migrating bars are gradually suppressed by a series of longer hybrid bars forming downstream of the transverse wall. After the period characterized by the average discharge (Q = 200 m^3/s), the small migrating bars are still present and with larger amplitude. They are further suppressed in the low-discharge period (Q = 151 m^3/s). The results show that the bar wave length increases whereas the bar amplitude decreases with the discharge. This is valid for both hybrid and free migrating bars. Table 3.4 presents bar development under variable discharge.

The analysis of bar evolution shows that, influenced by the forcing offered by the transverse wall, the first bar on the right side is the most stable one and the second bar on the right side has some variations in shape due to variable discharge. In order to observe clear effects of the variable discharge, the starting locations of the training wall refer to the second bar on the right side. Starting the longitudinal wall near one of the most downstream and variable bars could lead to different conclusions.

The results of the simulations with the longitudinal wall starting from the bed topography at the end of the tenth year of the reference case show bed evolution

Table 3.4: Bar development under variable discharge.

Q (m^3/s)	Period	B/h	Hybrid bars		Free migrating bars	
			Amplitude (m)	Wavelength (m)	Amplitude (m)	Wavelength (m)
590	Peak discharge	15	0.5	2200	0.3-1.5	1000-2000
267	End of flood wave	25	0.6-0.8	2000-2100	0.3-2.0	800-1400
200	Average discharge	30	0.9-1.2	1800-1900	0.5-2.5	600-1200
151	Low discharge	36	1.4-1.8	1600-1700	0.8-2.5	600-1400

trends that are similar to the cases with constant discharge (Figure 3.14): if the training wall starts in the upstream part of a steady bar the side channel silts up (Figure 3.14.a), whereas if the training wall starts in the downstream part of the same bar the side channel deepens (Figure 3.14.c). However, if the training wall starts near the bar top, the evolution is similar to the case in which the wall starts in the upstream part of the bar.

Figure 3.14 shows the water depth at the end of the 100th year at low flow for different width ratios. It might give the impression that one of the parallel channels always silts up completely but that is not true, since the plots refer to the final bed configuration at low flow condition. Figure 3.15 shows the temporal evolution of the ratio of side-channel discharge to total discharge (Q_1/Q_0). During the first 30 years, both channels remain open. From the 31st year on, both channels remain open during high flow, whereas one of the channels closes during low flow. The parallel-channel system does not find a dynamic equilibrium as occurs with a constant discharge if the training wall starts at Location 10 which is located at 2.2 km from the transverse wall (Figure 3.13, dash line). The conveyance of the silting channel slowly diminishes with time to reach a constant value after 70 years. This could be explained by the longitudinal variation of the reference bar shape due to variable discharge (Figure 3.13): the location of the initial bar-top is situated in the upstream part of a bar during average to moderate discharge and in a pool at the highest discharge, but for a relatively short duration.

3.4.4. Sensitivity analysis on the effects of transverse bed slope

A sensitivity analysis was carried out to assess the dependence of bifurcation stability on transverse bed slope, by increasing and decreasing its effects on sediment transport direction. This was obtained in the model by applying Koch and Flokstra [35]'s formulation, extended for the effect of bedforms, according to which the function $f(\theta)$ is calculated as:

$$f(\theta) = A_{sh}\theta^{B_{sh}}\left(\frac{D}{H}\right)^{C_{sh}} \tag{3.2}$$

where A_{sh}, B_{sh} and C_{sh} are calibration coefficients and θ represents the Shields parameter. The ratio D/H accounts for the effects of bedforms. Among the three parameters, A_{sh} is the most sensitive one. Increasing the value of A_{sh} decreases

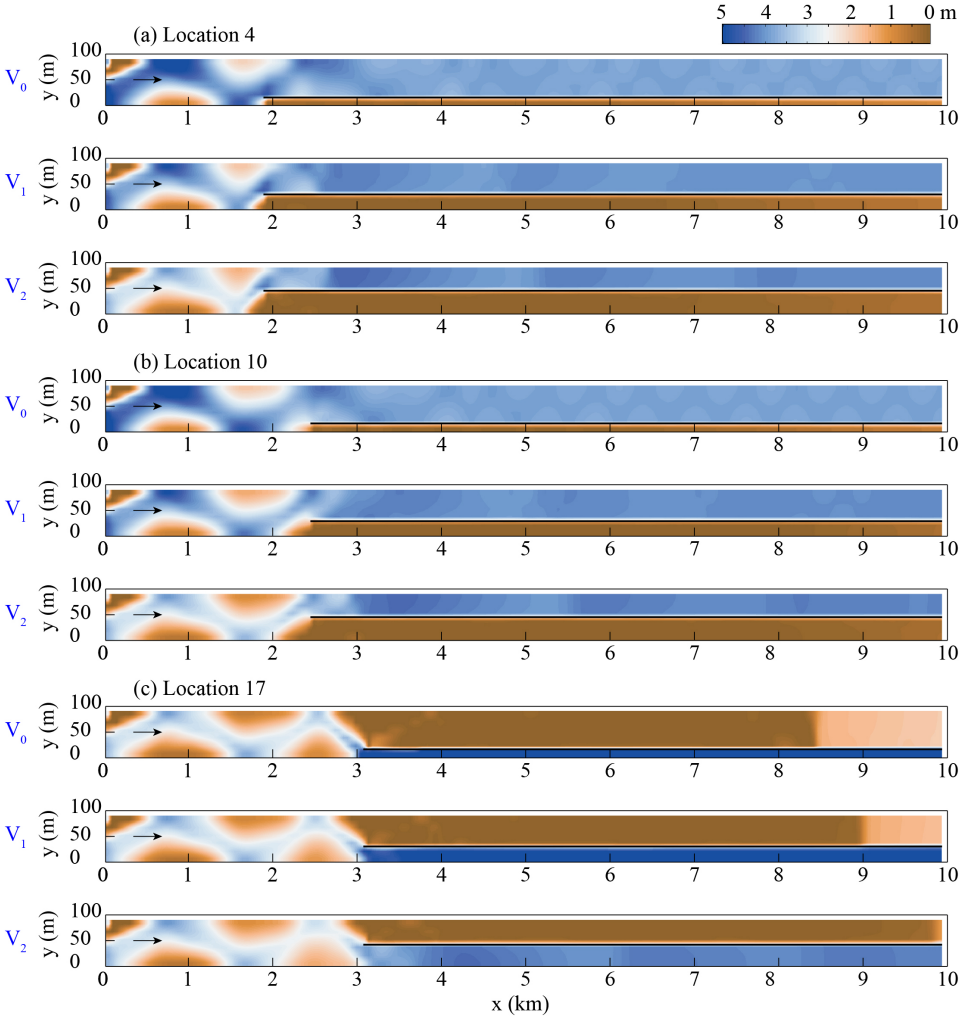

Figure 3.14: Results of variable discharge runs for different width ratios: water depth under variable discharge after 100 years. (a) Training wall starting at Location 4 (upstream of bar top). (b) Training wall starting at Location 10 (bar top). (c) Training wall starting at Location 17 (downstream of bar top). The figure shows the first 10 km after the transverse dam.

the effects of transverse slope on sediment transport direction [30]. The value of A_{sh} normally falls in the range 0.5 to 1.5 and this is the range of values used for the sensitivity analysis, whereas the value of the other calibration coefficients is kept constant: B_{sh} = 0.5 and C_{sh} = 0.3 [39].

The numerical simulations show that, starting from a flat bed, different values of A_{sh} resulted in different bar characteristics. Analysing the values in Table 3.5,

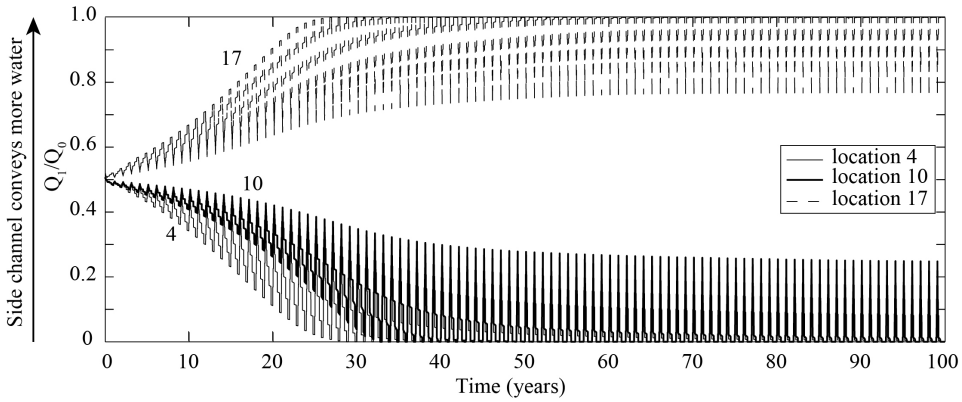

Figure 3.15: Evolution of discharge ratio for $B_1 : B_2$ = 1:1.

Table 3.5: Bar development with different magnitude of bed-slope effect.

A_{sh}	Bed slope effects	Bar amplitude (m)	Bar wavelength (m)	Duration of morphological evolution (days)	
				Location 4 (Upstream)*	Location 17 (Downstream)**
0.5	↑	0.95	1280	7130	3520
0.6		1.22	1350	6490	3070
0.7		1.82	1290	5760	2910
0.8		1.95	1200	5240	2840
0.9		2.03	1180	4630	2750
1.0		2.08	1175	3860	2630
1.1		2.15	1170	3810	2540
1.2		2.22	1165	3720	2420
1.3		2.25	1160	3660	2370
1.4		2.33	1140	3590	2360
1.5		2.27	1130	3570	2340

* Side channel silt-up
** Side channel erosion

we can observe that the bar wavelength increases if the bed slope effects increase (decreasing A_{sh}), whereas the opposite trend can be observed for the bar amplitude (stronger bed slope effects result in smaller amplitudes). Based on the equilibrium state, two locations for the starting point of the longitudinal training wall were selected: Location 4 in the upstream part of a bar and Location 17 in the downstream part. The results show that varying the effect of bed slope did not change the final configuration of the bifurcating channels. A training wall starting at Location 4 always resulted in side channel silt-up whereas a training wall starting at Location 17 always resulted in side channel erosion. However, stronger bed slope effects resulted in slower morphological evolution (Table 3.5), which is probably due to the smaller bar amplitude resulting in more equal sediment distribution between the channels.

3.4.5. Sinuous planform

In this section, the numerical simulations represent a sinuous channel with constant discharge of 200 m^3/s. In the reference case without longitudinal wall, point bars naturally formed near the inner bank of bends (Figure 3.16.a). The longitudinal training wall was set only after the point bars were fully-formed. Three locations for its starting point were selected: Location 4, in the upstream part of a point bar, Location 10 near the bar top and Location 17, in its downstream part. The obtained final configurations are shown in Figure 3.16. The results are similar to the ones obtained with a straight channel (Figure 3.8), indicating that the curvature of the channel and the presence of a relatively strong spiral flow [37] do not change the unstable character of the bifurcation created by a longitudinal training wall. The results indicate that the effects of the spiral flow are less important for the sediment transport direction and the sediment distribution between side and main channel than the main flow deviation and the bed slope caused by the presence of the point bar, at least in the cases examined.

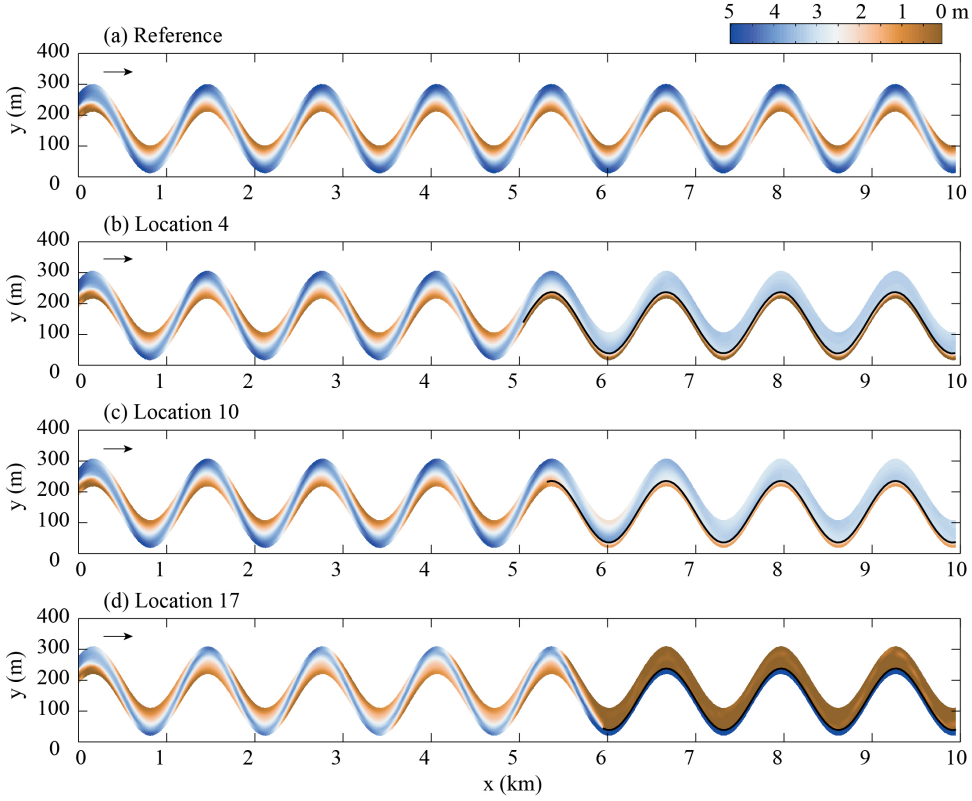

Figure 3.16: Sinuous channel simulations: water depth at the constant discharge of 200 m^3/s after 100 years. (a) Reference case without longitudinal training wall. (b) Training wall starting at Location 4 (upstream part of a point bar). (c) Training wall starting at Location 10 (bar top). (d) Training wall starting at Location 17 (downstream part of a point bar).

3.5. Discussion

In the previous sections, attention was paid to rather schematized and idealized examples. For more realistic applications a few aspects should be considered.

Cell drying was obtained numerically in a rather straightforward way, depending on an assigned critical local water depth. We believe that the areas that become completely dry under constant discharge in the numerical simulations would still convey some water in reality. The experimental study carried out by Le *et al.* [4] supports this, because aggrading channels were never found to silt up completely.

All tests were carried out with sediment transported as bed load. The results might be different in presence of substantial amounts of suspended load. This remains open for further research.

Keeping a constant value of the bed roughness, represented in the models by the Chézy coefficient, may have altered the dynamics of the system. The bed roughness should be a function of water depth, becoming gradually higher in the aggrading channel and lower in the deepening one. Similarly the bed roughness should vary with the discharge.

The numerical grid used in the computations contains six cells in the cross-section. Because two-dimensional aspects of water flow and sediment transport are important for bifurcation studies, we also performed other computational tests (not shown here) with 18 cells. The results of the finer grid confirmed the morphological developments obtained with the coarser grid. For this reason, we decided to use the coarser grid, which allowed for the computation of many different scenarios (in total 102 model runs).

An important issue in morphodynamic modelling is the use of a morphological factor (MF) which accelerates the bed development and decreases the computational time. In this study, we applied MF=10, but only for the cases with constant discharge, after having checked that it does not affect the results in a relevant way. To check this, we performed a computation using MF=1 (no morphological acceleration) and obtained after 10 years results that did not differ, when plotted, in an observable way from the results of one year using MF=10. For variable discharge, we represented the yearly hydrograph in a schematic way and performed the computation without any morphological acceleration. In this way we could distinguish the yearly effects of the variable discharge.

In computations with a constant discharge, the time corresponding to the morphological developments is merely theoretical. Using a morphological acceleration factor larger than 1 (after having checked that it does not affect the results) therefore does not affect the interpretation of the results, since the link with time is not clear anyway. With variable discharge, especially if a yearly hydrograph is used, applying a morphological acceleration factor larger than 1 creates an unclear distortion of time and hampers the interpretations of time developments. For this reason, we discourage the use of morphological acceleration in computations with variable discharge.

Redolfi *et al.* [3] investigated the stability of a symmetrical bifurcation under steady flow conditions, disregarding the presence of alternate bars in the main channel. This symmetrical configuration becomes unstable if the original (not yet

bifurcated) channel is at super-resonant conditions, because due to morphodynamics influence, a steady alternate bar forms just upstream of the bifurcation point. This bar tends to unbalance the flow and sediment partition between the bifurcating channels.

In the unsteady flow computations performed here, the width-to-depth ratio falls below the critical value for bar formation during peak flows and for this reason bars tend to disappear (Figure 3.13). At the end of the flood wave hybrid bars are incipient and short migrating bars are present. Hybrid bars are fully developed after the low-flow period, although some bar irregularities are present due to the interactions with remains of free bars. The conditions at average discharge, occurring after the flood wave, are close to resonance and at the lowest discharge the systems is super-resonant. According to Zolezzi and Seminara [7], upstream morphodynamic influence may occur only at the lowest flow rates. However, we do not observe any steady bar interfering with hybrid bars near the bifurcation at the end of the low-flow period. This is a sign of possible hybrid-bar dominance. As a consequence, we can conclude that upstream morphodynamic influence does not affect bifurcation stability at the conditions considered in this study.

Hypothetically, if super-resonant conditions were present for a longer period, i.e. also at higher discharges, a steady bar might develop near the bifurcation. In this case, the stability of the channel system would be determined by the competition between the steady bar at the node and the hybrid bars in the channel. Further investigations are needed to show at which conditions one of the two would prevail.

3.6. Conclusions and recommendations

This work addresses the stability of the system of two parallel channels separated by a longitudinal training wall. The effects of hybrid (steady) alternate bars near the bifurcation point on their morphological evolution have been investigated by means of a 2D numerical model developed using the Delft3D code.

The results of the numerical simulations show that the two-channel system with a training wall along one side of the river tends to become unstable, with the silting up of either the narrower side channel or the wider main channel. These results are valid for both straight and sinuous channels, with either constant or variable discharge. The results of the numerical simulations show three final scenarios, depending on the starting location of the longitudinal walls. In the first scenario, the training wall starts in the upstream part of a bar. In this case, all water flow eventually concentrates in the main channel and, as a result, the side channel gradually silts up. In the second scenario, the training wall starts in the downstream part of a bar. In this case, all water is eventually conveyed by the side channel and as a result the main channel gradually silts up. If the training wall starts in a limited area near the bar top, both channels reach a dynamic balance and remain open. However, this third scenario only occurs for constant discharge, since discharge variability results in the silting up of one channel in this case too. This is caused by the elongation and shortening of the bars that result from the discharge variations.

Changing the widths of the parallel channels did not change the trends observed in the base-case scenario. The most stable system is obtained if the longitudinal

wall subdivides the river in two equally-wide parallel channels. In this case, the morphological process appears much slower than in the other cases and the channel characterized by bed level rise does not appear to silt up completely.

This study shows that, in rivers with hybrid bars, the position of the upstream end of the training wall plays an important role in the morphological development of the system. Our results indicate that the upstream end of a training wall is best located near the top of a bar. This can be readily understood from the physical processes at the bifurcation. Bifurcation instability arises when the supply of sediment to a branch deviates from the transport capacity immediately downstream. Two factors play a role. First, this deviation between supply and transport capacity is smallest in river sections without streamwise gradients in flow field and bed topography, where lateral exchanges are at a minimum. Such sections are found at bar tops and in bar troughs. Second, deviations between sediment supply and transport capacity produce faster morphological changes in deeper areas where sediment transport is higher. Small deviations thus produce faster loss of stability in bar troughs than at bar tops. That makes bar tops the most suitable locations for the bifurcation. Yet, this does not guarantee stability in natural rivers where hybrid and point bars continuously change in length and position due to discharge variations [40], which means that the location of the training wall relative to a bar continuously changes with time. The upstream entrance of the side channel might therefore require an appropriate bank-line configuration or a control structure to enforce a favorable location since the first hybrid bars near a forcing are the most stable ones.

Discharge variations and the arrival of free migrating bars may produce cyclic growth and decay of bifurcated channels [6, 38]. Our findings suggest, however, that such cycles may also arise spontaneously as inherent system behavior if the development of bifurcated channels alters the relationship between sediment transport ratio and discharge ratio, e.g. expressed as a change in k (Equation 3.1).

The simulated systems were super-resonant, but close to resonant conditions [32]. In this case, steady bars may form also upstream of the bifurcation, due to the flow perturbation caused by the start of the longitudinal wall [3]. The obtained results, however, do not always show upstream influence of the bifurcation point, apart from a local bed deformation extending to a distance upstream on the order of magnitude of 3 bar wave-lengths (Figure 3.8). No bars formed upstream of the transverse forcing wall that was placed to generate a series of hybrid bars downstream.

In general, the evolution with constant discharge is faster than the evolution with variable discharge. This is because with constant discharge, location and size of the bar close to the bifurcation did not change and transported sediment was permanently deviated in the same way. With variable discharge, the bar tended to disappear during peak flows and the deviation of sediment towards the silting up channel was not always present. In our numerical simulations, when it does not reach a dynamic balance, the final bed configuration is obtained within the first 14 years. With variable discharges, the final configuration is obtained after 70 years (Figure 3.15). This result suggests that, in real rivers with natural discharges, the

morphological development after the construction of a longitudinal training wall may last for a long time.

The bifurcation formed by a longitudinal training wall is inherently unstable, but we found the condition at which the morphological changes develop rather slowly, which makes the bifurcation manageable. As a result, we recommend designing longitudinal training walls in such a way that the upstream starting point is located at the top of a bar. The bar top location can be fixated by constructing a groyne or structure upstream. If this is not possible, the optimal location of the starting point could be obtained by carefully studying the variation in bar length due to discharge variability. Channel maintenance is minimized if the two channels have more or less the same width.

Acknowledgments

This work is sponsored by Vietnam International Education Development (VIED), project 911.

References

[1] T. B. Le, A. Crosato, E. Mosselman, and W. Uijttewaal, *On the stability of river bifurcations created by longitudinal training walls. numerical investigation,* Advances in Water Resources **113**, 112 (2018), https://doi.org/10.1016/j.advwatres.2018.01.012.

[2] A. de Heer and E. Mosselman, *Flow structure and bedload distribution at alluvial diversions,* in *River Flow*, Vol. 2004 (2004) pp. 801–806.

[3] M. Redolfi, G. Zolezzi, and M. Tubino, *Free instability of channel bifurcations and morphodynamic influence,* Journal of Fluid Mechanics **799**, 476 (2016), https://doi.org/10.1017/ifm.2016.389.

[4] T. B. Le, A. Crosato, and W. Uijttewaal, *Long-term morphological developments of river channels separated by a longitudinal training wall,* Advances in Water Resources **113**, 73 (2018), https://doi.org/10.1016/j.advwatres.2018.01.007.

[5] N. Struiksma, K. Olesen, C. Flokstra, and H. De Vriend, *Bed deformation in curved alluvial channels,* Journal of Hydraulic Research **23**, 57 (1985), https://doi.org/10.1080/00221688509499377.

[6] W. Bertoldi and M. Tubino, *River bifurcations: Experimental observations on equilibrium configurations,* Water Resources Research **43** (2007), 10.1029/2007wr005907, https://doi.org/10.1029/2007wr005907.

[7] G. Zolezzi and G. Seminara, *Downstream and upstream influence in river meandering. Part 1. General theory and application to overdeepening,* Journal of Fluid Mechanics **438**, 183 (2001), https://doi.org/10.1017/S002211200100427X.

[8] G. Zolezzi, M. Guala, D. Termini, and G. Seminara, *Experimental observations of upstream overdeepening,* Journal of Fluid Mechanics **531**, 191 (2005), https://doi.org/10.1017/s0022112005003927.

[9] E. Mosselman, M. Tubino, and G. Zolezzi, *The overdeepening theory in river morphodynamics: Two decades of shifting interpretations,* River Flow 2006 , 1175 (2006).

[10] E. Hansen, *On the formation of meanders as a stability problem. progress report 13,* Coastal Engineering, Laboratory, Techn. Univ. Denmark, Basis Research (1967).

[11] R. Callander, *Instability and river channels,* Journal of Fluid Mechanics **36**, 465 (1969), https://doi.org/10.1017/S0022112069001765.

[12] F. Engelund, *Instability of erodible beds,* Journal of Fluid Mechanics **42**, 225 (1970).

[13] F. Engelund and O. Skovgaard, *On the origin of meandering and braiding in alluvial stream.* J. Fluid Mech. **57**, 289 (1973).

[14] G. Parker, *On the cause and characteristic scales of meandering and braiding in rivers,* Journal of fluid mechanics **76**, 457 (1976).

[15] J. Fredsøe, *Meandering and braiding of rivers,* Journal of Fluid Mechanics **84**, 609 (1978).

[16] S. Lanzoni, *Experiments on bar formation in a straight flume; 1. uniform sediment,* Water Resour. Res. **36**, 3337 (2000).

[17] A. Crosato and E. Mosselman, *Simple physics-based predictor for the number of river bars and the transition between meandering and braiding,* Water Resources Research **45** (2009), 10.1029/2008WR007242, https://doi.org/10.1029/2008WR007242.

[18] N. Struiksma and A. Crosato, *Analysis of a 2-D Bed Topography Model for Rivers* (Wiley Online Library, 1989) ISBN 0-87590-316-9.

[19] G. Duró, A. Crosato, and P. Tassi, *Numerical study on river bar response to spatial variations of channel width,* Advances in Water Resources **93**, 21 (2015), https://doi.org/10.1016/j.advwatres.2015.10.003.

[20] C. Flokstra, *De invloed van knooppuntsrelaties op de bodemligging bij splitsingspunten.*, Report R2166 (Waterloopkundig Laboratorium (WL | Delft Hydraulics), 1985) (in Dutch).

[21] Z. B. Wang, R. J. Fokkink, M. de Vries, and A. Langerak, *Stability of river bifurcations in 1D morphodynamic models,* Journal of Hydraulic Research **33**, 739 (1995).

[22] F. Engelund and E. Hansen, *A monograph on sediment transport in alluvial streams*, Tech. Rep. (TEKNISKFORLAG Skelbrekgade 4 Copenhagen V, Denmark., 1967).

[23] M. Bolla Pittaluga, R. Repetto, and M. Tubino, *Channel bifurcation in braided rivers: Equilibrium configurations and stability,* Water Resources Research **39**, 1046 (2003), https://doi.org/10.1029/2001WR001112.

[24] M. G. Kleinhans, H. R. A. Jagers, E. Mosselman, and C. J. Sloff, *Bifurcation dynamics and avulsion duration in meandering rivers by one-dimensional and three-dimensional models,* Water Resources Research **44**, W08454 (2008), https://doi.org/10.1029/2007WR005912.

[25] W. Bertoldi, L. Zanoni, S. Miori, R. Repetto, and M. Tubino, *Interaction between migrating bars and bifurcations in gravel bed rivers,* Water resources research **45** (2009), 10.1029/2008WR007086, https://doi.org/10.1029/2008WR007086.

[26] C. F. van der Mark and E. Mosselman, *Effects of helical flow in one-dimensional modelling of sediment distribution at river bifurcations,* Earth Surface Processes and Landforms **38**, 502 (2013), https://doi.org/10.1002/esp.3335.

[27] M. Colombini, G. Seminara, and M. Tubino, *Finite-amplitude alternate bars,* J. Fluid Mech. **181**, 213 (1987), https://doi.org/10.1017/S0022112087002064.

[28] Deltares, *Simulation of multi-dimensional hydrodynamic flows and transport phenomena, including sediments. User Manual Hydro-Morphodynamics Version: 3.15.34158 28, May 2014.*, edited by Deltares (Deltares, 2014) https://oss.deltares.nl/documents/183920/185723/Delft3D-FLOW_User_Manual .pdf.

[29] A. Defina, *Numerical experiments on bar growth,* Water Resour. Res. **39**, 1092 (2003), https://doi.org/10.1029/2002WR001455.

[30] F. Schuurman, W. A. Marra, and M. G. Kleinhans, *Physics-based modeling of large braided sand-bed rivers: Bar pattern formation, dynamics, and sensitivity,* Journal of geophysical research: Earth Surface **118**, 2509 (2013), https://doi.org/10.1002/2013JF002896.

[31] U. Singh, A. Crosato, S. Giri, and M. Hicks, *Sediment heterogeneity and mobility in the morphodynamic modelling of gravel-bed braided rivers,* Advances in Water Resources **104**, 127 (2017), https://doi.org/10.1016/j.advwatres.2017.02.005.

[32] P. Blondeaux and G. Seminara, *A unified bar-bend theory of river meanders,* Journal of Fluid Mechanics **157**, 449 (1985), https://doi.org/10.1017/S0022112085002440.

[33] E. Mosselman and T. B. Le, *Five common mistakes in fluvial morphodynamic modeling,* Advances in Water Resources **93**, 15 (2016), https://doi.org/10.1016/j.advwatres.2015.07.025.

[34] R. A. Bagnold, *An approach to the sediment transport problem from general physics* (Washington : U. S. Govt. Print. Off, 1966) https://doi.org/10.1017/S0016756800049074.

[35] F. Koch and C. Flokstra, *Bed Level Computations for Curved Alluvial Channels: Prepared for the 19th IAHR Congress, New Delhi, India, February 1981* (Waterloopkundig Laboratorium, 1981).

[36] A. Crosato, E. Mosselman, F. B. Desta, and W. S. J. Uijttewaal, *Experimental and numerical evidence for intrinsic nonmigrating bars in alluvial channels,* Water Resour. Res. **47**, W03511 (2011), https://doi.org/10.1029/2010WR009714.

[37] W. Ottevanger, *Modelling and parameterizing the hydro- and morphodynamics of curved open channels*, phdthesis, Delft University of Technology, Hydraulic Engineering (2013), https://doi.org/10.4233/uuid:9f19d0ea-5d89-4c15-b99d-3fb02fc28eb7.

[38] K. Hirose, K. Hasegawa, and H. Meguro, *Experiments and analysis on mainstream alternation in a bifurcated channel in mountain rivers,* River, Coastal and Estuarine Morphodynamics, Sanchez-Arcilla A, Bateman A (eds). IAHR: Madrid , 571 (2003).

[39] A. Talmon, N. Struiksma, and M. V. Mierlo, *Laboratory measurements of the direction of sediment transport on transverse alluvial-bed slopes,* Journal of Hydraulic Research **33**, 495 (1995), https://doi.org/10.1080/00221689509498657.

[40] N. Claude, S. Rodrigues, V. Bustillo, J.-G. Bréhéret, P. Tassi, and P. Jugé, *Interactions between flow structure and morphodynamic of bars in a channel expansion/contraction, loire river, france,* Water Resources Research **50**, 2850 (2014), https://doi.org/10.1002/2013WR015182.

4

Case study

Revisiting Waal River Training by Historical Reconstruction

The Dutch River Waal, a branch of the Rhine, has been trained for centuries to mitigate the effects of ice-jams and improve navigation. The works, started in 1850 AD, involved river straightening and narrowing by series of transverse groynes. Besides fulfilling their goal, the groynes also created the need to raise flood protection works and caused undesirable channel incision. We assess here the effectiveness of training the river with a longitudinal wall instead of with groynes. The investigation analyses the long-term response of the historical river with a 2DH morphodynamic model. The results show that the wall would create two parallel channels, one becoming deeper and the other one shallower. The former would be as suitable for navigation as an equally-wide channel obtained with groynes. The latter would contribute in conveying water during high flow events and improve the river ecology. Training the river with a wall would also lessen channel incision. The best performance is obtained if the wall is built on the channel centerline, starting just upstream of a point bar top.

This chapter is submitted to **Journal of Hydraulic Engineering (2018)** [1].

4.1. Introduction

4.1.1. Background information

The frequency of dike breaches and flooding increased along the Waal River, a branch of the Rhine, in the early modern period. At least 29 out of 51 river dike breaches between 1757 and 1926 were provoked by ice jams [2, 3]. As these ice jams formed preferentially at wider shallow sections with bars and islands, it was decided to give the river a narrow uniform width of 360 m using series of transverse groynes. The prescribed uniform width was called "normal width" and the corresponding river training programme "Normalization". The First Normalization (1850-1880) for the safe conveyance of ice, water and sediment was soon followed by further width reduction of the River Waal, this time to improve navigability: 310 m in the Second Normalization (1880-1893) and 260 m in the Third Normalization (1910-1916), when, next to narrowing, the river was also straightened and dredged. Figure 4.1 shows the different phases of the Normalization programme with a noticeable increase in the number of groynes over time.

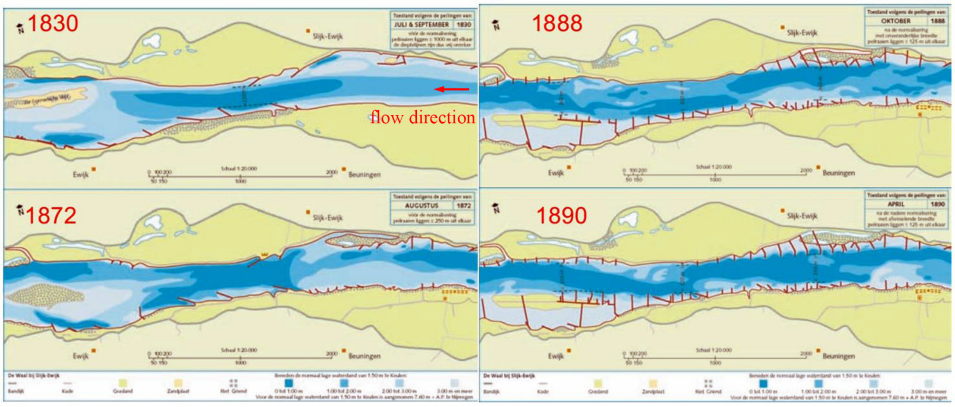

Figure 4.1: Normalization of the River Waal by straightening and narrowing by series of groynes (Source: Rijkswaterstaat – ministry of Public Works, the Netherlands). Red arrow indicates the flow direction, i.e. from right to left.

The morphological response of the river to narrowing, straightening and sediment extraction resulted in an incision process that reached the rate of 2 cm/year [4]. Besides floodplain draining and deterioration of riparian habitats, the lowering of the channel bed also posed problems to the hydraulic structures along the river, including the groynes. The conditions for navigation gradually deteriorated, because the connection between the river and the other elements of the inland waterway network, such as canals, ship locks and fluvial port facilities, became problematic. In addition, the presence of transverse groynes resulted also in other negative effects. For instance, groynes produce shallow ridges as a response to the formation of scour holes at their heads, which hampers navigation even further [5] and hinder the flow at high discharges forcing the water level to increase.

In 2013-2015, three series of transverse groynes were replaced by longitudinal training walls near Tiel, as an attempt to mitigate these effects (Figure 4.2). The main idea of this pilot project was to create a narrow and sufficiently deep navigation channel at low flows and a two-channel system to convey water at high flows, which would reduce the channel incision process and lower water levels. The new channel behind the training wall was expected improve the river ecological conditions, because it would form a freely flowing stream without intensive shipping traffic and with a more natural unprotected bank. Removing the groynes would finally also eliminate the problem of the shallow ridges that hamper navigation. However, the effectiveness of these interventions in achieving the goals has not been thoroughly investigated yet, particularly on the long-term.

Figure 4.2: Longitudinal training wall replacing transverse groynes in the Waal River near Tiel. Source: Rijkswaterstaat.

Navigation is common in low-land rivers, like the Waal, especially in the final part of their course, close to the sea. The bed of these rivers often presents bars and point-bars inside bends. These large sediment deposits are characterized by transverse bed slopes and produce helical flows, with the result that they locally modify the sediment transport direction and in particular the bed load direction. The presence of a nearby bar is thus expected to alter the distribution of sediment at the bifurcation created by the longitudinal training wall and hence to influence bifurcation stability (e.g. [6]). Le *et al.* [7, 8] carried out a series of experimental tests as well as numerical simulations showing that the parallel-channel system created by a longitudinal training wall tends to be unstable. The most stable configuration is obtained with equally-wide parallel channels. Both channels remain open, one deeper and one shallower, if the upstream end of the wall is located near the top of a steady alternate-bar or point-bar that is located at the same side of the river.

This work aims to assess the effectiveness of having a longitudinal training wall instead of groynes in the Waal River. In particular, we investigate the possibility of obtaining a navigation channel and increasing the water conveyance during high

flows by placing a longitudinal wall on a reach of the historical Waal River with a numerical model. The start year of the simulations is 1842, a short time before the beginning of the Normalization works, when the river channel was almost twice as wide as now. The large natural width of the historical Waal allows splitting the river in two equally-wide channels, each of them being large enough to potentially become a deep inland water way. The other channel, expected to become much shallower and with a natural bank, seems suitable to eventually host a richer riverine ecosystem than the current groyne fields. For this reason, we term here "navigation channel" the channel that becomes deeper and "ecological channel" the channel that becomes shallower. We analyze the effectiveness and convenience of training the river with a longitudinal wall by comparing the long-term morphological developments obtained with the wall to the ones obtained with series of groynes along both banks in a way similar to the current situation and to the "natural" development of the river (untrained case). We focus on channel incision, channel navigability and flood conveyance.

The long-term morphological responses are reproduced with a two-dimensional depth-averaged (2DH) model based on the open-source Delft3D code. The numerical approach adopted here is supported by Le et al. (2018a), who successfully reproduced the long-term morphological developments observed in an experimental channel separated by a longitudinal training wall; by Arboleda *et al.* [9], who simulated floodplain sedimentation in the historical Waal River; and by Vargas-Luna *et al.* [10], who successfully applied Baptist *et al.* [11]'s formulation for the assessment of the effects of floodplain vegetation on water levels.

4.1.2. Study area

The Waal River is the largest branch of the Rhine in the Netherlands, crossing the country from East to West. The study area is a 12 km long reach of the river between the cities of Nijmegen and Tiel (Figure 4.3), temporally placed in the first half of the nineteen century when the river was twice as large as now. The site was selected due to the availability of historical data. An old river map of 1800 AD showing the presence of three bars (Figure 4.3.a) and a set of 17 reconstructed cross-sectional profiles [12] allow for model calibration. Another map of the same area in 1842 AD, with 5 reconstructed cross-sectional profiles (Figure 4.3.b), allows for model validation and provides the start conditions for the simulations of the long-term morphological developments of the river trained either with a longitudinal wall or with groynes or without any training structures. Both historical maps fit well the current situation, showing their reliability (Figure 4.3.c). Note that the current river channel alignment is straighter than the original one.

In the study area, the pre-normalization channel width was approximately 400 m. By hypothetically dividing this channel in two equally-wide parts by means of a longitudinal wall we obtain one navigation and one ecological channel that are both 200 m wide. This width appears sufficient for navigation, considering that the current river width is 230-260 m.

The historical daily discharge time series were reconstructed by Arboleda *et al.* [9] based on the work of van Vuren [13] and they refer to the period 1790-1810.

From these time series we derived a daily mean discharge of 1,550 m^3/s, which is rather similar to the current value of 1,490 m^3/s, which we obtained from the time series of the period 2000-2010 (source: Rijkswaterstaat). The estimated historical bankfull discharge in the study area is 2,350 m^3/s. This value is smaller than the current one, which is approximately 300 m^3/s larger (it depends on location). This is mainly due to the channel incision process which has followed the normalization works.

In the early 1800s, the median sediment grain size was 850-1000 µm [12], slightly smaller than the present one [14, 15]. Arboleda *et al.* [9] showed that suspended solids concentrations were similar to the actual ones, ranging between 85 and 95 mg/l. The composition of suspended sediment being silt and fine sand [16].

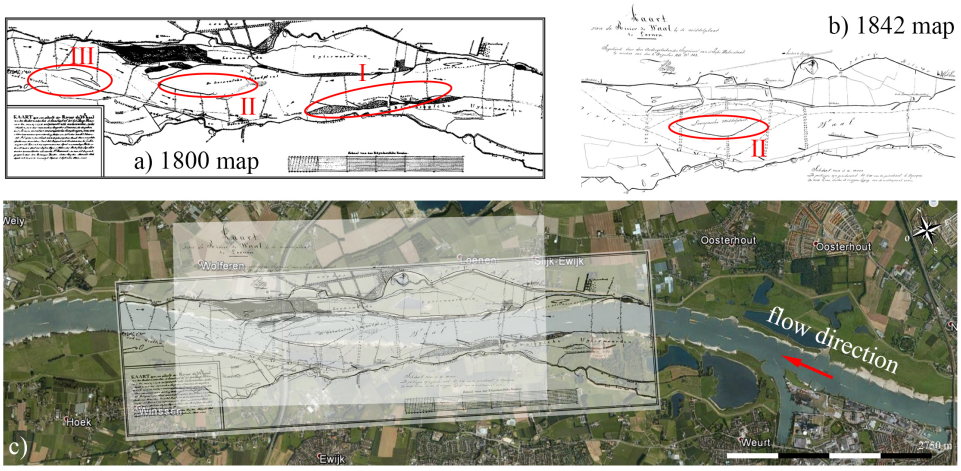

Figure 4.3: Study area: Waal River near Winssen, Slijk Ewijk and Weurt, between the cities of Nijmegen and Tiel. a) 1800 map. b) 1842 map. c) Historical maps superimposed on current situation (Google Earth © 2005). Bars are numbered I, II and III to be recognized and compared in the calibration and validation steps.

4.2. Materials and Methods

4.2.1. General description

The effectiveness and convenience of training the Waal River with a longitudinal wall are studied by means of a numerical model. The approach is to compare the long-term natural river evolution, i.e. without any interventions, with the long-term river adjustments to either a longitudinal wall or transversal groynes focusing on river navigability, high flow conveyance and channel incision. In this study, the longitudinal wall subdivides the river in two equally-wide channels, as recommended by Le *et al.* [7, 8]. Two wall scenarios are considered: wall at the channel centerline starting upstream of point bar I top (Figure 4.3), and wall starting more

downstream. Two groyne-scenarios are considered:

1. channel width between groynes heads equal to the current Waal River width (260 m). In this case the comparison allows establishing whether the implementation of a longitudinal wall instead of the historical normalization works would have resulted in better conditions for navigation, high flow conveyance and river ecology in the present river.

2. channel width equal to the one of the navigation channel obtained with the longitudinal wall (200 m). This comparison allows analyzing the differences between the river adjustment to the wall and the river adjustment to the groynes for the same navigation channel width.

The considered temporal scale corresponds to the time needed to achieve morphodynamic equilibrium. This is the condition in which the long-term temporal changes of 2D and 1D bed topography (bar configuration and longitudinal slope) become negligible. The morphodynamic models used for the investigation are built from Arboleda *et al.* [9]'s setup, who reconstructed the historical Waal River using the open-source Delft3D code, but include some important modifications, as for instance having a mobile instead of a fixed main channel bed.

Delft3D solves the Reynolds equations for incompressible fluid and shallow water in three dimensions with a finite-difference scheme [17]. The sediment transport rates are computed by means of sediment transport capacity formulas. The bed level changes are either derived by applying the Exner approach, i.e. by assuming immediate response of the sediment transport rate to the local hydraulic conditions, which is valid only for bed load, or by applying a sediment balance equation in which sediment deposition and entrainment rates are obtained from suspended solids concentrations, hydrodynamic parameters and soil characteristics. The evolution of suspended solids concentration is computed with an advection-diffusion equation. In this study we assume sediment to be transported as bed load and apply the Exner approach. The effects of transverse slope and spiral flow on bed load direction are important for the simulation of the evolution of the river bed topography [18], in particular for the reproduction of bars (e.g. [19]) and to simulate the sediment distribution between bifurcating channels (e.g. [20]). For the combined effect of transverse slope and spiral flow, Struiksma *et al.* [21] derived the direction β_s of sediment transport (bed load) as:

$$tan\beta_s = \frac{sin\beta_\tau - \frac{1}{f(\theta)}\frac{\delta z}{\delta y}}{cos\beta_\tau - \frac{1}{f(\theta)}\frac{\delta z}{\delta x}} \tag{4.1}$$

where $\delta z/\delta y$ is the transverse slope; $\delta z/\delta x$ is the streamwise slope; β_τ is the bed shear stress; $f(\theta)$ is a function to account for the effects of transverse bed slope on bed load direction, in which θ represents the Shields parameter. Considering the effects of spiral flow, which become relevant if the stream lines have a sinuous path, as in channel bends and around bars, the bed shear stress (β_τ) is derived as follows [21]:

$$\tan \beta_\tau = \frac{v}{u} - A\frac{h}{R} \tag{4.2}$$

where u and v are the streamwise and transverse velocity, respectively (m/s); h is the local water depth (m); R is the streamline radius of curvature (m); A is a coefficient that weights the influence of the spiral flow, derived as follows [21]:

$$A = \frac{2\varepsilon}{\kappa^2}\left(1 - \frac{\sqrt{g}}{\kappa C}\right) \tag{4.3}$$

with ε (≈ 1) being a calibration coefficient (in this study ε = 1), κ (= 0.4) being the Von Kármán constant, g and C being the acceleration due to gravity (m/s^2) and the Chézy roughness coefficient (m$^{1/2}$/s), respectively.

The function $f(\theta)$ is derived by applying the formulation suggested by Koch and Flokstra [22], extended by Talmon *et al.* [23]:

$$f(\theta) = A_{sh}\theta^{B_{sh}}\left(\frac{D}{H}\right)^{C_{sh}} \tag{4.4}$$

where D_{50} is the median sediment size and A_{sh}, B_{sh} and C_{sh} are calibration coefficients, with A_{sh} being the most sensitive one with a value that normally falls between 0.1 and 1.0. The effects of transverse slope on sediment transport direction decrease if the value of A_{sh} increases [19] and vice versa. A sensitivity analysis is carried out in the framework of this study to assess the effects of transverse bed slope by varying the value of A_{sh} whereas the values of the other calibration coefficients are kept constant with the values suggested by Talmon *et al.* [23]: B_{sh} = 0.5 and C_{sh} = 0.3.

In the morphodynamic model, the drying/wetting of cells is obtained based on the value of the local water depth. The cells that become dry are removed from the computational domain and remain dry until higher discharge floods them again. Dry cells may also re-become wet by bank erosion, but this is not considered in our computations. In this study, the threshold value below which cells become dry is 10 cm.

In presence of vegetation, as for instance on flood plains during high flow events, the Delft3D code corrects the local Chézy coefficient according to Baptist *et al.* [11]'s formulation:

$$C = \frac{1}{\sqrt{\frac{1}{C_b^2} + \frac{C_D n h_v}{2g}}} + \frac{\sqrt{g}}{\kappa} ln\left(\frac{h}{h_v}\right) \tag{4.5}$$

in which C_b is the bed roughness without vegetation (m$^{1/2}$/s), C_D is the drag coefficient associated with the vegetation type (-), for which Vargas-Luna *et al.* [24] suggest using the value of 1, corresponding to rigid cylinders; n is the vegetation density (m^{-1}), being $n = mD$, where m is the number of cylinders per unit area (m^{-2}) and D is the cylinder diameter (m); h_v is the vegetation height (m).

In the framework of this study, the following morphological model simulations are performed:

- Pre-runs: different model setups are run several times to check computational stability and to assess the time that is necessary to achieve morphodynamic equilibrium at the cross-sectional and reach scales (bar shape and longitudinal slope).
- Model calibration runs: starting with a flat (mobile) bed and with the (fixed) bank alignment and the other boundary conditions of 1800 AD, the model simulates the 2D development of the river bed topography for the time that is necessary to achieve morphodynamic equilibrium. The results are then compared to the bed topography measured in 1800 AD. The value of unvegetated-bed roughness coefficient is the one previously derived by Arboleda *et al.* [9]. The calibration parameter here is A_{sh} (Equation 4.4), weighing the effects of transverse slope on sediment transport direction, which strongly influences the 2D bed topography.
- Model validation run: starting from the measured bed topography of 1800 AD the model simulates the river bed evolution for 42 years. The results are then compared to the reconstructed bed topography of 1842 AD.
- Model run without any interventions (untrained river = base-case): starting with the reconstructed bed topography of 1842 AD, the model is run for the time that is necessary to achieve morphodynamic equilibrium.
- Model runs with longitudinal wall (wall scenarios): starting with the reconstructed bed topography of 1842 AD, the model is run for the time that is necessary to achieve morphodynamic equilibrium. Two starting points of the wall are considered, one upstream of point bar I top and one more downstream.
- Model runs with groynes (groyne scenarios): starting with the reconstructed bed topography of 1842 AD, the model is run for the time that is necessary to achieve morphodynamic equilibrium. Two scenarios are considered. In the first one the main river channel constrained by groynes has the same width as the current Waal River (260 m). The implemented series of groynes have the general characteristic of the ones that are currently present in the Waal River [5]: the groyne length protruding transversally to the flow in the river is 70 m on average; the groyne crest level is the same as the river bank level on average; and the groyne field length (distance between two subsequent groynes) is 200 m. In the second scenario the constrained channel is as large as the navigation channel in the wall scenarios (200 m). The groyne length protruding transversally to the flow is 100 m on average, whereas the other characteristics of the groynes are the same as in the first scenario. In both scenarios the channel alignment does not coincide with the present one, which has been straightened. Channel straightening would be an additional intervention leading to river adjustment and for this it is not considered here.

To compare the navigability and the high flow conveyance of the river in the different scenarios, the models are used again, this time with a fixed bed, to simulate the hydraulic conditions at selected values of the discharge (hydraulic models). For the Waal River, the discharge Q_{low} = 680 m^3/s is currently used as the lowest value for which it is necessary to guarantee a minimum navigation depth of 2.80 m for a channel width of 150 m. The discharge of Q_{design} = 10,600 m^3/s is strongly recommended for the design of flood protection works. Another important reference discharge corresponds to the 1995 flood: 8,000 m^3/s. These are the discharges considered in the hydraulic computations. The flow conveyance of the river is inferred by comparison of computed water levels at the same high discharge. Lower water levels indicate increased river conveyance whereas higher levels indicate decreased conveyance. The water levels are computed at a specific reference cross-section in the middle of the model domain.

4.2.2. Numerical model setup

The curvilinear grid follows the alignment of the historical main channel with the embankments being used as land boundaries. The modelled river reach is about 12 km long and 1 km wide on average, the width of the main channel (historical Waal River) being approximately 400 m. The models are built focusing on the main channel, which is described using a 40×20 m grid, finer than the grid used for the floodplains (40×40 m). This configuration allows having a sufficient amount of data points along the cross section with a reasonable computational time. Moreover, it also allows schematizing the longitudinal training wall in the middle of the main stream and the transversal groynes along the river banks in a realistic way. The morphological computations are not accelerated [25].

For the calibration run, the initial main channel bed and the floodplains are horizontal in transverse direction but sloping in longitudinal direction, with slope i_0 = 1×10^{-4}, the floodplains being 5.5 m higher than the channel bed. For the validation run, the initial bed topography is the one derived from the 1800 map (Figure 4.3). For the model simulations, the initial bed topography is the one derived from the 1842 map (Figure 4.3).

The upstream hydraulic boundary condition is flow discharge. A representative yearly hydrograph (Figure 4.4.b) is derived from the mean duration curve of the period 1790-1810 (Figure 4.4.a) obtained from the data provided by Arboleda *et al.* [9]. The total volume of transported sediment computed using the representative yearly hydrograph (Figure 4.4.b) remains unchanged compared to the one obtained using the mean yearly duration curve (dotted red line in Figure 4.4.a). The bed material, assumed uniform, has a diameter of 900 μm.

The representative yearly hydrograph is repeated every year for the entire duration of the computational period. The approach minimizes the problems related to model instability because it decreases the sudden inflow changes that are present in the reconstructed daily discharge time series, while maintaining the same yearly sediment transport rates and almost the same yearly discharge distribution. The same approach has been already successfully used for long term morphological simulations by, for instance, Yossef *et al.* [26]. The downstream hydraulic boundary

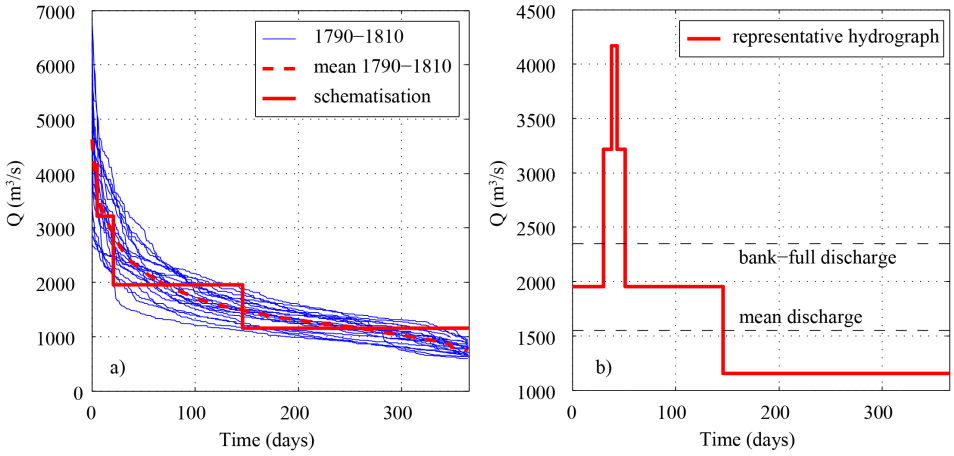

Figure 4.4: a) Yearly daily discharge duration curves, mean duration curve and schematized duration curve of the period 1790-1810. b) Representative daily discharge hydrograph used in this study.

condition is a flow-dependent water level. In this study the water level at the end of the model domain is assumed to coincide to the one corresponding to uniform flow.

The upstream boundary condition for the sediment component is balanced sediment transport (recirculation: input = output). The downstream boundary condition is given by the free sediment transport condition. This allows undisturbed bed level changes up to the end of the model domain. The bed-load transport rate is computed with the Engelund and Hansen [27] formula, valid for sand-bed rivers. The unvegetated bed roughness is represented by a constant Chézy coefficient, whereas the value of Chézy coefficient of vegetated areas is computed by applying Equation 4.5.

The distribution of floodplain vegetation cover is derived from the reconstructed ecotope maps of 1830 AD provided by Maas *et al.* [12], see Figure 4.5, and the vegetation parameters used in the model are the ones suggested by van Velzen *et al.* [28], see Table 4.1. The computations are carried out assuming that floodplain vegetation has not changed much in the 50 years covered by the simulations. The historical Waal River characteristics at average discharge are listed in Table 4.2.

Table 4.1: Selected vegetation types from typical floodplain vegetation [28]. The value of C_D, drag coefficient, is imposed equal to 1, following Vargas-Luna *et al.* [24]

Vegetation type	$h_v(m)$	$n(m^{-1})$	C_D (-)
Natural grass	0.1	21.6	1
Reed	2.5	0.6624	1
Softwood	10	0.042	1

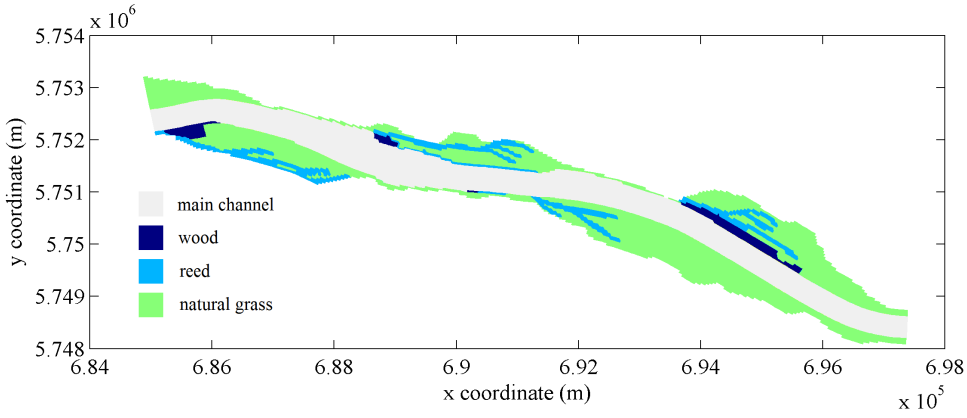

Figure 4.5: Spatially varying vegetation cover in 1830 AD according to historical ecotope maps [12]. Coordinates are in the Universal Transverse Mercator (UTM) system.

Table 4.2: Reach-scale characteristics of the Waal River at average discharge in 1800s and sources

Parameters	Notation	Unit	Value	Source
River width	B_0	m	400	Maas *et al.* [12]
Normal depth	h	m	6.0	Maas *et al.* [12]
Longitudinal bed slope	i_0	-	10^{-4}	Maas *et al.* [12]
Chézy coefficient	C	$m^{1/2}/s$	50	Arboleda *et al.* [9]
Froude number	Fr	-	0.160	This study
Shields parameter	θ	-	0.026	This study
Width-to-depth ratio	B/h	-	30 to 70	This study

4.2.3. Implementation of training wall and groynes

The longitudinal training wall is schematized as a local rise of the channel bed at the channel centerline having the same elevation as the river bank. The wall divides the river in two channels having the same width (200 m on average). This schematization allows the wall to emerge during low-flow conditions and to be submerged during high flows. Two scenarios for the longitudinal training wall are considered: in one the wall starts just upstream of point bar I top (Figure 4.3) and in the other one the wall starts near the downstream end of the same bar.

Groynes are schematized as a local rise of the channel bed in the center of a series of grid cells covering the transverse groyne length and being as high as the river bank. This configuration allows for groyne overtopping by high-water flows. Two scenarios are considered. In one scenario the flow width between the groyne heads is 260 m, the same as in the current situation. In the other scenario the flow width is 200 m, the same as the navigation channel of the wall scenarios.

4.3. Results

4.3.1. Pre-runs

These runs are meant to: assess the stability of the model vs. the time step and estimate the simulation time. In some of the pre-runs the value of the discharge is kept constant. The results show that a time step t = 0.5 minute ensures numerical stability and that after 50 years the system reaches a state of morphodynamic equilibrium. The computational time of a 50-year simulation is 5 to 6 days.

4.3.2. Model calibration and validation

Calibration is carried out to optimize the value of the most influencing parameter weighing the transverse bed slope effects on sediment transport direction, A_{sh} (Equation 4.4). Applying the boundary conditions, i.e. discharge hydrograph (Figure 4.4.b) and bank alignments of 1800 AD, for a period of 50 years, the computed channel bed finally reaches an equilibrium state, characterized by negligible temporal changes. The computed bed topography is then compared with the reconstructed bed topography from the 1800 map.

Figure 4.6 shows the results of model calibration. The computed bed topography presents three alternate bars in the main channel (Figure 4.6.b). These bars are present and have similar size in the reconstructed bed topography (Figure 4.6.a). Figure 4.6.c shows both the reconstructed cross-section A-A and the computed one, for different values of the calibration parameter. The best result is obtained for A_{sh} = 0.4. The results confirm what reported by Le *et al.* [8]: larger A_{sh} (smaller bed slope effects) leads to larger bar amplitudes, shorter bar wavelengths and smaller longitudinal slopes. The value of A_{sh} = 0.4 results in the longitudinal slope i_{1800} = 1.03×10^{-4}, which is equal to the reconstructed longitudinal bed slope.

The model is then validated on its ability to reproduce the reconstructed bed topography from 1842 AD starting from the reconstructed bed topography from 1800 AD and applying the most suitable value of A_{sh} = 0.4. Figure 4.7 shows the results of model validation. The model reproduces the chute cutoff that occurred in the period 1800-1842, resulting in the formation of a middle bar (Figure 4.7.b) which is similar to the one that can be observed from the reconstructed bed topography 1842 (Figure 4.7.a). Computed and reconstructed bars have similar lengths, but the model tends to underestimate the chute cutoff channel depth (Figure 4.7.c). The computed longitudinal bed slope is i_{1842} = 1.03×10^{-4}, which equals the reconstructed longitudinal bed slope. The satisfactory results of validation allow trusting the model in its ability to reproduce realistic bed topographies in the study area.

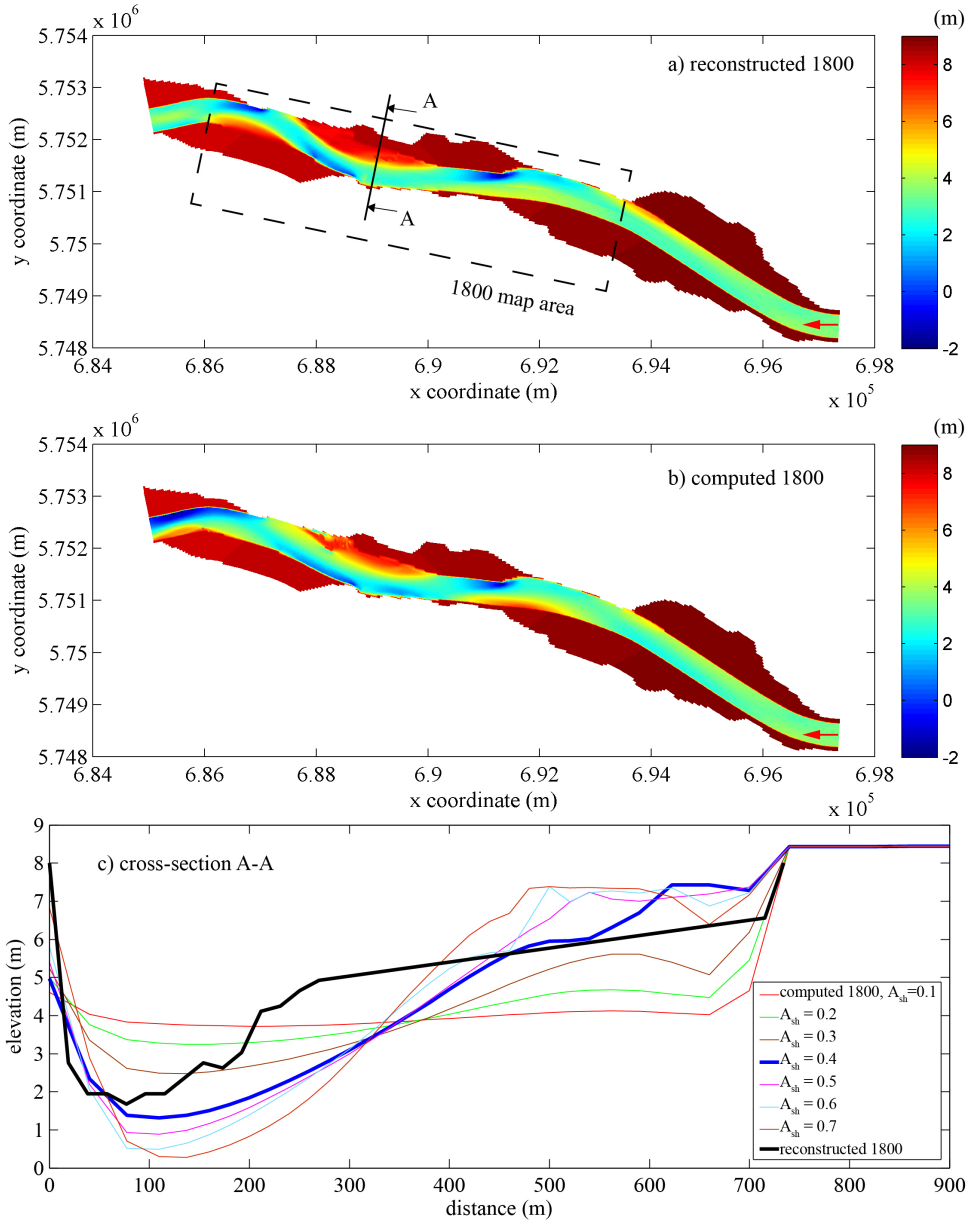

Figure 4.6: Results of model calibration. a) Reconstructed bed topography 1800. b) Computed bed topography 1800 with A_{sh} = 0.4. Coordinates are in the Universal Transverse Mercator (UTM) system. c) Computed and reconstructed Cross-Section A-A. The best fit corresponds to A_{sh} = 0.4.

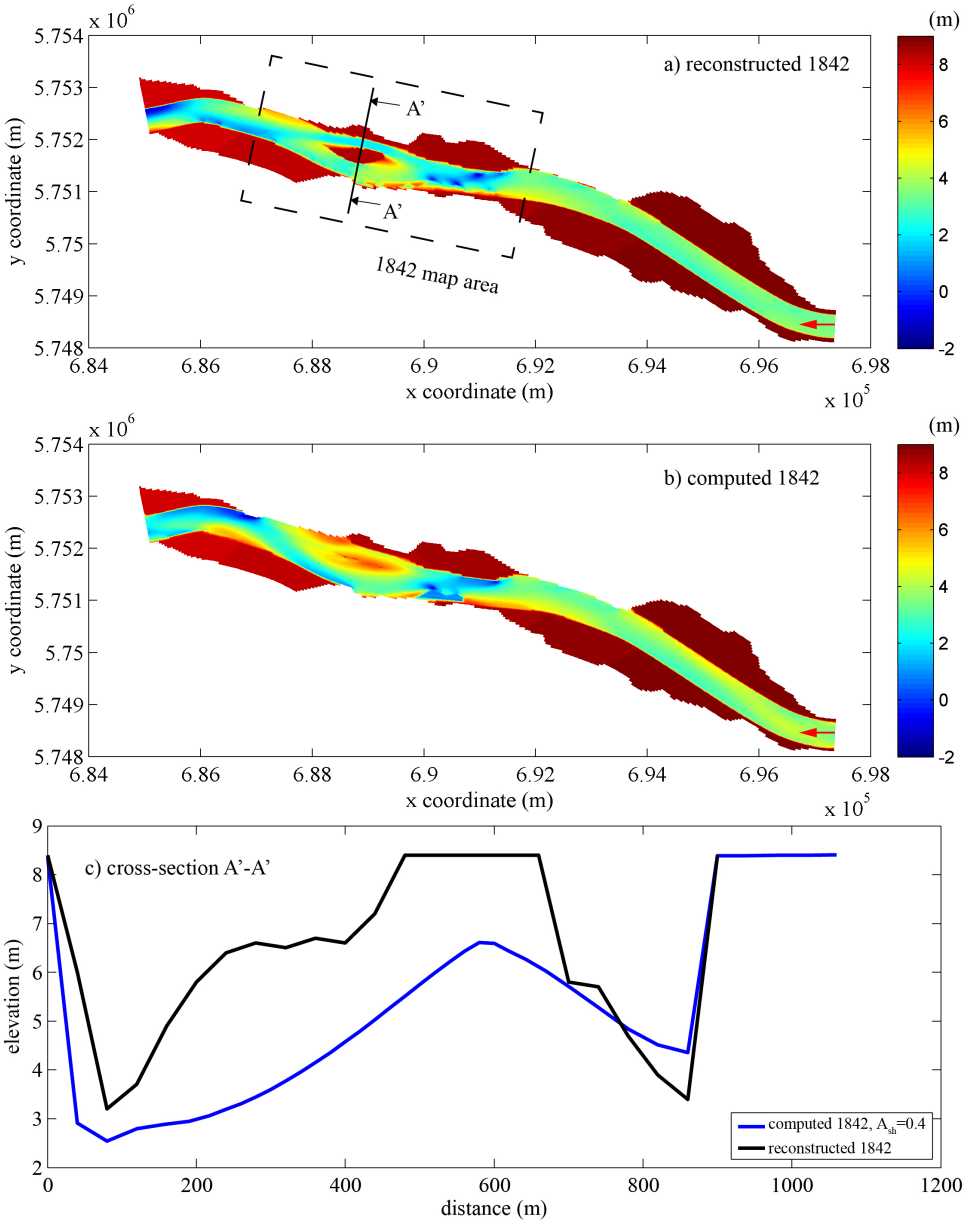

Figure 4.7: Results of model validation. a) Reconstructed bed topography 1842. b) Computed bed topography 1842 with A_{sh} = 0.4. Coordinates are in the Universal Transverse Mercator (UTM) system. c) Computed and reconstructed Cross-Section A'-A'.

4.3.3. Long-term morphological developments with and without interventions

The simulated scenarios include the base-case scenario, characterized by the absence of any anthropogenic intervention. This is the reference case to assess the

effects of interventions with respect to the "natural" evolution of the river. The runs also include two wall scenarios, differing in the starting point of the longitudinal wall, and two groyne scenarios, differing in the channel width. The starting condition of all scenarios is the reconstructed bed topography of 1842 AD. The discharge hydrograph used as upstream boundary condition is the schematized yearly hydrograph 1790-1810 (Figure 4.4). The computations, without any morphological acceleration, cover the period of 50 years.

The computed bed topography (Figure 4.8) of the base-case scenario shows that at the end of 1892 AD around the middle bar the left channel tends to silt up whereas the right channel has become the main stream. Because the model does not simulate bank erosion, the main stream narrows to 120 m. This result is qualitatively supported by the performed historical works belonging to the "Normalization" program (Figure 4.1). Due to its decreased size since 1872, the left channel was finally abandoned after the construction of groynes (1888 and 1890), whereas the right channel was artificially straightened and enlarged to 310 m (see Section 4.1) by removing the middle bar. The averaged longitudinal bed slope at the end of the 50-year evolution is the same as the 1842 slope: $i_{untrain}$ = 1.03×10^{-4}.

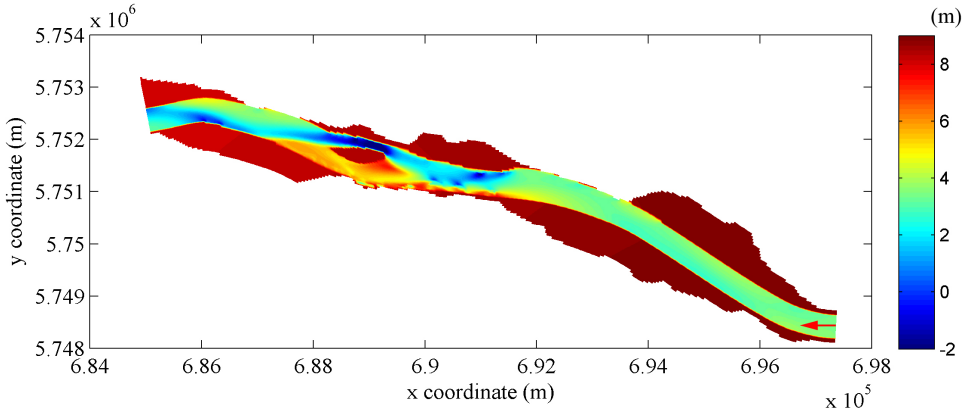

Figure 4.8: Base-case scenario (untrained river): computed bed topography at the end of 1892 AD. Coordinates are in the Universal Transverse Mercator (UTM) system.

The results of the wall scenarios are shown in Figure 4.9. If the training wall starts upstream of point bar I top, the left channel gradually silts up and the right channel deepens (Figure 4.9.a). Instead, if the longitudinal training wall starts downstream of the same point bar top, the left channel deepens and the right channel silts up (Figure 4.9.b). The system results always in a deeper and a shallower channel and the starting point of the longitudinal training wall with respect to a bar plays an important role in system instability. These results confirm the experimental and computational findings of Le *et al.* [7, 8].

Compared to the base-case scenario, the averaged bed level of the navigation channel lowers by either 3.57 m or 3.66 m for the starting locations at the upstream or downstream of point bar I top, respectively. The bed slopes become milder than

in the base-case scenario: 0.91×10^{-4} and 0.89×10^{-4}, respectively, compared to $i_{untrain}$ = 1.03×10^{-4}. The bed level of the ecological channel raises by either 3.38 m or 3.76 m, respectively, and its bed slope becomes steeper than the one of the untrained river (base-case scenario): 3.80×10^{-4} and 3.77×10^{-4}, respectively.

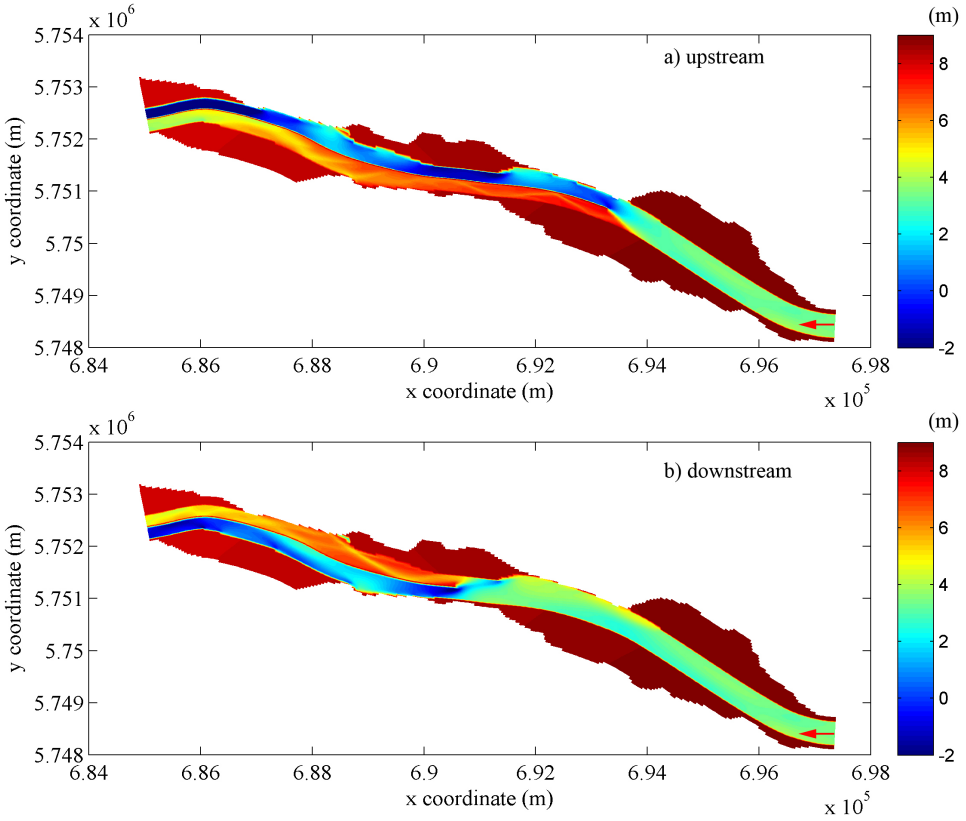

Figure 4.9: Wall scenarios. Computed bed topography at the end of 1892 AD. a) The longitudinal training wall starts upstream of point bar top. b) The longitudinal training wall starts downstream of point bar top. Coordinates are in the Universal Transverse Mercator (UTM) system.

In the two groyne scenarios the channel between groyne heads has either the width of the current Waal River (260 m) or the width of the navigation channel in the wall scenarios (200 m). The resulting long-term bed topographies after 50 years, corresponding to the hypothetical river situation at the end of 1892 AD, are presented in Figure 4.10. In this figure, the river channel has clearly deepened, as described by Suzuki *et al.* [29] and Spannring [30]. Compared to the untrained river scenario (base-case), the averaged bed level lowers by either 2.33 m or 4.04 m for the river width of 260 m or 200 m, respectively. The bed slope becomes milder than in the base-case scenario: 0.93×10^{-4} and 0.87×10^{-4}, respectively, compared to $i_{untrain}$ = 1.03×10^{-4}. The results agree with the general trends that can be

expected after river narrowing (e.g. Duró *et al.* [31]).

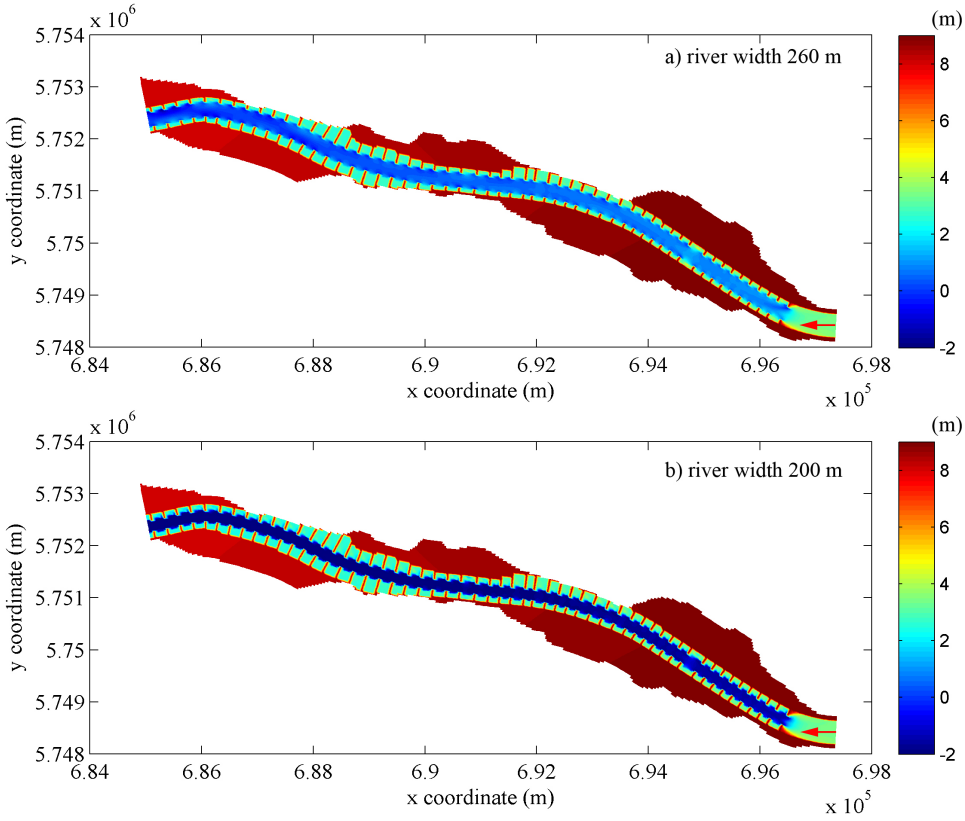

Figure 4.10: Groyne scenarios. Computed bed topography at the end of 1892 AD. a) River width equal to 260 m. b) River width equal to 200 m. Coordinates are in the Universal Transverse Mercator (UTM) system.

4.3.4. Results of the hydraulic models

The models are used again to assess the available depth for navigation at low flow and the water levels at high flow with reference to the morphological conditions in 1892 AD, i.e. at the new equilibrium state. In these runs the models do not allow for bed level changes and compute the flow conditions at fixed constant discharges. The hydraulic simulations are listed in Table 4.3. The selection of the discharges is described in Section 4.2.1.

River navigability

The present criteria for navigation in the Waal River are: a minimum depth of 2.8 m for a minimum width of 150 m. These conditions should be fulfilled at all discharges equal to or higher than 680 m^3/s. The results relative to the discharge of 680 m^3/s,

Table 4.3: Hydraulic simulations summary

Scenarios	Bed topography	Constant discharge			Detail
		Low discharge	Highest in history	Design discharge	
Base-case	Computed bed topography 1892	680	8,000	10,600	Untrained river
Wall scenarios	Computed bed topography 1892	680	8,000	10,600	Two starting points: upstream of point bar I top and downstream
Groyne scenarios	Computed bed topography 1892	680	8,000	10,600	No straightening, current groyne character, width: 260 and 200 m

shown in Figure 4.11.a, indicate that in the base-case scenario the river fulfills the criterion for navigation depth only in the right channel around the middle bar, but only for a width of 120 m, which is smaller than the minimum requirement of 150 m. This supports the reason to train the river to achieve navigability. In the wall scenarios (Figure 4.11.b, c), if the longitudinal training wall starts upstream of point bar I top, the average depth in the navigation channel is 5.13 m. If the longitudinal training wall starts downstream of that point bar, the depth is 5.16 m. In both cases, the minimum depth of 2.8 m is exceeded everywhere, i.e. for a width of 200 m. In the groyne scenarios (Figure 4.11.d, e), if the river width is 260 m the average depth is 3.99 m. If the river width is 200 m the average depth is 5.17 m. In both cases the water depth of 2.8 m is exceeded everywhere.

The results indicate that the wall and the groyne scenarios having the same navigation channel width (200 m) present similar navigation depths. Compared to the groyne scenario having a channel width of 260 m, constructing a longitudinal wall in the middle of the historical river results in a deeper but narrower navigation channel.

High flow conveyance

The effects of river training on water levels are represented by ΔZ_{water}, which is the difference between the average water level in the considered trained river case and the averaged water level in the untrained river (base-case) at Cross-Section A'-A' (Figure 4.7.a). If ΔZ_{water} is negative, the training method results in lower water levels, which indicates increased high flow conveyance of the river and vice versa if it is positive. The computed water levels at Cross-Section A'-A' are listed in Table 4.4.

The results show that the longitudinal training wall increases the high flow conveyance even compared to the untrained river. The reason for this is the lowering of bed elevation in the navigation channel (see next section). The most appropriate starting location of the wall is upstream of the point bar top. Instead, training by means of series of groynes decreases the high flow conveyance of the river.

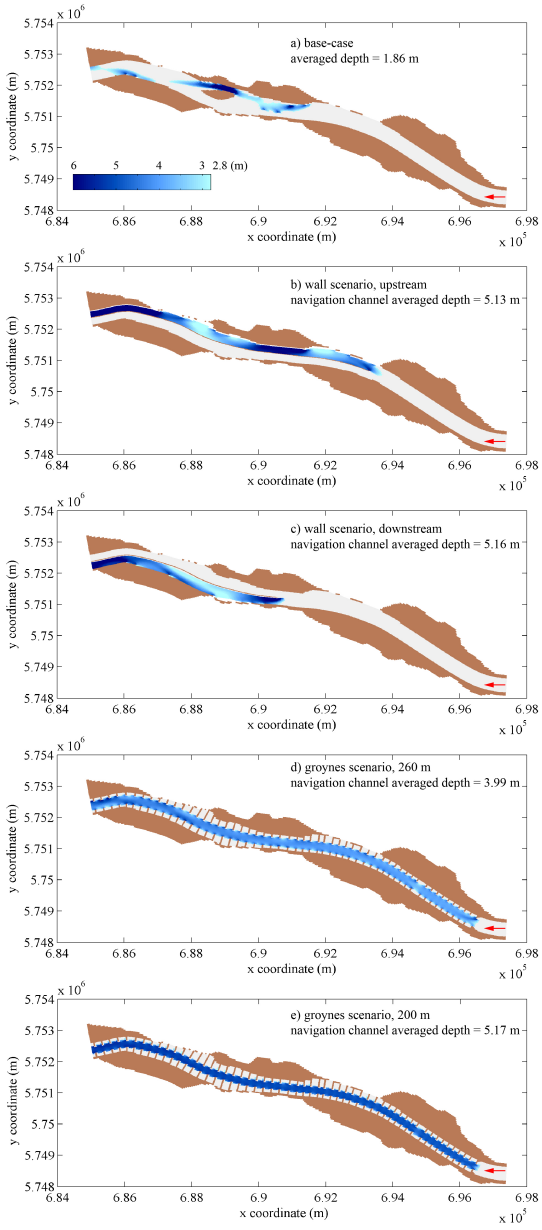

Figure 4.11: Water depth at Q_{low} = 680 m³/s. Flood plains and training structures are colored brown. Grey areas in the water body indicate local water depth less than 2.8 m. a) Base-case scenario. b) Wall starts upstream of point bar I top. c) Wall starts downstream of point bar I top. d) Groyne scenario with river width of 260 m. e) Groyne scenario with river width of 200 m. Coordinates are in the Universal Transverse Mercator (UTM) system.

Table 4.4: Average water levels at Cross-Section A'-A' in 1892 AD (computed equilibrium bed topographies)

Scenarios	$Q_{history}$ = 8000 m^3/s		Q_{design} = 10600 m^3/s	
	Water level (m)	ΔZ_{water} (m)	Water level (m)	ΔZ_{water} (m)
Base-case	11.02	-	13.08	-
Wall scenarios, upstream	10.77	-0.25	12.95	-0.13
Wall scenarios, downstream	10.90	-0.12	13.06	-0.02
Groyne scenarios, river width 260 m	11.12	+0.10	13.15	+0.07
Groyne scenarios, river width 200 m	11.20	+0.18	13.20	+0.12

Channel incision

Jansen *et al.* [32] and Duró *et al.* [31] show that channel narrowing inevitably leads to river incision in the narrowed reach and upstream. The latter is caused by longitudinal slope reduction in the narrowed reach resulting in lower water levels at its upstream end. At equilibrium these lower water levels correspond to equally lower bed levels and cause thus channel incision. The lowering is theoretically equal to the slope reduction multiplied by the length of the narrowed reach. This means that the training setup that results in the smallest longitudinal slope has the highest upstream effect. Table 4.5 lists the equilibrium longitudinal slopes of all considered scenarios. The results show that the groyne scenario with river width of 200 m causes the highest upstream incision, whereas the groyne scenario with river width of 260 m the lowest. The differences in slope between the training scenarios appear as negligible, being between 0.02×10^{-4} and 0.06×10^{-4}, resulting in 2 to 6 cm of upstream incision every ten kilometers of narrowed reach. However, considering that narrowing of the Wall River is present for a length of the order of 100 km, these small differences might lead to extra upstream incision of the order of 20-60 cm.

Table 4.5: Longitudinal navigation channel slope at equilibrium (1892 AD) and average navigation channel deepening with respect to the untrained case

Scenario	Longitudinal bed slope (-)	Averaged bed level with respect to base-case scenario (m)
Untrained river (base-case)	1.03×10^{-4}	0
Wall scenario, upstream (W1)	0.91×10^{-4}	-3.57
Wall scenario, downstream (W2)	0.89×10^{-4}	-3.66
Groyne scenario, river width 260 m (G1)	0.93×10^{-4}	-2.33
Groyne scenario, river width 200 m (G2)	0.87×10^{-4}	-4.04

In the trained reach, incision is also caused by local bed level lowering. Table 4.5 lists also the average channel bed deepening in the navigation channels with respect to the untrained case. The maximum value of channel deepening occurs in the 200 m large channel with groynes which is also the one that produces the smallest longitudinal slope (maximum upstream incision), whereas the minimum value of

channel deepening corresponds to the 260 m large channel with groynes, which presents also the largest longitudinal slope (minimum upstream incision).

For an equally-wide navigation channel (200 m), the construction of a longitudinal wall results in smaller channel incision compared to channel narrowing by means of groynes. However, compared to the 260 m wide channel with groynes that is present today, a longitudinal training wall in the middle of the Waal River starting from a location upstream of a bar top would be the cause of 1.24 m extra channel bed lowering, whereas extra upstream incision would be of the order of 20 cm every 100 km of narrowed length. Thus, from the point of view of incision, the current groynes setup is preferable to a longitudinal wall in the middle of the historical pre-normalization channel.

At this point it is interesting to analyze what it would mean for the Waal River to have a navigation channel of 260 m obtained by means of a longitudinal wall. In this case, the training wall would not divide the river in two equally-wide channels, as recommended by Le *et al.* [8]. To study the long-term implications of this training set up, an extra simulation has been carried out, starting the wall just upstream of point bar I top (W3 run). The results show a longitudinal slope $i = 0.98 \times 10^{-4}$, whereas bed level lowering compared to the base-case scenario is 2.30 m. This means that this setup of the longitudinal wall reduces channel incision compared to the groyne scenario having the same width of 260 m and improves high flow conveyance as well. However, this setup presents some shortcomings, since at the low flow of 680 m^3/s the navigation channel would need flattening of bar tops to maintain a depth of 2.8 m over the entire channel width (Figure 4.12). It is interesting to observe that the formation of bars leading to local water depths smaller than 2.8 m does not occur in the groyne scenario having the same width (G1 run, Figure 4.11.d). Observing the results of W3 run (Figure 4.12) we can notice that bars form only in local widening areas characterized by larger width-to-depth ratios [33]. Local widening areas are absent in the model with groynes, in which the river width is strictly kept constant. However, bar tops flattening is regularly carried out in the current Waal River having the same width of 260 m (personal communication Rijkswaterstaat).

4.4. Discussion

The results presented here are affected by uncertainties. However, the computed values are only used to compare scenarios and for this reason the approach can be still considered appropriate, even if we recognize that some aspects can be more relevant in one scenario rather than in another one. For more realistic results a few aspects should be considered.

The investigation is based on the use of 2DH models, which cannot correctly simulate the flow that overtops the wall and the groynes at high discharge conditions. Water levels at flows above bankfull are strongly affected by the resistance of groynes and wall. There is still debate whether the groyne resistance is properly calculated by 2DH models [5]. In any case the groynes and the flow around and above them are not well resolved. This might lead to important errors on water levels estimates. Similarly, errors can be caused by inaccurate representation

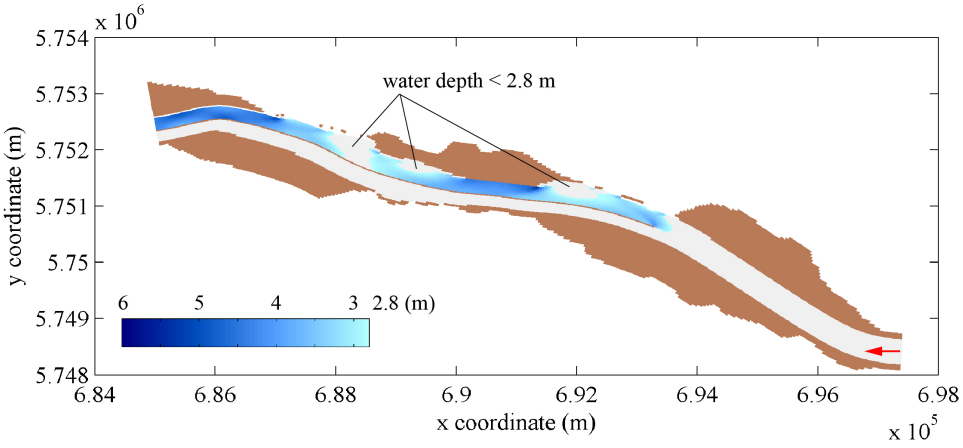

Figure 4.12: Water depth at Q_{low} = 680 m³/s in W3 run. Flood plains and training structures are colored brown. Grey areas in the water body indicate local water depth less than 2.8 m. Coordinates are in the Universal Transverse Mercator (UTM) system.

of the flow along and above the wall. This means that the results regarding the flow conveyance of the river are not conclusive and further investigation is needed. With particular regard to the wall scenarios, the models do not reproduce well also the working of the system navigation-ecological channel when important flow exchanges between the two channels can be expected. To improve the results, a 3D model with Detached Eddy Simulation (DES) is needed. Such a model would also allow studying the effects of suspended solids, which are not taken into account in the present study. Deposition of fine material might accelerate sedimentation in the ecological channel and increase its final bed level rise.

Another aspect that has not been investigated in this study is bank erosion. Whereas it is clear that bank protection is needed along the navigation channel, the results indicate that the ecological channel can maintain a natural bank. However, bank erosion can occur also along the ecological channel, in particular during high flow conditions, when ship waves can reach the unprotected bank. Preliminary data collected in the framework of the project "Waalsamen" along the ecological channels behind the three pilot longitudinal dams built in the Waal River (Figure 4.2) indicate the occurrence of bank erosion during high flow conditions (personal communication Rijkswaterstaat). This means that future research should include also bank processes.

The models simulate strongly schematized scenarios. For instance, the longitudinal wall is represented without any openings, i.e. without any water exchange between the two parallel channels. Due to this, the channels present different water levels. Moreover, the model domain is a relatively short river reach. The results are thus affected by the boundary conditions.

Topographical information of the floodplains in the nineteenth century is not available, so floodplains were schematized as horizontal surfaces with a longitudinal

slope $i_0 = 1\times10^{-4}$ (Figure 4.5). This approximation needs further improvements, because the present floodplain levels of the Waal floodplains can vary by 3-4 m [34].

Finally, the investigation did not consider colonization and growth of vegetation in the ecological channel during low-flow conditions. This, by increasing the hydraulic resistance, might have the following effects: rise of water levels at high flow conditions; increased sedimentation in the ecological channel leading to its total closure. Future investigations should consider these aspects and investigate the effects of different vegetation management strategies, as well as dredging strategies.

4.5. Conclusions and recommendations

This work addresses the long-term developments of the historical Waal River with different training techniques to assess whether a longitudinal training wall subdividing the river in two parallel channels would have resulted in more favorable conditions than the current groyne fields. The morphological evolution and the hydraulic conditions have been investigated by means of a 2DH numerical model developed using the Delft3D code. Several training scenarios are considered. The analysis is based on the comparison between river morphology, navigability level and high flow conveyance at equilibrium, considering also the "natural" untrained river case.

The model is calibrated and validated on the reconstructed bed topographies of 1800 and 1842 AD, respectively. The results show that the historical morphological developments are reproduced in a satisfactory way and that the model can then be used for this type of investigations.

The results of the numerical simulations covering 50 years starting from the river bed topography of 1842 AD show that separating the Waal River by a longitudinal training wall always leads to the formation of one deeper and one shallower channel. The starting position of the wall with respect to a steady bar determines which channel becomes the deeper "navigation channel" and which one becomes the shallower "ecological channel". This agrees with the findings of Le *et al.* [7, 8]. The reach-scale characteristics of the navigation channels obtained with different starting positions of the longitudinal wall do not differ much, but starting the wall just upstream of a point bar top reduces river incision, which arises from local bed level lowering and longitudinal slope reduction (e.g. [32] and [31]). In general, the deepening of the navigation channel shows the need of protecting its bank, whereas bank protection might not be necessary for the ecological channel.

The results of the computations with respect to river navigability show that the implementation of a longitudinal wall instead of series of groynes would not result in substantially different navigation channels. In all considered cases the minimum criteria for navigation are satisfied. These criteria are not met in the untrained river case, showing that River Waal navigability can only be achieved by means of river training, which is in fact what has happened in reality. The results show also that a longitudinal wall is preferable when considering the high-flow conveyance of the river. Also with respect to this criterion the most appropriate starting location of the

wall is just upstream of a point bar top. The presence of a shallow channel with a natural bank is another reason to prefer the longitudinal wall to the groynes, since this is expected to increases the river ecological value [35].

Table 4.6 summaries the advantages and disadvantages of longitudinal walls. Single plus indicates improvement with respect to the groyne scenario having the same navigation channel width. Double plus indicates improvement with respect to all considered groyne scenarios. Zero value indicates neutral effect and minus indicates negative effect compared to groyne scenarios.

Table 4.6: Summary of advantages and disadvantages of river training with a longitudinal wall with respect to groynes in the Waal River

Scenario (width in m)	Navigability	High flow conveyance	Incision	Potential river ecology
W1 (200)	0	++	+	++
W2 (200)	0	++	+	++
W3 (260)	-*	++	+	++

* Requires flattening of bar tops for low-flow navigability. This can be solved by proper protection and alignment of the navigation channel bank.

The results of this study suggest that a longitudinal training wall might be an appropriate intervention to train wide low-land rivers as water ways. It is advisable to carefully select the location of the upstream end of the wall if steady bars or point bars are present. In this case, the most favorable location to start the wall is just upstream of a steady bar or point bar top. Placing the wall in the middle of the channel maximizes system stability. The bank of the navigation channel should be protected and properly aligned, whereas the study does not indicate the need for ecological-channel bank protection.

Acknowledgments

This work is sponsored by Vietnam International Education Development (VIED), project 911. The authors wish to acknowledge the useful comments provided by Wim S.J. Uijttewaal and Erik Mosselman.

References

[1] T. B. Le, A. Crosato, and A. Arboleda, *Revisiting waal river training by historical reconstruction,* Journal of Hydraulic Engineering (2018), (submitted).

[2] J. Wijbenga, J. Lambeek, E. Mosselman, R. Nieuwkamer, and R. Passchier, *Toetsing uitgangspunten rivierdijkversterkingen,* in *Deelrapport 2: Maatgevende belastingen, Waterloopkundig Laboratorium and European-American Center for Policy Analysis, Delft, the Netherlands.* (1993) (in Dutch).

[3] J. Wijbenga, J. Lambeek, E. Mosselman, R. Nieuwkamer, and R. Passchier, *River flood protection in the netherlands,* in *Proceedings of International Con-*

ference on River Flood Hydraulics. York, England, Eds. W.R. White & J. Watts, Wiley, Paper 24 (1994) pp. 275–285.

[4] J. Sieben, *Sediment management in the dutch rhine branches,* International Journal of River Basin Management **7**, 43 (2009), https://doi.org/10.1080/15715124.2009.9635369.

[5] M. F. M. Yossef, *Morphodynamics of rivers with groynes*, Ph.D. thesis, Delft University of Technology (2005).

[6] W. Bertoldi and M. Tubino, *River bifurcations: Experimental observations on equilibrium configurations,* Water Resources Research **43** (2007), 10.1029/2007wr005907, https://doi.org/10.1029/2007wr005907.

[7] T. B. Le, A. Crosato, and W. Uijttewaal, *Long-term morphological developments of river channels separated by a longitudinal training wall,* Advances in Water Resources **113**, 73 (2018), https://doi.org/10.1016/j.advwatres.2018.01.007.

[8] T. B. Le, A. Crosato, E. Mosselman, and W. Uijttewaal, *On the stability of river bifurcations created by longitudinal training walls. numerical investigation,* Advances in Water Resources **113**, 112 (2018), https://doi.org/10.1016/j.advwatres.2018.01.012.

[9] A. M. Arboleda, A. Crosato, and H. Middelkoop, *Reconstructing the early 19th-century waal river by means of a 2d physics-based numerical model,* Hydrological processes **24**, 3661 (2010), https://doi.org/10.1002/hyp.7804.

[10] A. Vargas-Luna, C. Alessandra, A. Niels, H. A. J.F., K. S. D., and U. W. S.J., *Morphodynamic effects of riparian vegetation growth after stream restoration,* Earth Surface Processes and Landforms **43**, 1591 (2018), https://onlinelibrary.wiley.com/doi/pdf/10.1002/esp.4338 .

[11] M. J. Baptist, L. V. van den Bosch, J. T. Dijkstra, and S. Kapinga, *Modelling the effects of vegetation on flow and morphology in rivers.* Large Rivers , 339 (2005), https://dx.doi.org/10.1127/lr/15/2003/339.

[12] G. Maas, H. Wolfert, M. Schoor, and H. Middelkoop, *Classificatie van riviertrajecten en kansrijkdom voor ecotopen, Report 552*, Tech. Rep. (DLOStaring Centrum, Wageningen, the Netherlands, 1997) (in Dutch).

[13] W. van Vuren, *Verdeling zomer- en winterhoogwaters voor de Rijntakken in de periode 1770-2004.*, Tech. Rep. (Memo WRR 2005-012. WRR, The Hague., 2005) (in Dutch).

[14] R. M. Frings and M. G. Kleinhans, *Complex variations in sediment transport at three large river bifurcations during discharge waves in the river rhine.* Sedimentology **55**, 1145 (2008).

[15] R. Frings, M. Berbee Bastiaan, G. Erkens, M. G. Kleinhans, and M. J. P. Gouw, *Human-induced changes in bed shear stress and bed grain size in the river waal (the netherlands) during the past 900 years,* Earth Surface Processes and Landforms **34**, 503 (2009), https://onlinelibrary.wiley.com/doi/pdf/10.1002/esp.1746 .

[16] H. Middelkoop, *Embanked floodplains in The Netherlands. Netherlands Geographical Studies.*, Ph.D. thesis, University of Utrecht, Utrecht, The Netherlands (1997), ISBN 90-6266-146-7.

[17] Deltares, *Simulation of multi-dimensional hydrodynamic flows and transport phenomena, including sediments. User Manual Hydro-Morphodynamics Version: 3.15.34158 28, May 2014.*, edited by Deltares (Deltares, 2014) https://oss.deltares.nl/documents/183920/185723/Delft3D-FLOW_User_Manual .pdf.

[18] E. Mosselman and T. B. Le, *Five common mistakes in fluvial morphodynamic modeling,* Advances in Water Resources **93**, 15 (2016), https://doi.org/10.1016/j.advwatres.2015.07.025.

[19] F. Schuurman, W. A. Marra, and M. G. Kleinhans, *Physics-based modeling of large braided sand-bed rivers: Bar pattern formation, dynamics, and sensitivity,* Journal of geophysical research: Earth Surface **118**, 2509 (2013), https://doi.org/10.1002/2013JF002896.

[20] M. G. Kleinhans, H. R. A. Jagers, E. Mosselman, and C. J. Sloff, *Bifurcation dynamics and avulsion duration in meandering rivers by one-dimensional and three-dimensional models,* Water Resources Research **44**, W08454 (2008), https://doi.org/10.1029/2007WR005912.

[21] N. Struiksma, K. Olesen, C. Flokstra, and H. De Vriend, *Bed deformation in curved alluvial channels,* Journal of Hydraulic Research **23**, 57 (1985), https://doi.org/10.1080/00221688509499377.

[22] F. Koch and C. Flokstra, *Bed Level Computations for Curved Alluvial Channels: Prepared for the 19th IAHR Congress, New Delhi, India, February 1981* (Waterloopkundig Laboratorium, 1981).

[23] A. Talmon, N. Struiksma, and M. V. Mierlo, *Laboratory measurements of the direction of sediment transport on transverse alluvial-bed slopes,* Journal of Hydraulic Research **33**, 495 (1995), https://doi.org/10.1080/00221689509498657.

[24] A. Vargas-Luna, A. Crosato, G. Calvani, and W. S. Uijttewaal, *Representing plants as rigid cylinders in experiments and models,* Advances in Water Resources **93**, 205 (2015), ecogeomorphological feedbacks of water fluxes, sediment transport and vegetation dynamics in rivers and estuaries.

[25] F. Carraro, D. Vanzo, V. Caleffi, A. Valiani, and A. Siviglia, *Mathematical study of linear morphodynamic acceleration and derivation of the masspeed approach.* Advances in Water Resources **117**, 40 (2018).

[26] M. Yossef, C. Stolker, S. Giri, A. Hauschild, and S. van Vuren, *Calibration of the multi-domain model. Report Q4357.20*, Tech. Rep. (WL | delft hydraulics, 2008).

[27] F. Engelund and E. Hansen, *A monograph on sediment transport in alluvial streams*, Tech. Rep. (TEKNISKFORLAG Skelbrekgade 4 Copenhagen V, Denmark., 1967).

[28] E. van Velzen, P. Jesse, P. Cornelissen, and H. Coops, *Stromingsweerstand vegetatie in uiterwaarden. Tech. Rep. No. 2003D028*, Tech. Rep. (Rijkswaterstaat, RIZA, 2003) (in Dutch).

[29] K. Suzuki, M. Michiue, and O. Hinokidani, *Local bed form around a series of spur-dikes in alluvial channels,* in *Proceedings, 22nd Congress IAHR* (1987) pp. 316–321.

[30] M. Spannring, *Degradation of the river bed after building of groynes,* in *28th IAHR congress, Graz, Austria* (1999) pp. 1–7.

[31] G. Duró, A. Crosato, and P. Tassi, *Numerical study on river bar response to spatial variations of channel width,* Advances in Water Resources **93**, 21 (2015), https://doi.org/10.1016/j.advwatres.2015.10.003.

[32] P. Jansen, L. van Bendegom, J. van den Berg, M. de Vries, and A. Zanen, *Principles of river engineering. The non-tidal alluvial river.* (Pitman, London, Facsimile edition. Published in 1994 by Delftse Uitgevers Maatschappij., 1979) ISBN 90 6562 146 6.

[33] A. Crosato and E. Mosselman, *Simple physics-based predictor for the number of river bars and the transition between meandering and braiding,* Water Resources Research **45** (2009), 10.1029/2008WR007242, https://doi.org/10.1029/2008WR007242.

[34] H. Middelkoop and N. E. M. Asselman, *Spatial variability of floodplain sedimentation at the event scale in the rhine-meuse delta, the netherlands,* Earth Surface Processes and Landforms **23**, 561 (1998).

[35] F. Collas, A. Buijse, L. van den Heuvel, N. van Kessel, M. Schoor, H. Eerden, and R. Leuven, *Longitudinal training dams mitigate effects of shipping on environmental conditions and fish density in the littoral zones of the river Rhine,* Science of The Total Environment **619-620**, 1183 (2017), https://doi.org/10.1016/j.scitotenv.2017.10.299.

5

Discussion

This chapter discusses the qualitative comparison with previous work and field observations on the usage of longitudinal training walls; the experimental tests; the numerical simulations; and the future works.

5.1. Qualitative comparison with previous work and field observations

Three Longitudinal training walls have been built in 2013-2015 near Tiel, Dreumel and Ophemert in the Waal River, a branch of the Rhine in The Netherlands (Figure 5.1). The engineers built them with side slopes and prefer to call them Longitudinal Training Dams (LTDs). This is a pilot project to test the effectiveness of LTDs for river training. The parallel channels created by three pilot LTDs have been monitored since 2013 in the framework of the "Waalsamen" project. The first data sets on short-term morphological evolution and sediment composition have been processed by Weerdenburg [1].

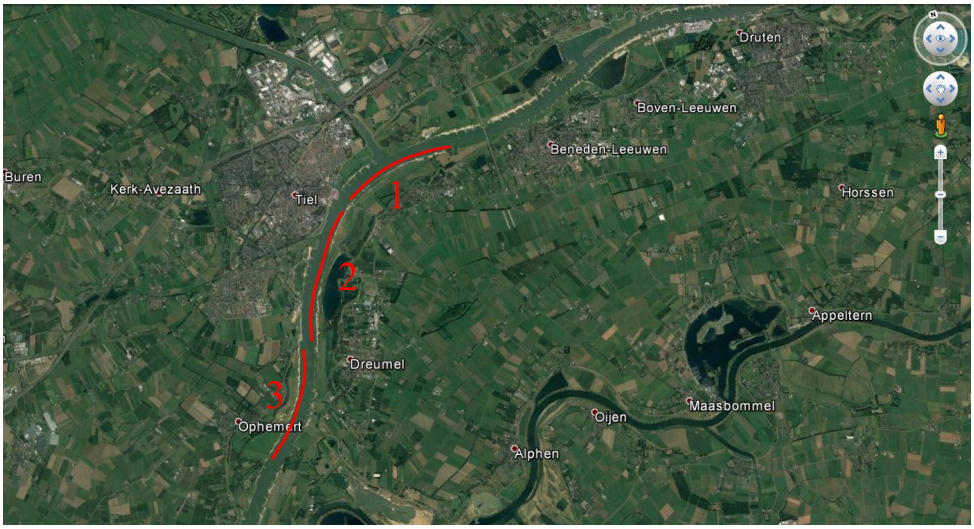

Figure 5.1: Three pilot LTDs on the Waal River (named 1, 2, and 3). Source: Google Earth © 2017. Flow direction from right to left. The red lines are the LTDs.

The early predictions by Huthoff [2] using a two-dimensional Delft3D model focusing on the navigation channel show that the morphological response of the Waal River due to the construction of the three LTDs can be rather quick (1-2 years). The navigation channel along the first and second LTD is shown to silt up, whereas the third one becomes deeper. These predictions are not supported by the current measurements on the pilot projects [1]. In particular, Huthoff [2]'s results show the potential of main river channel to recover from the on-going incision. They also show that this process of bed aggradation could become undesirable on the long term (Figure 5.2).

The measurements data that were analysed by Weerdenburg [1] reveal the first 3.5 years of morphological response to the pilot LTDs. The results show that the average bed level in the side channels has increased much for all three LTDs (bed level rise by 0.5 m - 1.0 m). However, the average bed level of the side channel

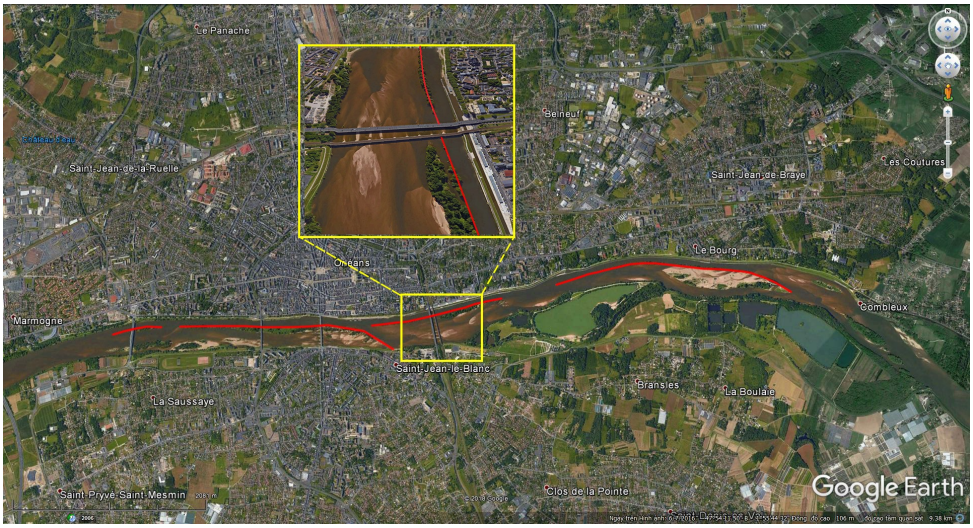

Figure 5.2: Larger channel silt up in the Loire River near Orleans, France when LTDs start upstream of a point bar top. Source: Google Earth © 2017. Flow direction from right to left. The red lines are the LTDs.

along the first LTD has been increasing continuously, whereas the average bed level of the other two side channels has become more or less stable. The first two LTDs start upstream of a point bar top and near the point bar top, respectively. Their development so far agrees with the findings of this research (chapter 2 and 3) and not as predicted by Huthoff [2]. The effects of the third LTD are still unclear.

In a separate setting, i.e. the Loire River near Orleans in France, see Figure 5.2, even the larger channel silts up when LTDs start upstream of a point bar top. This agrees with the results of this research (chapter 2 and 3): the width ratio of the parallel channels does not affect their final bed level configuration. The location of the starting point of the LTD is the governing factor establishing which of the two channels silts up and which one erodes.

These qualitative comparisons show that the results of this research are supported by some field data on river channels separated by LTDs. This gives some confidence on their applicability on real rivers.

5.2. Experimental tests

In this study, the experimental tests were carried out in a small flume, 14 m long and 40 cm wide. This limited the formation of bars inside the flume in terms of magnitude, i.e. the bars had the height of 2 cm (water depth: 4 - 6 cm). Furthermore, there were ripples undulating the bed of the flume. This made it difficult to detect the bars and identify the location of the relative starting point of the training wall. Another issue is the length of the flume. During the test case S1 (Chapter 2), the longitudinal training wall could not be placed starting at the downstream part

of a bar because of the flume being too short. Experimental tests should be thus carried out in a larger flume to better reproduce the bars and therefore enhance the quality of the measurements.

At the time of the experimental investigation carried out during this research, larger facilities were not available. For this reason using a larger flume is hence a recommendation for future study.

Another tip to advance the bar formation in the flume and to reduce the formation of ripples is to properly select the sediment size and distribution. The effects of different sediment characteristics were clearly visible during the experimental tests (Figure 5.3).

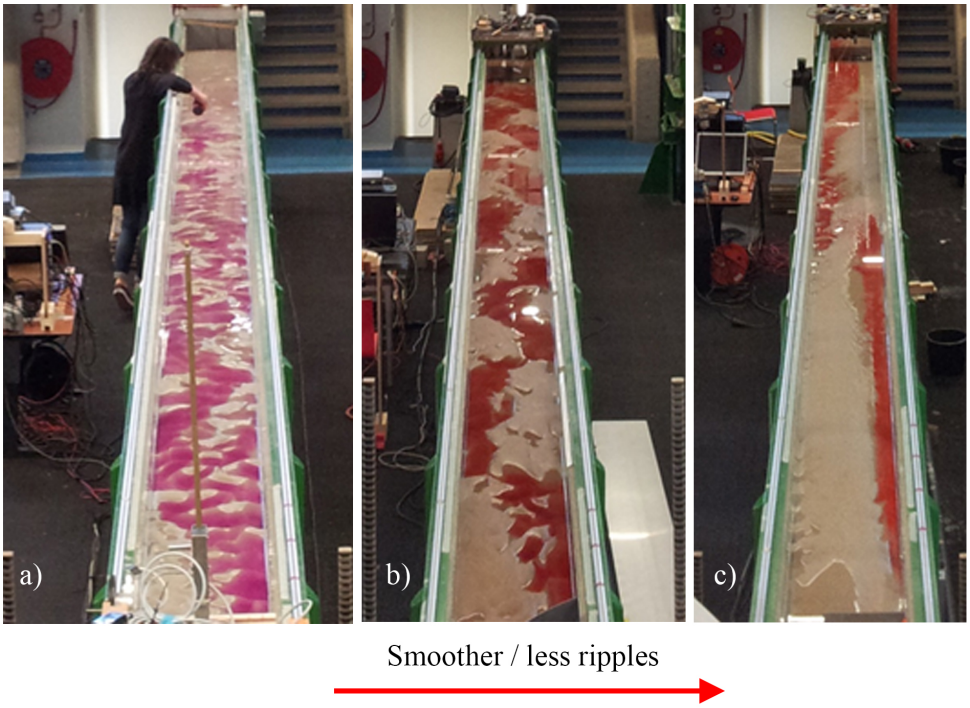

Figure 5.3: Effects of different sediment characteristics on bar and ripple formation. a) S1 test, rather uniform sediment with D_{50} = 0.37 mm; b) Base-case, rather uniform sediment with D_{50} = 0.50 mm; and c) S2 test, graded sand with D_{50} = 1.00 mm.

5.3. Numerical simulations

In this study, a two-dimensional depth-averaged (2DH) approach is used to simulate the effects of three dimensional (3D) processes, namely spiral flow and transverse bed slope. They have opposite effects on bar development and bifurcation stability. The results of this study present the combined effects of these two processes in

straight channels with alternate bars and in sinuous channels with point bars. A specific sensitivity analysis was carried out to study the effects of transverse bed slope on bifurcation stability. Spiral flow is the result of flow curvature; it develops around bars and is particularly strong inside river bends. The numerical simulations carried out in this study have shown that the same results are obtained in the straight and in the sinuous channels, indicating that the effects of spiral flow on bar formation and bifurcation are smaller than the effects of transverse slopes related to the presence of bars and point bars. However, this result cannot be considered generally valid. Further investigations should analyze the effects of spiral flow on bifurcation stability if the longitudinal wall starts or presents important openings inside river bends, particularly in relation to the curvature of the channel.

The numerical approach presents some limitations which could affect the results. For instance, we use the sediment transport formula of Engelund and Hansen [3] for the simulation of sand-bed river (chapter 3) and of Meyer-Peter and Müller [4] for the simulations of gravel-bed rivers (chapter 2). For the historical simulation of the Waal River evolution sediment transport was computed by the Engelund and Hansen [3] formula. However, other researchers used different formula for the Waal River. For instance Yossef *et al.* [5] used the Van Rijn [6] formula. This means that: it is not clear which formula performs best for the conditions of the Waal River; and that the results can be affected by the chosen formula. It is therefore recommended to perform a sensitivity analysis on the effects of choice of sediment transport formula on the morphological developments of the system.

Sediment sorting was not included in this research due to the long duration of the computations. However, based on the results of previous studies [7, 8], in the Waal River we could expect: 1) negligible changes in bed composition if the channel had remained untrained; 2) gradual coarsening of river bed material in case of narrowing by groynes. This was observed by Sieben [9] when he analyzed sediment on the Waal River compared to the past; 3) in case of channel subdivision by a LTD, gradual coarsening of the river bed material in the channel that becomes deeper and fining in the silting up channel. The latter was observed in the deposition areas by Weerdenburg [1] in the pilot study (section 5.1).

Bank erosion is another issue in this study. The simulation results show that due to bed deepening and flow concentration in the navigation channel, the bank of this channel will need to be protected against erosion. Instead, the bank of the shallower ecological channel might not need to be protected. However, ship wave propagation inside this channel, especially in presence of openings in the longitudinal wall might cause localized bank erosion. This has been observed along the Waal River in The Netherlands behind the three longitudinal walls in the pilot project (personal communication with Rijkswaterstaat).

To assess the necessity to protect the river banks requires using a numerical model with a good representation of the bank erosion process. The current version of the Delft3D code does not allow for this type of investigation, because bank erosion is only roughly represented through a factor that allows a dry-cell adjacent to a wet cell to be eroded. Moreover, ship waves pose additional complications for the representation of the bank erosion process.

Others issues regarding the numerical simulations carried out in this study have contributed to the definition of the best practices in 2D morphodynamic modelling of rivers. Five mistakes are common when modelling alluvial rivers [10]. They include: (1) codes with inadequate representation of physical processes; (2) inputs that impose morphodynamic patterns; (3) inadequate upscaling; (4) confusion of physical and numerical phenomena; and (5) belief that 2D and 3D models require more data than 1D models.

5.4. Future works

5.4.1. Setting of longitudinal training walls

This study focuses on the morphological effects of a single longitudinal wall. What would happen if two walls are built along both sides of the river? The results of a preliminary investigation are presented in Appendix A. They suggest that alternating walls, i.e. wall first along one side and then along the other side of the river might be helpful to reduce the amplitudes of bars forming in the navigation channel. However, more work still needs to be done to figure out what are the correct length of the walls and the distance between them.

In this study, the longitudinal walls are considered as a continuous structure. As a result, the parallel channels become completely separated from each other at low discharge rates. This leads to different water levels and to the development of different longitudinal bed slopes in the channels. In practice, engineers prefer opening the walls at some points for many purposes, for example allowing for river crossings (ferry route). This could help balancing the water levels on both sides of the wall. The setting of openings requires more attention in future investigations.

Although the results of this work indicate that equally-wide parallel channels might result in the most stable system, this does not mean that engineers should always build the wall right in the middle of the river. If the navigation channel requires a specific width, engineers should consider placing the wall in such a way that one of the parallel channels has the required width. Moreover, building the wall right in the middle of the river might require more material and facing more technical issues which were not considered in this study, mainly focusing on the long-term morphological developments. Further investigations should be carried out with an economic-technical assessment to balance the interest of the relative-width selection.

Another issue regarding longitudinal walls is their body structure: should the wall be seal off (such as a concrete or steal plate) or open for suspended load to be penetrated (like a rock fill dam)? In many low-land rivers, suspended load is important and the exchange between the parallel channels above and through the wall body might become not negligible. This point needs further investigation too.

5.4.2. On the river ecological potential

In this study, the longitudinal training walls were assessed with focus on morphological effects. The river ecological aspects were not investigated. However, the presence of a shallow channel (that does not exist with groynes) might offer a better

condition for the river fauna (fish) and flora (riparian vegetation). Collas *et al.* [11] confirm an increasing in fish numbers in the side channel behind the longitudinal wall that was implemented in the Waal River (pilot study, see section 5.1) compared to the situation before with groynes. However, river ecological is more than "some species" benefitting. Therefore, more broader works are advised to fully understand the potential benefits for all relevant fauna and flora in the river reach with longitudinal training walls compared to the situation with series of groynes.

References

[1] R. Weerdenburg, *Morphological development in the Waal River near longitudinal training dams*, Master's thesis, Delft University of Technology (2018).

[2] F. Huthoff, *Longitudinal dams as an alternative to wing dikes in river engineering,* in *Smart River 2011 conference, New Orleans, Louisiana, USA.* (2011).

[3] F. Engelund and E. Hansen, *A monograph on sediment transport in alluvial streams*, Tech. Rep. (TEKNISKFORLAG Skelbrekgade 4 Copenhagen V, Denmark., 1967).

[4] E. Meyer-Peter and R. Müller, *Formulas for bed-load transport,* in *Proc., 2nd Meeting, IAHR* (Stockholm, Sweden, 1948) pp. 39–64.

[5] M. Yossef, C. Stolker, S. Giri, A. Hauschild, and S. van Vuren, *Calibration of the multi-domain model. Report Q4357.20*, Tech. Rep. (WL | delft hydraulics, 2008).

[6] L. C. Van Rijn, *Sediment Transport, Part I: Bed Load Transport,* Journal of Hydraulic Engineering **110 (10)**, 1431 (1984).

[7] R. M. Frings and M. G. Kleinhans, *Complex variations in sediment transport at three large river bifurcations during discharge waves in the river rhine.* Sedimentology **55**, 1145 (2008).

[8] R. Frings, M. Berbee Bastiaan, G. Erkens, M. G. Kleinhans, and M. J. P. Gouw, *Human-induced changes in bed shear stress and bed grain size in the river waal (the netherlands) during the past 900 years,* Earth Surface Processes and Landforms **34**, 503 (2009), https://onlinelibrary.wiley.com/doi/pdf/10.1002/esp.1746 .

[9] J. Sieben, *Sediment management in the dutch rhine branches,* International Journal of River Basin Management **7**, 43 (2009), https://doi.org/10.1080/15715124.2009.9635369.

[10] E. Mosselman and T. B. Le, *Five common mistakes in fluvial morphodynamic modeling,* Advances in Water Resources **93**, 15 (2016), https://doi.org/10.1016/j.advwatres.2015.07.025.

[11] F. Collas, A. Buijse, L. van den Heuvel, N. van Kessel, M. Schoor, H. Eerden, and R. Leuven, *Longitudinal training dams mitigate effects of shipping on environmental conditions and fish density in the littoral zones of the river Rhine,* Science of The Total Environment **619-620**, 1183 (2017), https://doi.org/10.1016/j.scitotenv.2017.10.299.

6

Conclusion

Originally, there is no road on earth,
but as people walk this way again and again, a path appears.

Lu Xun

6.1. Main conclusions

The results of this study have brought some important conclusions regarding the effectiveness of training a river with longitudinal walls:

On the degree of stability of the parallel-channel system created by a longitudinal wall

The work addressed this topic by combining the results of experimental and numerical investigations. The results show that a bifurcation created by a longitudinal training wall tends to be unstable and eventually results in a shallow channel and a deeper channel. The location of the upstream end of the longitudinal training wall with respect to a steady alternate bar or a point bar, if inside a river bend, is found to play an important role on this stability. Starting the wall at a location in the upstream part of a bar leads to the silting up of the channel at the bar side and to deepening of the other channel. The opposite occurs if the wall starts downstream of a bar top. The most desirable location for starting the longitudinal training wall is near the bar top. In this case, both channels remain open for a long time. In case of sinuous channels the best starting location is near a point bar top.

The physical processes at the bifurcation can explain these observations. Bifurcation instability arises if the supply of sediment to a branch deviates from the

transport capacity immediately downstream. Two factors play a role. First, the deviation between supply and transport capacity is smallest in river sections without streamwise gradients in flow field and bed topography, where lateral exchanges are at a minimum. Such sections are found at bar tops and in bar troughs. Second, deviations between sediment supply and transport capacity produce faster morphological changes in deeper areas where the sediment transport is higher. Small deviations thus produce faster loss of stability in bar troughs than at bar tops. This makes bar tops the most suitable locations for the bifurcation.

The effects of varying the widths of the parallel channels were assessed by means of both experimental and numerical investigations. The results of the experimental tests and of the simulations agreed with each other and showed that varying the width-ratios does not change the final configuration of the parallel channels system. The most stable system is obtained if the longitudinal training wall subdivides the river in two equally-wide parallel channels. In this case, the morphological process appears much slower than in the others cases and the channel characterized by bed level rise does not silt up completely.

On the role of discharge regime on bifurcation stability

The role of the discharge regime was assessed by means of numerical simulations. The results obtained with a constant discharge were compared with those obtained with a variable discharge (representative hydrograph). The morphological evolution was faster with a constant discharge than with a variable discharge. This is because with a constant discharge both the location and the size of the bar close to the bifurcation did not change and the transported sediment was permanently deflected in the same way. With variable discharge, bars tend to disappear during peak flows and the deviation of sediment towards the silting up channel was not always present. This suggests that in real rivers with natural discharges the morphological development after the construction of a longitudinal training wall may last for a long time.

The discharge regime affects also the stability of the parallel channels if the longitudinal wall starts near an alternate bar top or near the top of a point bar inside a river bend. The channels reach a dynamic equilibrium if the discharge is constant. Instead, if the discharge is variable the channel at the side of the bar tends to slowly silt up

On the degree of river navigability

In this study, the degree of navigability of the channel becoming deeper was assessed by considering the minimum width and depth requirements at low-flow conditions. This investigation was carried out using a numerical model to simulate a real river case: the Waal River before the normalization works. Three scenarios were compared: untrained river; river trained with a longitudinal wall; river trained with transverse groynes. The results show that a longitudinal wall and series of

groynes guarantee the same level of navigability with low flow if the obtained navigation channel width is the same.

On flood conveyance

The flood conveyance in rivers trained with a longitudinal wall was analyzed by means of numerical simulations reproducing the conditions of the Alpine Rhine River and of the Waal River. In both cases, the flood conveyance was interpreted by comparing the water levels for the same high discharge. Lower water levels than in the reference scenario indicate better flood conveyance and vice versa.

In the canalized Alpine Rhine River, a limited wall (in length) is placed in the river which is characterized by the absence of floodplains. The water levels obtained with the longitudinal wall are compared to the ones of the reference scenario (without wall) based on longitudinal profiles. The results show that placing the wall upstream or downstream of a steady bar does not affect the flood conveyance at the highest discharge. Within the length of the wall, the water levels locally drop, whereas just downstream of the wall, there is a slight increase in water levels. This could be the influence of the confluence where the two parallel channels merge again.

In the Waal River, the longitudinal wall extends to the end of the model domain and flood plains are present. The water levels are compared at one cross-section in the middle of the calculation domain. The results show that a longitudinal training wall is better than transverse groynes in conveying high discharges. The wall scenario is even better than the untrained river in this task. The reason for this is river incision lowering the main channel bed and thus increasing its conveyance.

On long-term channel incision

Training a river with a longitudinal wall indeed leads to main channel incision compared to the untrained river. Bed lowering is a result of two factors: general deepening and longitudinal slope becoming milder by river narrowing. Compared to the traditional transverse groynes, a longitudinal wall leads to less incision. This is related to the higher high-discharge conveyance, which can be regarded as "less narrowing" (on hydraulic resistance) of the river even if the navigation channel has the same width.

6.2. Summary of conclusions and recommendations

The major conclusions of this study are:

- The most desirable location for starting the longitudinal training wall is near a bar top or near a point bar top in case of a sinuous channel.
- The most stable system is obtained if the longitudinal training wall subdivides the river in two equally-wide parallel channels.
- The morphological evolution is faster with a constant discharge than with a variable discharge.

- In comparison with groynes producing the same navigation channel width, a longitudinal wall provides the same level of channel navigability, a higher flood conveyance, less river incision, whereas the presence of a shallow side channel might offer more suitable conditions for fish.

Recommendations regard future research:

- Erosion of unprotected banks along both the deeper and the shallower channel, particularly in presence of ship waves, at high and low discharge.
- The effects of openings of the wall allowing for water exchange.
- The effects of suspended solids on channel stability.
- The effects of vegetation growth in the shallower channel.

The investigation should consider the data measured in the framework of the Waalsamen project, monitoring the three pilot longitudinal walls constructed in the Waal River.

With its advantages compared to the traditional transverse groynes, longitudinal training walls will receive more attention from engineers and authorities in the future. With time they will find their way to come to the rivers.

A

Appendix

Effects of longitudinal walls on both sides of the river

This appendix analyzes the effects of having training walls along both sides of the river channel, with the aim to obtain a navigation channel in the middle and two parallel side channels along the banks. The analysis considers the same starting locations as for one single training wall (Locations 1 to 18, Figure 3.7). The straight channel presents hybrid (steady) alternate bars. The conditions considered in these simulations are the same as for one single training wall: discharge is kept constant (200 m^3/s) and the simulation is run for 10 years with morphological factor 10 (it simulates 100 morphological years).

The results of having training walls along both sides of the river are presented in Figure A.1. The reference case without longitudinal wall is displayed again (Figure A.1.a is the same as Figure 3.8.a) for the sake of comparison. If the right training wall starts at positions 3 to 9, i.e. at the upstream part of a bar (Figure A.1.b) and the left training wall starts thus at the downstream part of the bar located near the opposite bank, the results of the simulations agree with those obtained with a single training wall (Sections 3.4.1): the left-side channel bed is eroded whereas the right-side channel and the main channel silts up.

The opposite is obtained if the right-side training wall starts at position 12 to 17, i.e. at the downstream part of a bar (Figure A.1.d). In this case, the left-side training wall starts at the upstream part of the opposite bar. Again the results comply with those obtained with a single training wall. The right-side channel bed is eroded whereas the left-side channel and the main channel silts up.

If the right-side training walls starts at position 1, 2, 10 or 11, i.e. at a location close to the top of a bar (Figure A.1.c), the left-side wall starts at a location close to a pool. In this case, the results of the simulations show a more complex morphodynamic behavior. Initially, the right-side channel remains open in a way similar to the dynamic balance illustrated in Figure 3.9. The channel at the opposite side is first quickly eroded, but then it silts up once a new bar forms in the main channel

A

near its opening. After the left-side channel has silted up almost completely, the right-side channel starts aggrading, to finally completely silt up too. At this point, all water is conveyed by the main channel where all bars quickly disappear. This disappearance complies with theory [1], since the bar mode decreases from 1.0 (alternate bars) to 0.6 (strongly damped alternate bars).

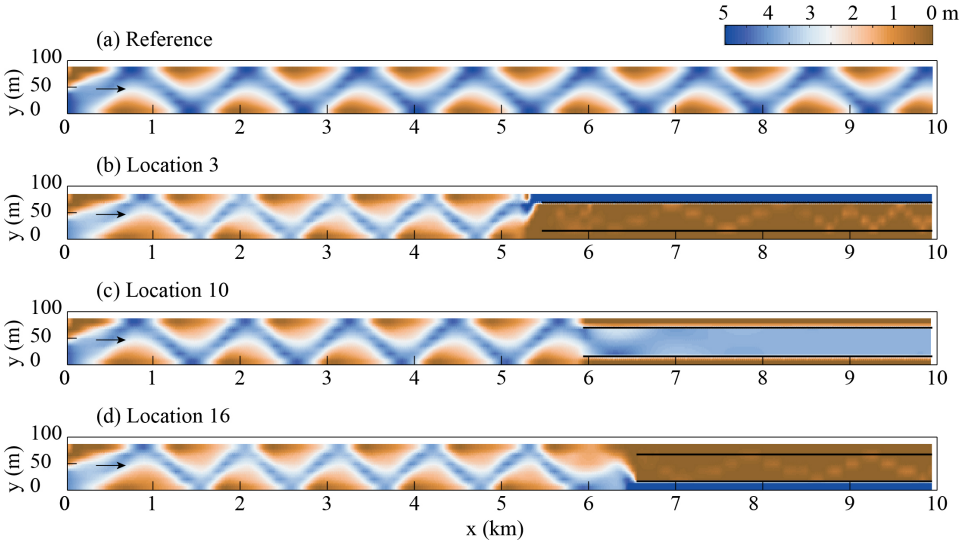

Figure A.1: Longitudinal training walls along both sides of the river. Equilibrium water depth at the constant discharge of 200 m^3/s. a) Reference case without training walls. b) Right side training wall start at location 3. c) Right side training wall start at location 10. d) Right side training wall start at location 16.

At this point an interesting question arises: can alternate walls on both sides of the river starting each one near a hybrid steady bar top minimize bar formation in the navigation channel? This would reduce both the extension of the structures in the river and dredging to maintain the navigation route. Preliminary results show that this might be a solution (Figure A.2). Possible reason for this bar reduction is that after the short wall the bar need spatial recovery. However, more investigations should be carried out to correctly identify the length of the walls and the distance between them.

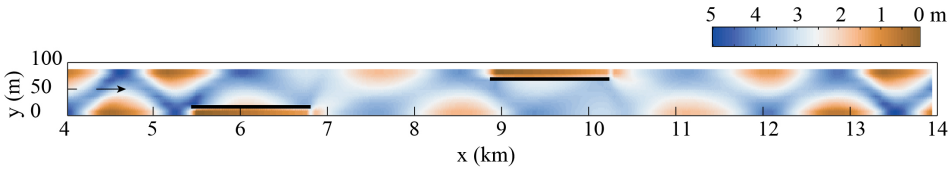

Figure A.2: Alternate training walls on both sides of the river starting near bar tops. Equilibrium water depth at the constant discharge of 200 m^3/s. Bars in the navigation channel tend to be reduced compared to the ones in the original channel.

References

[1] A. Crosato and E. Mosselman, *Simple physics-based predictor for the number of river bars and the transition between meandering and braiding,* Water Resources Research **45** (2009), 10.1029/2008WR007242, https://doi.org/10.1029/2008WR007242.

Acknowledgements

This thesis is definitely a great prize for the hard work,
but I know life still has many important things for us.
So my friend, keep working for the beautiful future.

Thai Binh LE (2010)

My PhD started in 2014 after a wonderful talk with Alessandra Crosato and Wim S.J. Uijttewaal. Since then, they have continuously supported me and enabled me to carry out my work with their important guidance and direction. I would like to show my deep respect for their knowledge and thank them for what they did during my study.

At the beginning, I was confident with the scientific aspect of the topic but I did not have any ideas on the technical support I might receive. Now I want to say that the help I received was almost ”perfect” in terms of a scientific support. I would like to thank the technical staff of the Environmental Fluid Mechanics Laboratory of Delft University of Technology. I thank my students Floortje Roelvink, Anouk Lako, Johan Jansen, Tim van Domburg and Arthur Pinkse for their help in the laboratory.

I thank Hendrik Havinga for providing me important information at the very beginning of this study. He gave me a wonderful talk on longitudinal training dams when I knew nothing about the topic.

I thank Erik Mosselman for his expert support. Together with him, many aspects of this study became clear.

I would like to thank an anonymous reviewer who rejected my very first paper and recommended that it should split in two different ones. Following this advice, my work was easier and more successful.

I thank Delft University of Technology for its working space and resources to make this study possible.

I also thank the Vietnam International Education Development (VIED) for its financial support to complete this study.

I thank my university (Thuy Loi University) and my professors in Vietnam (Nguyễn Trọng Tư, Lê Văn Hùng, Nguyễn Quang Kim). With their help and support, I can be here to learn new things and have a chance to improve myself.

Now about my life.

First, I would like to thank all of my friends of the Vietnamese Community in Delft (VCiD) and the international colleagues in my section. With them, I enjoyed a nice and friendly life here in Delft.

Special thanks are due to my family, especially, my beloved sister, Natalie Nga Le. Without their support and encouragement, I would have not gone this far.

Finally, I want to show special thanks to my wife, Lê Thị Hằng. She came and smoothed all unpredictable things in my life. Without her, I even do not know that life is still beautiful outside the office when I started the last year of my PhD. My dear, I want to go with you till the end of the time.

Delft, June 2018

Thai Binh LE

Curriculum Vitæ

Thai Binh LE

18-04-1983 Born in Quang Nam, Vietnam.

Education

2001–2006 Thuyloi University, Hanoi, Vietnam

2010 MSc. Hydraulic Enginering
Unesco-IHE, Delft, The Netherlands
Thesis: Effects of groyne lowering along the Waal River
Supervisor: Prof.dr. N. Wright
Daily supervisor: Dr. A. Crosato

2018 PhD. Hydraulic Engineering
Delft University of Technology, Delft, The Netherlands
Thesis: Training Rivers with longitudinal walls. A long-term perspective
Promoter: Prof.dr.ir. Wim S.J. Uijttewaal
Co-promoter: Assoc.prof.dr. A. Crosato

Awards

2006 Third prize, Loa Thanh 18^{th} Prize for excellent students in Civil Engineering and Architecture in Vietnam (nationwide contest).

2008 Fellowship by IHP-Tertiary Water Education Grants Program (IHP-TWEGP) for a MSc study at UNESCO-IHE, Delft, The Netherlands.

2013 Fellowship by Vietnam International Education Development (VIED). Project 911 for PhD student.
Subject: The effects of longitudinal training walls on river morphological development

List of Publications

Articles

4. **T.B. Le, A. Crosato, A. Montes Arboleda**, *Revisiting Waal River Training by Historical Reconstruction.*, Journal of Hydraulic Engineering. (2018, submitted).

3. **T.B. Le, A. Crosato, W.S.J. Uijttewaal**, *On the stability of river bifurcations created by longitudinal training walls. Numerical investigation*, Advances in Water Resources 113, 112 (2018).

2. **T.B. Le, A. Crosato, W.S.J. Uijttewaal**, *Long-term morphological developments of river channels separated by a longitudinal training wall*, Advances in Water Resources 113, 73 (2018).

1. **E. Mosselman, T.B. Le**, *Five common mistakes in fluvial morphodynamic modeling*, Advances in Water Resources 93, 15 (2016).

Conference proceedings

7. **T.B. Le, A. Crosato, W.S.J. Uijttewaal**, *Stability of parallel river channels created by a longitudinal training wall*, Book of Abstracts RCEM 2017 - Back to Italy, Trento-Padova, September 15-22 (Stefano Lanzoni, Marco Redolfi and Guido Zolezzi Eds.), pp. 212. Publisher: RCEM2017 Organizing Committee, ISBN: 978-88-8443-752-5 (2017).

6. **T.B. Le, A. Crosato, W.S.J. Uijttewaal**, *Longitudinal training walls: optimization of river width subdivision*, Book of Abstracts NCR-Days 2017, Wageningen, February 1-2, NCR-PUBLICATION 41-2017 (AJ.F. Hoitink, T.V. de Ruijsscher, T.J. Geertsema, B. Makaske, J. Wallinga, J.H.J. Candel, J. Poelman Eds.), pp. 46-47. Publisher: Netherlands Centre for River Studies (NCR), ISSN 1568-234X (2017).

5. **T.B. Le, A. Crosato, W.S.J. Uijttewaal**, *Experimental study on the effects of longitudinal training walls*, River Flow 2016. Constantinescu, Garcia & Hanes (Eds.). © 2016 Taylor & Francis Group, London, ISBN 978-1-138-02913-2 (2016).

4. **T.B. Le, A. Crosato, W.S.J. Uijttewaal**, *Longitudinal training walls: morphodynamic effects of the starting point*, Book of Abstracts NCR-Days 2015, Nijmegen, October 1-2, NCR-PUBLICATION 39-2015 (HJR Lenders, FPL Collas, GW Geerling and RSEW Leuven Eds.), pp. 69-72. Publisher: Netherlands Centre for River Studies (NCR), ISSN 1568-234X (2015).

3. **F.E. Roelvink, A. Lako, T.B. Le, A. Crosato**, *Challenges in morphodynamic laboratory experiments*, Book of Abstracts NCR-Days 2015, Nijmegen, October 1-2, NCR-PUBLICATION 39-2015 (HJR Lenders, FPL Collas, GW Geerling and RSEW Leuven Eds.), pp. 38-41. Publisher: Netherlands Centre for River Studies (NCR), ISSN 1568-234X (2015).

2. **T.B. Le, A. Crosato, W.S.J. Uijttewaal**, *Long term effects of longitudinal training wall: a numerical study*, IAHR world congress 07/2015. The Hague, The Netherlands (2015).

1. **T.B. Le, A. Crosato, W.S.J. Uijttewaal**, *Longitudinal training walls: optimization of channel geometry*, Book of Abstracts NCR-Days 2014, Enschede, October 2-3, NCR-PUBLICATION 38-2014 (D.C.M. Augustijn and J.J. Warmink (eds.), pp. 41-42. Publisher: Netherlands Centre for River Studies (NCR), ISSN 1568-234X (2014).

Invited presentations

2. **T.B. Le, A. Crosato, W.S.J. Uijttewaal**, *Numerical and experimental studies on longitudinal training walls*, WaalSamen meeting, Wamel, April 20th (2016).

1. **T.B. Le, A. Crosato, E., Mosselman, W.S.J. Uijttewaal**, *Long-term morphological effects of longitudinal training walls*, WaalSamen meeting, Westervoort, April 5th (2018).

MSc thesis

T.B. Le, *Effects of groyne lowering along the Waal River*, MSc thesis, Unesco-IHE, The Netherlands. (2010).